
ANL-76-XX-8

NORTHWESTERN UNIVERSITY

PHOTOEXCITATION IN SUPERCONDUCTORS

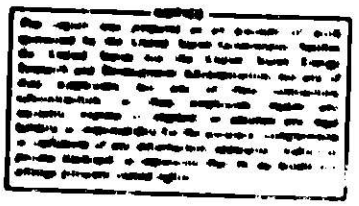

A DISSERTATION

SUBMITTED TO THE GRADUATE SCHOOL

IN PARTIAL FULFILLMENT OF THE REQUIREMENTS

for the degree

DOCTOR OF PHILOSOPHY

Field of Physics

By

IVAN SCHULLER

Evanston, Illinois

June 1976

CONTRACT NO. N-31-109-ENG-38

Preface

Since this work is the culmination of many years of study, I will take the liberty of making a small philosophical digression.

One of the most important things I have learned is that scientific research as a whole is one of the most exciting human activities irrespective of the specific problem or area than one pursues. As long as a problem is challenging and one involves himself deeply in it, the excitement will be there. The only disappointment is that it took me so many years to find out what Woodstock learned in one cartoon (see following figure).

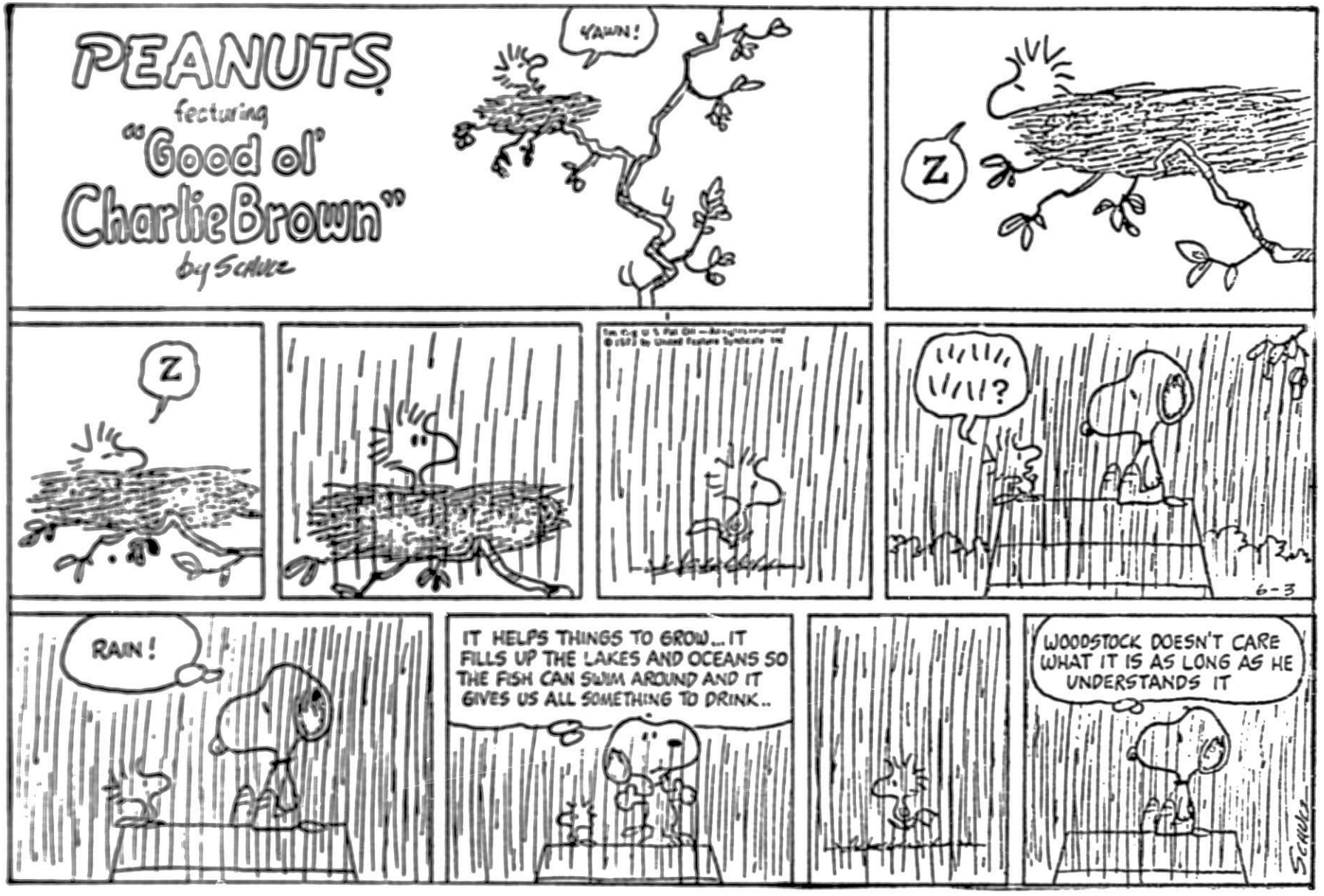

Acknowledgments

I would like to thank Dr. Kenneth E. Gray who suggested the idea for the experiments that are described in this thesis. I would like to thank him for his guidance and willingness to discuss my ideas, however trivial they were, and for his help in the actual experimental work.

I am deeply indebted to my advisor, Professor John Ketterson, who very generously permitted me to choose a subject accordingly to my personal taste and preference. His interest and guidance as well as his constant questioning were very important for my education as a physicist.

It is a pleasure to thank Dr. O. C. Simpson and Dr. D. L. Price of the Solid State Science Division of Argonne National Laboratory for the financial support and for the use of the excellent experimental facilities during the period of this work. To the machinists Edmund E. Klocek, the late Robert Lemke, Elmer I. Kondla, and Don Rabe for bringing to reality my rough drafts and vague ideas and for teaching me many of the things I know about plants, many thanks. The fine typing work on this thesis is due to Mrs. Carol Oleferchik whose help I appreciate. Many thanks to Carol Cohen for gluing somewhat my broken English.

I am thankful to Dr. L. Welsh who guided my first steps in experimental solid state. Special thanks to Dr. Charles Falco for long discussions, advice and for helping me face the disappointments with a smile.

My thanks to Northwestern University for a University Fellowship and for support to attend conferences.

I would like to acknowledge United Feature Syndicate Inc. for permission to use the first figure of this thesis.

Last, but not least, many thanks to my wife Jackie for her constant support since my undergraduate days in Chile.

Abstract

We have performed a study of the behavior of superconductors under light illumination. In one of the experiments the acoustical coupling of two thin superconducting films forming a tunnel junction was measured. The experiment was performed by photoexciting quasiparticles in one film and studying the resulting charge in the energy gap. A detailed comparison shows agreement of the experimental results with Little's theory of the acoustical coupling of solids. In addition, the results indicate that the acoustic coupling of a thin lead film to the helium bath is much stronger than to the underlying tin film and substrate.

In another experiment we have measured directly for the first time the relaxation time τ of the superconducting energy gap. We show that near the superconducting transition temperature T_c the relaxation time diverges as predicted by several authors. By also measuring the equilibrium energy gap Δ we find $\tau \propto \Delta^{-1}$ very near T_c in agreement with calculations of Schmid and Schön. It is observed for the first time that near T_c ($\sim$ 10 mK below T_c) the equilibrium energy gap does not obey the BCS temperature dependence, a result which is attributed to inhomogeneities in the films.

Table of Contents

Table of Contents (contd.)

Table of Contents (contd.)

I. Introduction

Superconductivity is a phenomenon exhibited by many metals and alloys at low temperatures. At particular critical temperature T_c, the metal undergoes a second order phase transition in which a finite fraction of the electrons pair up and condense into a "superfluid" exhibiting macroscopic quantum phenomena. In their now classical paper, Bardeen, Cooper, and Schrieffer (BCS57) layed down the basis for the understanding of superconductivity from a microscopic point of view. Their theory (BCS) predicts the existence of a temperature-dependent energy gap $\Delta(T)$ in the excitation spectrum of the electrons. This microscopic theory was able to explain such striking phenomena as zero resistivity and the Meissner effect. Subsequently many theoretical predictions, such as of superconducting tunneling and the Josephson effect (Jo62), were experimentally confirmed (Gi60, AR63).

Since the equilibrium properties of superconductors are now fairly well understood (Parks 69), there has recently been extensive work done in the study of nonequilibrium superconductivity (La74, La75). Most of these studies were done at small deviations from equilibrium so that many equilibrium concepts could be extended to the nonequilibrium situation. Extensive experimental as well as theoretical work was dedicated to the measurement of relaxation times in superconductors, since precisely these relaxation times are the ones that set the time scale for nonequilibrium phenomena. Most of the relaxation time measurements were performed on thin films deposited on insulator substrates immersed in liquid helium. It was recognized (RT67) that the phonons play an important role in these measurements since the relaxation times are enhanced by a factor that

depends on the coupling of the phonons to the surrounding environment. An attempt to measure the phonon coupling of two superconducting thin films is the subject of Chapter IV of this thesis.

Because superconductors close to the transition temperature T_c obey the Landau second order phase transition theory very closely, it is to be expected that the prediction of a time-dependent second order phase transition will be an indication of the nonequilibrium behavior of superconductors close to T_c. Landau and Khalatnikov (LK54) predicted that the relaxation time of the order parameter (i.e., energy gap in superconductors) should diverge as T_c is approached. A measurement of this relaxation time in a superconductor is the subject of Chapter V of this thesis.

Nonequilibrium situations are established in superconductors by (a) photoexcitation (illumination with a laser), (b) superposition of AC and DC currents, (c) driving currents through a normal-superconductor interface, or (d) by injecting quasiparticles through a thin oxide barrier. In this study the nonequilibrium situation was established by photoexcitation and the behavior of the superconductor during or after illumination was studied. The superconductor which was disturbed from equilibrium was a thin film which was part of a tunnel junction. This permitted simultaneous measurements of the energy gaps and of relaxation times.

In Chapter II we describe briefly the microscopic theory (BCS), the phenomenological Ginzburg-Landau theory and superconducting tunneling. In Chapter III we describe the different relaxation times in superconductors as well as the experiments and theories for photoexcitation. In Chapter IV we give a detailed discussion of Little's theory of

acoustic coupling of solids and the theory and experiment for the acoustic coupling of thin superconducting films. In Chapter V we describe a phenomenological and microscopic theory for the relaxation of the superconducting order parameter as well as an experiment in which this relaxation time was measured directly for the first time.

II. Equilibrium Superconductivity

II.1. Introduction

At low temperature (around the liquid helium range) many metals and alloys show a second order phase transition to a thermodynamic state in which, among many other striking phenomena, the DC resistivity of the metals or alloys drops to zero. This new thermodynamic state is the so-called superconducting state. Although the phenomenon of superconductivity was discovered in 1911, it took 50 years to develop a microscopic theory (BCS57). This can be understood by the fact that the binding energy of an electron in a normal metal is of the order of the Fermi energy ($\sim$ 1 eV) and on the other hand the "condensation energy" (the difference between the binding energy in the normal and in the superconducting state) is about 6 order of magnitude smaller. Because of this, in order to apply a perturbation theory, it is necessary to have a normal state theory which is correct at least to one part in a million. Since no normal state theory is correct to this accuracy, any perturbation scheme is doomed to fail.

The equilibrium properties of superconductors are well established from an experimental as well as a theoretical (macroscopic and microscopic) point of view. Although the present work is a research on the nonequilibrium properties of superconductors, we will briefly describe some of the equilibrium concepts which are carried over to nonequilibrium situations.

We will briefly describe the macroscopic Ginzburg-Landau (GL50) second order phase transition theory as well as the Bardeen-Cooper-Schrieffer (BCS) (BCS57) microscopic theory. From the experimental

point of view we are only going to describe superconducting tunneling and we are not going to detail the very interesting phenomena of zero resistance and Meissner effect.

II.2. The BCS Theory

The success of the BCS theory is due to the fact that instead of trying to correct the normal state theory, BCS isolated the interaction that is responsible for producing superconductivity and assumed that all the other interactions are the same in the normal and superconducting states.

The ground work was laid down by Fröhlich (Fr50), who showed how a short range electron-phonon interaction can give rise to a long range electron-electron interaction. Intuitively, what happens is that an electron attracts (via the Coulomb interaction) the surrounding ions, deforming the lattice locally. Since the typical frequencies of a phonon are of the order of 10^{-13} sec and the Fermi velocity of an electron is of the order of 10^{16} Å/sec, the electron can move 10^3 lattice spacings before the lattice can relax back to its equilibrium position. Another electron "in passing" feels the force due to these displaced ions and indirectly, then, is interacting with an electron which is far away (10^3 lattice spacings). Later Cooper (Co57) showed that two electrons outside a Fermi sea that interact with an attractive potential will pair and have a bound state of opposite moments.

Based on these ideas, BCS proposed a model Hamiltonian in which they assumed that since different metals show superconductivity, the crystal symmetry is unimportant and there are going to be only small changes in total energy with the superconducting transition. The

electron-phonon interaction is a good candidate for the interaction for the following: strong coupling metals (Pb, Hg, etc.) are superconductors whereas weak coupling metals (Cu, Na, etc.) are not; the electron-phonon interaction is attractive; superconductors show an isotope effect in which the transition temperature increases with isotopic mass. The ground state was assumed to be formed by electron pairs (of the type described by Cooper), and the interactions present to be the phonon mediated electron-electron interaction. Assuming a square well potential for the attractive interaction BCS were able to predict the existence of a temperature-dependent forbidden energy gap $\Delta_{eq}(T)$ for the electrons. They showed that the distribution function for the excitations is Fermi-like

$$f_k = \frac{1}{1 + \exp(\epsilon_k / k_B T)} \tag{II-1}$$

where ϵ_k is the excitation energy of momentum k (here ϵ_k is a function of Δ_{eq} and T). The energy gap is given implicitly in the equation

$$1 = N_0 V \int_{\Delta_{eq}}^{\hbar\omega_D} \frac{d\xi}{\sqrt{\xi^2 + \Delta_{eq}^2}} \left[1 - 2f(\xi^2 + \Delta_{eq}^2)\right] \tag{II-2}$$

where N_0 is the density of states at the Fermi surface in the normal metal, V is the depth of the potential well and ω_D is the Debye frequency. This reduces at zero temperature to

$$\Delta_{eq}(0) = 1.76\, k_B T_c \tag{II-3}$$

where T_c is the transition temperature and close to T_c

$$\Delta_{eq}(T) \sim 3.2\, k_B T_c (1 - T/T_c)^{1/2} \tag{II-4}$$

II.3. The Phenomenological Ginzburg-Landau Theory

In the vicinity of the transition temperature, the free energy of a superconductor, in the absence of magnetic fields and inhomogeneities, is written as

$$F(P,T,\psi_{eq}) = F_0(P,T) + A(P,T)\psi_{eq}^2 + C(P,T)\psi_{eq}^4 \qquad \text{(II-5)}$$

where ψ_{eq}, the order parameter, is zero at high temperatures and continuous across the transition into the ordered phase. From general consideration of stability, Ginzburg-Landau assumed $C > 0$ and $A < 0$ below T_c and $A > 0$ above T_c. The transition point is determined from the condition $A(P,T) = 0$.

In the vicinity of T_c, $A(P,T)$ is expanded in series in the difference $T-T_c$, and neglecting higher order terms one writes

$$A(P,T) = a(P)(T - T_c) \quad . \qquad \text{(II-6)}$$

The temperature dependence of the order parameter is determined from the condition that the free energy has to be a minimum in equilibrium. This yields

$$\psi_{eq}^2 = -\frac{A}{2C} = \frac{a}{2C}(T_c - T) \quad . \qquad \text{(II-7)}$$

This is the same temperature dependence as the energy gap in the BCS theory close to T_c, and it has been shown by Gorkov (Go59) that in equilibrium close to T_c, the BCS theory is equivalent to the G-L theory, with $\psi_{eq} = \Delta_{eq}$. It was also shown by Gorkov that ψ_{eq} is the wavefunction for the superconducting electrons and so $|\psi_{eq}|^2 = n_s$ the density of Cooper pairs.

II.4. Superconducting Tunneling

Since the experiments described in this thesis were performed on superconducting tunnel junctions, we will describe in this section the phenomenon of superconducting tunneling.

If a superconductor is separated from a normal metal or another superconductor by a thin ($\sim$ 10 Å) insulator, a very sharp structure appears in the I-V characteristic of this system. Because of the existence of a forbidden energy gap Δ in the excitation spectrum, an electron with an energy $eV < \Delta$ will not be able to tunnel across the oxide barrier into the forbidden energy states. Consequently, for voltages such that $eV < \Delta$, no current will flow across the junction. At a voltage for which $eV = \Delta$, current will start flowing across the junction because now the electrons will be able to tunnel into the allowed energy states above the gap. At much higher voltages the characteristic will approach the normal state characteristic of the oxide. A measurement of the equilibrium energy gaps made from this I-V characteristic agrees well with the predictions of the BCS theory (described in this chapter) although close to T_c deviations from the theoretical behavior, which are presumably due to inhomogeneities or edge effects in the junctions, are observed (see Chapter V). A series of characteristic curves for a superconductor-insulator-superconductor tunnel junction is shown in Fig. II-1 (Ta63).

If the tunnel junction is formed from two different superconductors, structure can be seen in the I-V characteristic at the sum and difference of the energy gaps. From this structure the energy gaps of both superconductors can be determined. If the two superconductors have quite

Fig. II-1: I-V characteristic for an Al-Al_2O_3-Al superconducting tunnel junction. Notice the sharp structure at $eV = \Delta_{Al}$ (after Ta63).

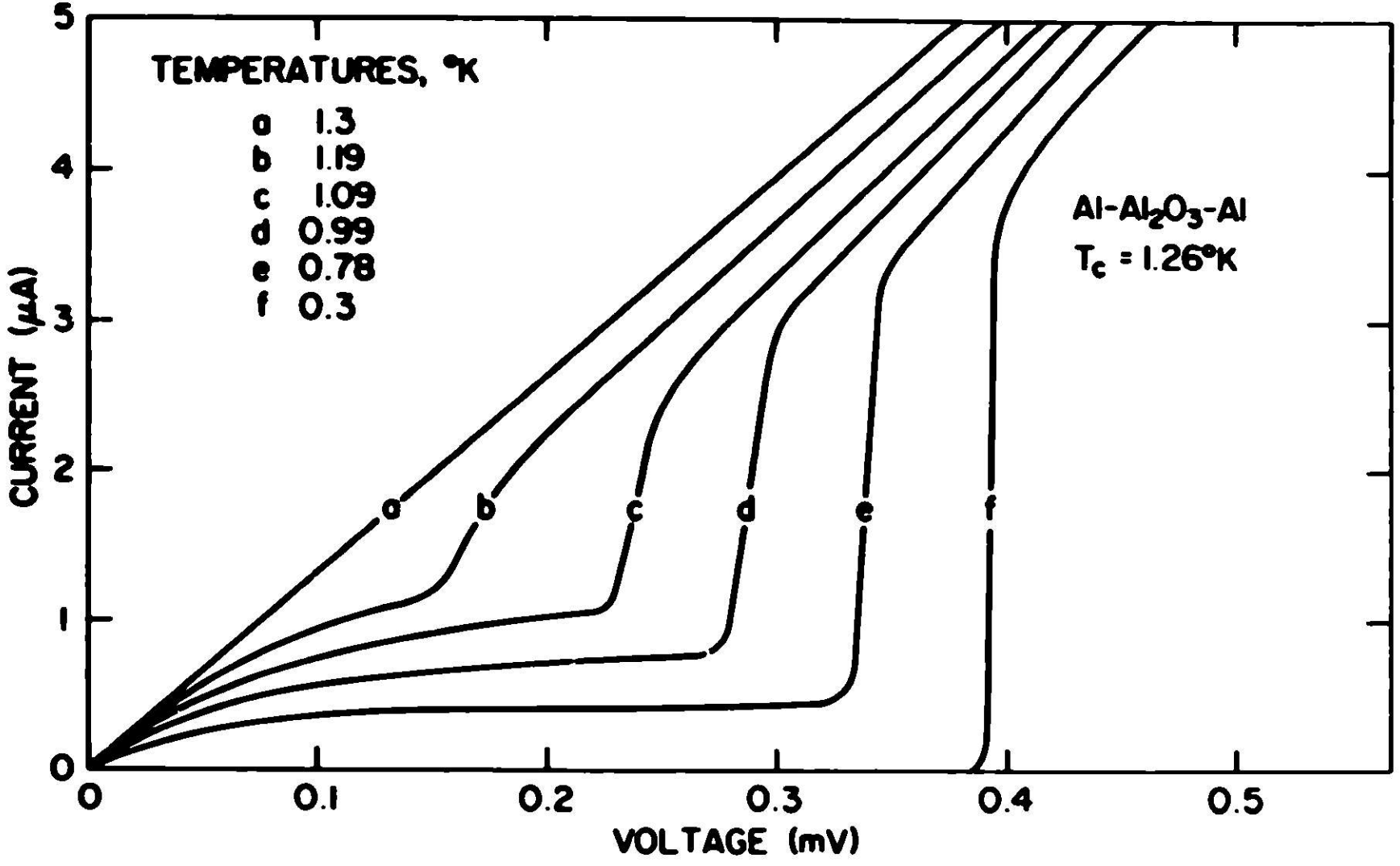
TEMPERATURES, °K
a 1.3
b 1.19
c 1.09
d 0.99
e 0.78
f 0.3
Al-Al2O3-Al
Tc = 1.26°K
CURRENT (μA)
VOLTAGE (mV)
0
1
2
3
4
5
0
0.1
0.2
0.3
0.4
0.5
a
b
c
d
e
f

different transition temperatures, the energy gap of one of the superconductors (the one with lowest transition temperature) can be determined more precisely in this way than by using a junction made of the same material. This is because the structure in the I-V characteristics, close to T_c, is sharper in this case (see Chapter V). An example of I-V characteristics for a tunnel junction made of dissimilar superconductors is shown in Fig. II-2.

Fig. II-2: I-V characteristic for an Sn-SnO-Pb tunnel junction. Notice the sharp structure at $eV = (\Delta_{Sn} + \Delta_{Pb})$ and at $eV = (\Delta_{Pb} - \Delta_{Sn})$ (after Ta63).

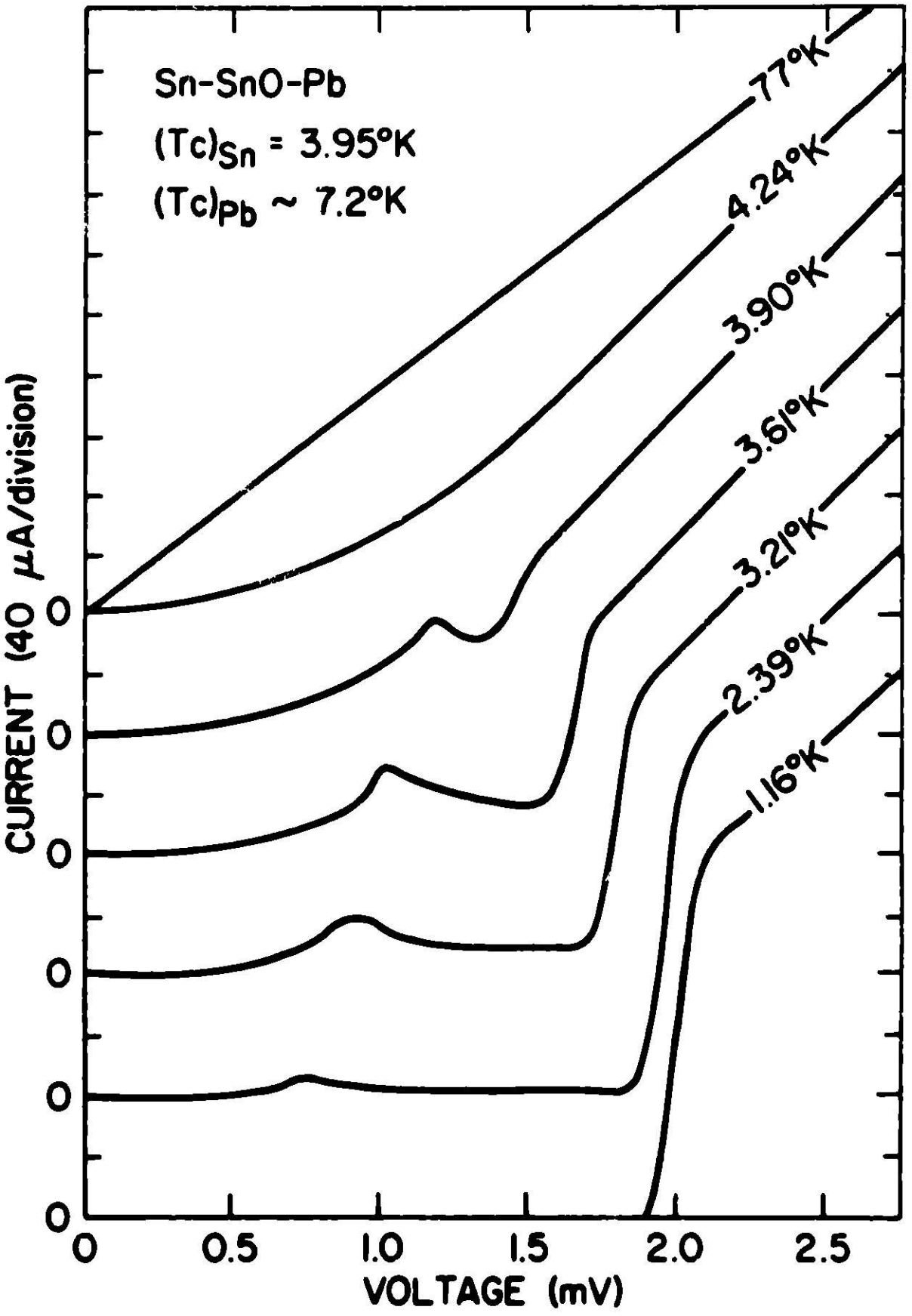
Sn-SnO-Pb
(Tc)Sn = 3.95°K
(Tc)Pb ~ 7.2°K
77°K
4.24°K
3.90°K
3.61°K
3.21°K
2.39°K
1.16°K
CURRENT (40 μA/division)
0
0
0
0
0
0
0.5
1.0
1.5
2.0
2.5
VOLTAGE (mV)

III. Nonequilibrium Superconductivity

III.1. Introduction

Recently there has been a considerable amount of work done in order to characterize the nonequilibrium properties of superconductors. Since in most applications (superconducting magnets, transmission lines, etc.) the superconductors are used in a nonequilibrium situation, it is important from an applied as well as a fundamental point of view to understand their nonequilibrium behavior.

Since the macroscopic and microscopic theories are so successful in explaining the equilibrium properties of superconductors, it is reasonable to carry over to nonequilibrium situations many of the concepts used in equilibrium. It is assumed that it is still legitimate to describe the superconductor through a local energy gap or order parameter and a local excitation spectrum. It was suggested (GE68, VK74) that due to the existence of the energy gap, a simple relaxation scheme is not valid for a superconductor. Because of the singularity in the excitation spectrum all related quantities will have a singularity in their frequency spectrum (Yu74). This singularity will manifest itself as an oscillatory behavior in the nonequilibrium relaxation phenomena. Since the characteristic frequency for this oscillation is the "gap frequency", for longer times, it is expected that the concept of a relaxation time will be valid.

For small deviations from equilibrium it is expected that these assumptions are valid, but even for large deviations from equilibrium we will have to start and extend from the equilibrium concepts. Since the quasiparticles, the Cooper pairs and the phonons form a coupled system,

there are many possible relaxation processes. These relaxation processes include (La75): (a) inelastic scattering of quasiparticles and phonons, (b) recombination and pair breaking with emission of phonons at low temperatures and relaxation of the energy gap at temperatures close to the transition temperature, (c) diffusion of excited quasiparticles and phonons, and (d) escape of phonons into the substrate or liquid helium. In the next sections we will describe the relaxation times associated with this processes.

In order to study the nonequilibrium properties of a superconductor a nonequilibrium situation is created by: (a) injecting quasiparticles into a superconductor through a tunnel junction (LH68, GLA69, Gr71, C&72, CP74), (b) driving a current through a region where the energy gap changes spatially, as at a normal superconductor interface (YM72, Yu74), (c) applying alternating currents to the superconductor (PM73), or (d) illuminating the superconductor with a laser (Te71, PW72, HDN74, Sa74, Pa75, SG75). In the present experiments the superconductor was perturbed by illuminating it with a laser, and because of this in Section 3 of this chapter we will describe the current theories for the photoexcitation of a superconductor.

III.2. Relaxation Times in Superconductors

Since the time scale for the time-dependent phenomena is set by the various relaxation times, we are going to review the subject in this section. Even for small perturbations from equilibrium there are a large number of relaxation times measured. Up to date there have been only two theoretical efforts by Kaplan et al. (Ka75), and Gray (Gr75) to describe these relaxation times. (Ka75) have been able to calculate

the low energy quasiparticle and phonon lifetimes using the low frequency part of the weighted phonon density of states $\alpha^2(\Omega)F(\Omega)$. On the other hand (Gr75) was able to classify the various relaxation times close to T_c using a scheme suggested by Schmid and Schön (SS75). In this section we will describe the various relaxation times and their dependence on temperature. We will also give a compilation of the relaxation times measured to date.

The relaxation times that were first measured were the quasiparticle recombination lifetimes (MD67, LH68, GLA69, LH71, PW72, HDW74, Pa74), the most complete study being that of (Gr69) in aluminum. These (Gr69) measurements were done on a double tunnel junction as illustrated in the inset of Fig. III-1. One of the junctions was used to inject quasiparticles in the nonequilibrium region where the increase in the steady state quasiparticle distribution is proportional to the relaxation time. This increase is measured with the second tunnel junction, and the results obtained by (Gr69) indicate that the recombination lifetime is given by $\tau_R \propto T^{-1/2}\, e^{\Delta_{eq}/kT}$ as shown in Fig. III-1, in good agreement with the theoretical predictions (SG62, RC63). The same temperature dependence was measured later in lead (PW72) and tin (HDW74, Pa74), so we conclude that the temperature dependence of the quasiparticle recombination lifetimes is well established, and that theory and experiment are in good agreement. It should be pointed out that in these lifetime experiments the time that is measured is an effective lifetime which is different from the actual recombination lifetime by a factor $(1 + \beta/2\gamma)$, where β is the pair breaking probability and γ is the escape probability for phonons from the energy range $h\omega \geq 2\Delta_{eq}$ by processes other than pair

Fig. III-1: Recombination lifetimes vs Δ_{eq}/kT (Δ_{eq}; the equilibrium energy gap) as measured in the steady state experiments of Gray (Gr69). The solid line is the theoretical prediction. The inset shows a schematic of the experiment as described in the text.

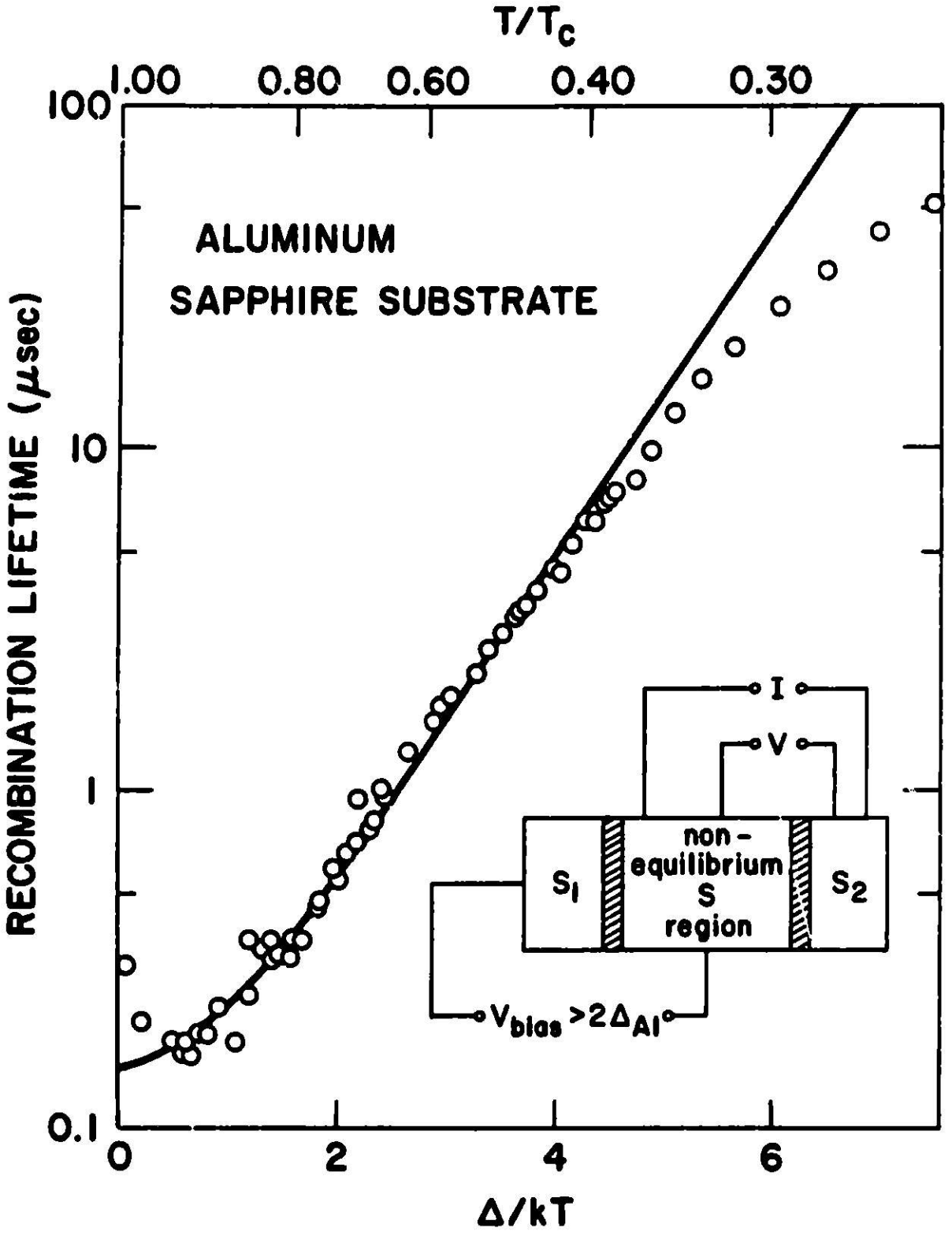
T/Tc
1.00
0.80
0.60
0.40
0.30
100
10
1
0.1
ALUMINUM
SAPPHIRE SUBSTRATE
RECOMBINATION LIFETIME (μsec)
I
V
S1
non-
equilibrium
S
region
S2
Vbias >2ΔAl
0
2
4
6
Δ/kT

breaking. The conclusions of (GLA69) indicate that $0.2 \leq \beta/2\gamma \leq 1$ for their experiment, whereas the recent results of Smith and Mochel (SM75) conclude that $7.5 \leq \beta/2\gamma \leq 8.7$ (although there are objections that can be raised (Gr75) to this last experiment). Because the phonons can modify substantially the measured lifetimes, it is important to determine the role they play in this type of recombination experiment. A determination of γ will be the subject of Chapter IV of this thesis, which will help in clarifying this problem.

One of the relaxation times that received the least amount of attention from the experimental (MD67) and the theoretical (Th72) points of view is the thermalization time τ_{Th}. In all lifetime experiments it is assumed that the relaxation process of the excited quasiparticles at low temperature occurs in two steps. First, the highly excited quasiparticles relax (thermalize) with a characteristic time τ_{Th} to a quasiequilibrium distribution (close to the gap edge) and then recombine with a much longer characteristic time τ_R, the recombination lifetime. The measurements of Miller and Dayem (MD67), shown in Fig. III-2, indicate that $\tau_{Th} \propto \exp[-3.34(E - \Delta_{eq}/\Delta_{eq})]$ where E is the energy of the excited quasiparticle and Δ_{eq} is the equilibrium energy gap. These results are not convincing. The recombination lifetime they measure has a different temperature dependence from other experiments and theoretical predictions; however, this discrepancy has been explained (Gr75). A theoretical calculation of Tinkham (Th72) shows that the important steps in the thermalization process are the low energy steps so that the time is independent of the initial energy distribution. (Th72) finds that the thermalization time t to a temperature T* is given by the relationship $T^* \propto t^{-1/3}$.

Fig. III-2: Thermalization time as calculated from the steady state experiments of Miller and Dayem (MD67). (Here Δ refers to the equilibrium energy gap.)

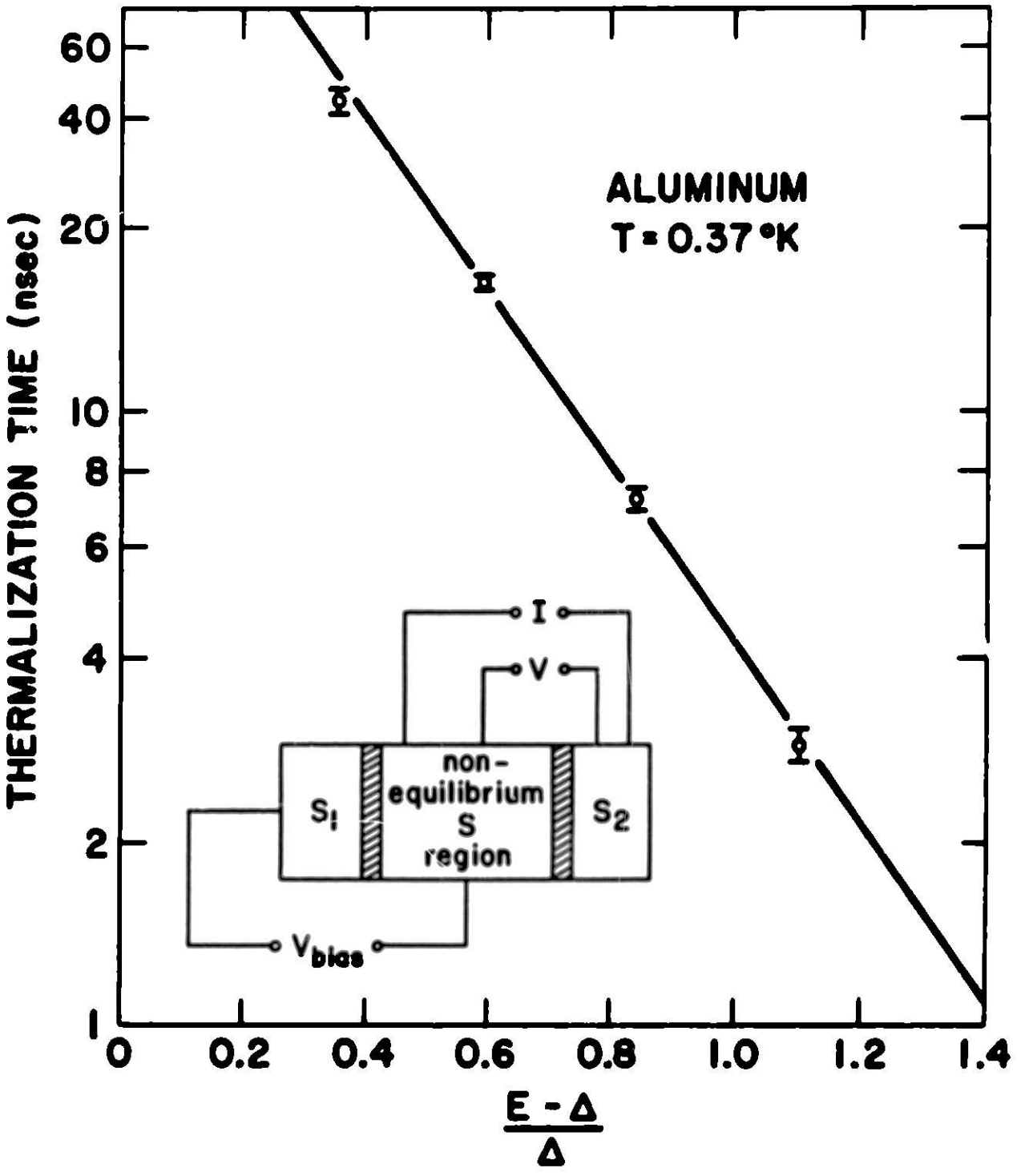
ALUMINUM
T = 0.37 °K
THERMALIZATION TIME (nsec)
60
40
20
10
8
6
4
2
1
0
0.2
0.4
0.6
0.8
1.0
1.2
1.4
E - Δ / Δ
I
V
S1
non-equilibrium S region
S2
Vbias

Yet another nonequilibrium situation can be induced in a superconductor if the electron and hole branches of the excitation spectrum are not populated equally. This can be done, for instance, by injecting quasiparticles into a superconductor through a tunnel junction at $V >> \Delta$. The relaxation time τ_Q (branch mixing time) back to equilibrium, where both branches are equally populated, was shown to be proportional to $1/\Delta_{eq}$ and hence diverge close to T_c (Ct72, Pa73, CP74). Here Δ_{eq} is the equilibrium energy gap. This is in agreement with a theory developed by Tinkham and Clarke (TC72) in which it is assumed that branch imbalance implies that the chemical potential for the pairs is different from the chemical potential for the quasiparticles. It is this difference in the chemical potentials that gives rise to the branch imbalance. A graph of the experimental results of Paterson (Pa73) and a diagram (TC72) illustrating the experiment are shown in Fig. III-3. A theory (SS75) that will be described in Chapter V predicts that the branch imbalance relaxation is equivalent to the relaxation of the phase of the superconducting order parameter, and also predicts that τ_Q diverges as $1/\Delta_{eq}$ in agreement with the experimental results.

By studying the responses of a microwave biased SQUID (Superconducting Quantum Interference Device), Rochford et al. (RRRH75) found that the minimum response time of a SQUID, τ_f, is also proportional to $1/\Delta_{eq}$. It was suggested by them that this might reflect the characteristic time for the response of a supercurrent to an electric field. In an earlier calculation (Ma70) it was predicted that this time should diverge as $1/\Delta_{eq}$ for superconducting microbridges of width less than the coherence length. The measurements and theory are in quantitative agreement (see Fig. III-4) although it was suggested (Pa75) that this experiment might

Fig. III-3: Branch mixing time vs the reduced temperature measured by Paterson (Pa73).

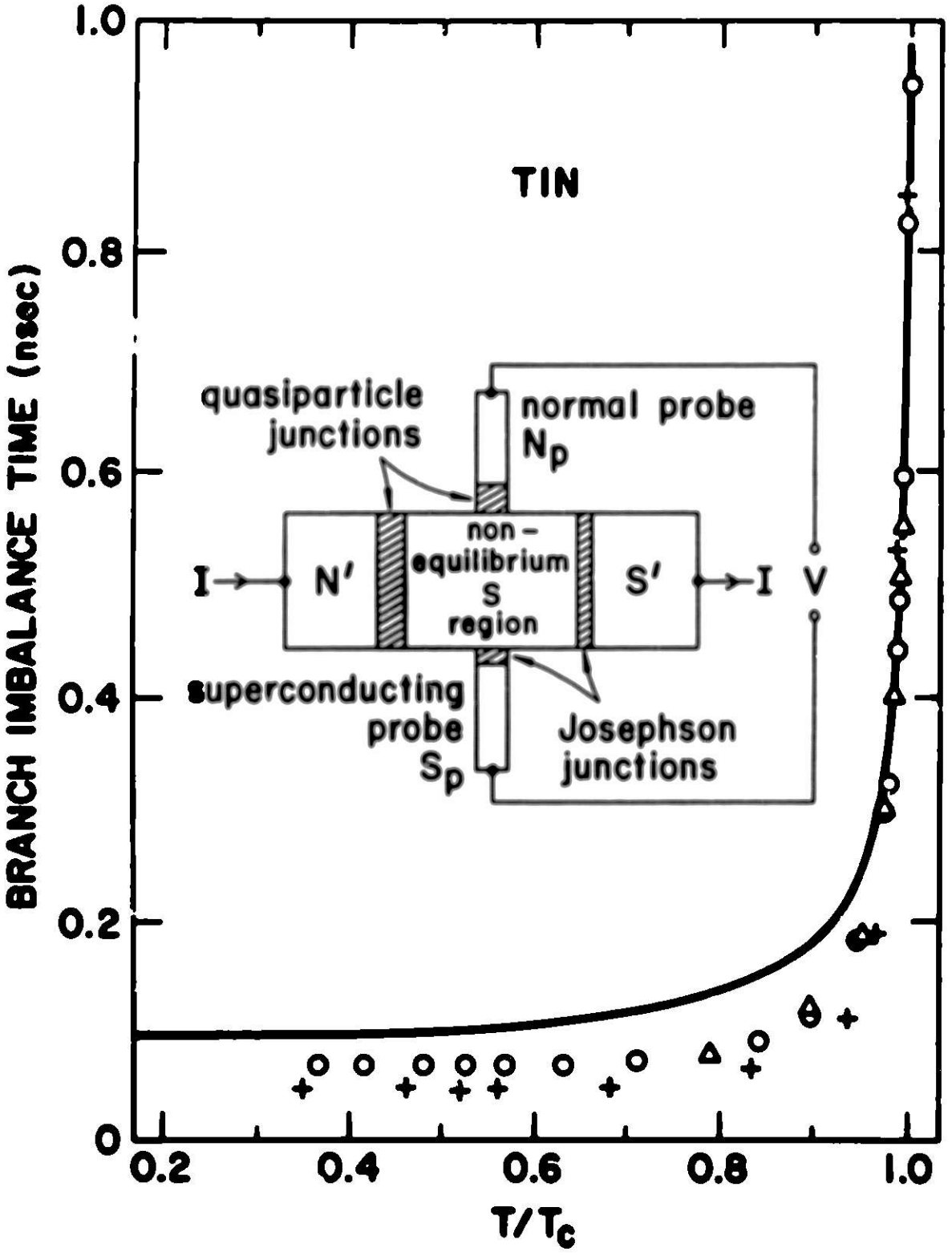
TIN
BRANCH IMBALANCE TIME (nsec)
1.0
0.8
0.6
0.4
0.2
0
0.2
0.4
0.6
0.8
1.0
T/Tc
quasiparticle junctions
normal probe Np
non-equilibrium S region
I
N'
S'
I V
superconducting probe Sp
Josephson junctions

Fig. III-4: Limiting flux passage time in a SQUID vs $\Delta_{eq}(0)/\Delta_{eq}(T)$ measured by Rachford et al. (RWH75).

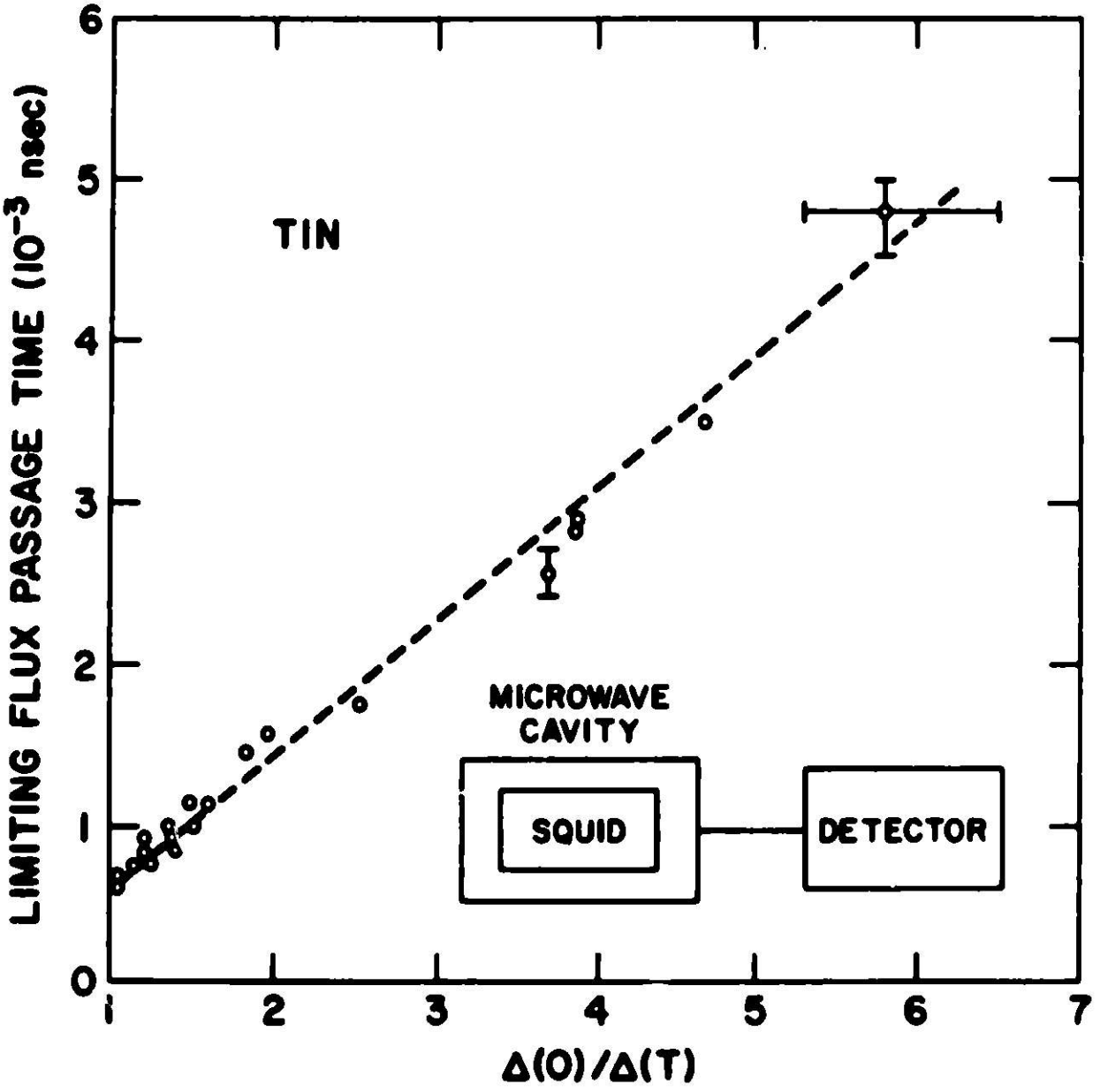
LIMITING FLUX PASSAGE TIME (10^{-3} nsec)
TIN
MICROWAVE CAVITY
SQUID
DETECTOR
Δ(0)/Δ(T)
0
1
2
3
4
5
6
7

be only a measurement of the temperature variation of the resistance of the weak link in the SQUID.

For a superconductor above the transition temperature it is expected that the superconducting fluctuations will relax with a characteristic time that diverges as $1/\Delta^2$ in approaching T_c (see Chapter V). This was studied experimentally (Ca75) by measuring the excess current in a tunnel junction in which one of the electrodes was well below the transition temperature and the other just above its transition temperature (Fig. III-5). It was found that the relaxation time is in good agreement with the theoretical prediction described in Chapter V based on the Ginzburg-Landau theory.

In studying the response time of a superconductor to an AC current, Peters and Meissner (PM73) derived from measurements a relaxation time for the Cooper pair density which diverges as $(T_c - T)^{-1/2}$ as predicted (Sch69). This measurement is not conclusive since the experimental data shows only an increase of about a factor of 2 and a substantial scatter. In Chapter V a measurement of the relaxation time of the superconducting order parameter will be described. For the sake of completeness we will just state that the results are consistent with recent theoretical predictions (SS75) which conclude that the relaxation time of the order parameter diverges as $1/\Delta_{eq}$.

In conclusion, at low temperatures the recombination lifetimes in type-I superconductors, the branch mixing time and the relaxation time of the magnitude of the order parameter, are well established theoretically as well as experimentally. The relaxation of the quasiparticle density and

Fig. III-5: Ginzburg-Landau relaxation time vs reduced temperature as measured by Carlson (Ca75). The solid line is the theoretical prediction described in Chapter V.

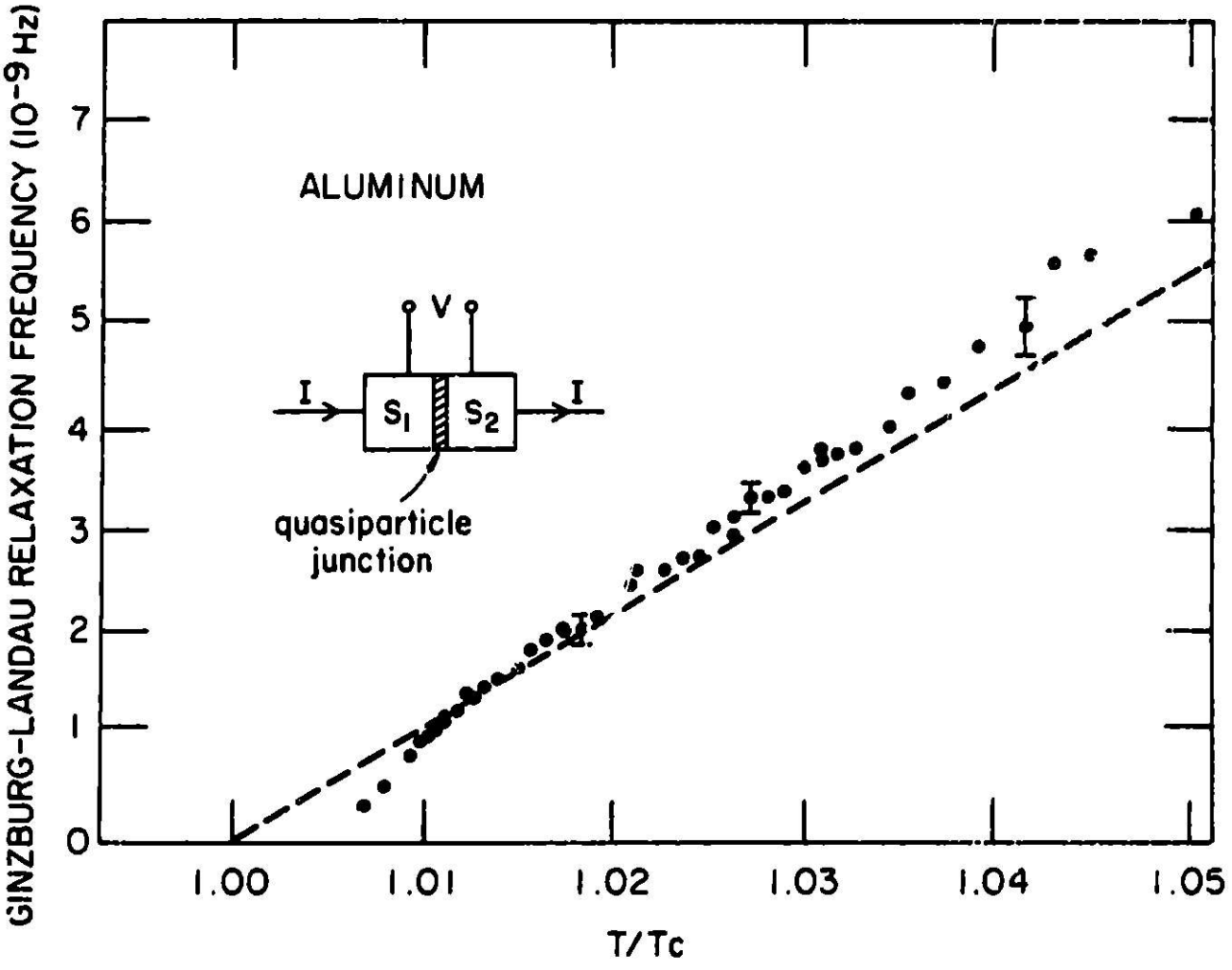
GINZBURG-LANDAU RELAXATION FREQUENCY (10⁻⁹ Hz)
ALUMINUM
V
I
S1
S2
I
quasiparticle
junction
0
1
2
3
4
5
6
7
1.00
1.01
1.02
1.03
1.04
1.05
T/Tc

the condensate is only determined (in the whole superconducting temperature range) for aluminum.

Experimental work is still needed to measure the recombination lifetimes in type II superconductors and to clarify the behavior the thermalization times at all temperatures. A table of the experimentally measured relaxation times are shown in Table III-1. Because of the different values for density of states, film thicknesses, etc., that are used in their determination, these lifetimes must be corrected for a detailed comparison (see Chapter IV).

III.3. Photoexcitation: Experiments and Theory

Several methods (transport current, AC currents, tunnel injection, photoexcitation, etc.) have been used in order to create a nonequilibrium situation in a superconductor. From the experimental point of view, illumination with a laser (photoexcitation) is a very convenient way of inducing a nonequilibrium situation in a superconductor, since light produces no additional electronic noise in the measuring apparatus.

The first photoexcitation experiments were those of Testardi (Te71) in which the DC resistance of a lead film under laser illumination was studied. From these experiments it was concluded that the superconductivity can be destroyed by light, and that simple lattice-heating ("thermal effects") cannot account for this. They also conclude that this is a phenomenon involving the electrons.

Owen and Scalapino (0872) developed a model of a superconductor considering an electron gas containing Cooper pairs and unpaired excited quasiparticles. In their model, the ratio of paired to unpaired

Table 1. Experimental values of relaxation times.

Name	Symbol	Value	Material and Temperature	Comments	Reference
Auger	τ_{auger}	$\sim 10^{-13} - 10^{-14}$		Estimated	(La74)
Thermalization	τ_T	1.11×10^{-7}			
		$\times \exp(-3.34\frac{E-\Delta}{\Delta})$	Al(0.37°K)		(MD67)
		10^{-9}/100 Å	Sn	Films	(Sa74)
	τ_{T*}	5.5×10^{-10}	Sn($T_f^* = T_c$)	T_f^* = final temperature Estimated	(Th72)
Recombination Lifetime	τ_R	$6 \times 10^{-8} T^{-1/2} e^{\Delta/kT}$	Al	Extrapolated to 0 film thickness, tunneling	(Gr71)
		$7 \times 10^{-9} T^{-1/2} e^{\Delta/kT}$	Al	Injection at V = 4Δ	(SM75)
Effective Lifetime	τ_{eff}	$4 \times 10^{-9} T^{-1/2} e^{\Delta/kT}$	Sn	He/3500 Å Sn/sapphire	(Pa74)
		$9 \times 10^{-10} T^{-1/2} e^{\Delta/kT}$	Sn	He/3200 Å Sn/glass	(HDN74)
		$6 \times 10^{-10} T^{-1/2} e^{\Delta/kT}$	Sn	He/4000 Å Sn/sapphire	(ED67)
		2.5×10^{-7}	Sn (1°K)	He/3000 Å Sn/sapphire	(Da72)
		$1 \times 10^{-9} T^{-1/2} e^{\Delta/kT}$	Sn	He/400 Å Sn/quartz	(La75)
		$1.9 \times 10^{-9} T^{-1/2} e^{\Delta/kT}$	Sn	He/750 Å Sn/quartz	(La75)
		$2.5 \times 10^{-9} T^{-1/2} e^{\Delta/kT}$	Sn	He/900 Å Sn/quartz	(La75)

Table I. (cont.)

Name	Symbol	Value	Material and Temperature	Comments	Reference
		$8 \times 10^{-12} T^{-1/2} e^{\Delta/kT}$	Pb	He/1000-2000 Å Sn/sapphire or glass	(PW72)
Branch imbalance	τ_Q	$(1 \pm 0.2) \times 10^{-10}$ $\Delta(0)/\Delta(T)$	Sn	Close to T_c	(CP74)
		3×10^{-10} $\Delta(0)/\Delta(T)$	Sn dirty	$T/T_c \gtrsim 0.7$	(CP74)
		0.65×10^{-10}	Ta (0°K)		(Yu74)
Minimum flux passage	$\tau_f(0)$	$(0.6 \pm 0.1) \times 10^{-12}$	Pb-40%-Th		(RWNH75)
	τ_f	$(0.7 \pm 0.1) \times 10^{-12}$ $\Delta(0)/\Delta(T)$	Sn		(RWNH75)
Ginzburg-Landau	τ_{GL}	$\frac{\hbar\pi}{8k} \frac{1}{T - T_c}$	Al	Above T_c	(ACG72)
Order-Parameter Relaxation	τ_Δ	1.4×10^{-10} $\Delta(0)/\Delta(T)$	Sn($0.95 \leq T/T_c \leq 0.995$)		(PM73)
		1.5×10^{-8} $\Delta(0)/\Delta(T)$	Al($0.99 \leq T/T_c \leq 1.0$)		(SG76)

electrons is artificially specified instead of being uniquely determined by the temperature. The electron gas is assumed to be in thermal equilibrium with the lattice, but the Cooper pairs and the quasiparticles are not in chemical equilibrium. Their calculation is similar to BCS with an additional constraint on the total quasiparticle excitation number. The effect of this additional constraint is to introduce a new chemical potential μ^* in the quasiparticle distribution function so that the distribution function is $f(E) = (1 + \exp\beta(E - \mu^*))^{-1}$ where $\beta = 1/kT$. In the low temperature limit they find two algebraic equations

$$\left(\frac{\Delta}{\Delta_o}\right)^3 = \left\{\left[\left(\frac{\Delta}{\Delta_o}\right)^2 + n^2\right]^{1/2} - n\right\}^2 \qquad \text{(III-1)}$$

$$n = \left(\frac{\mu^{*2}}{\Delta_o^2} - \frac{\Delta^2}{\Delta_o^2}\right)^{1/2} \qquad \text{(III-2)}$$

where Δ_o is the zero temperature equilibrium energy gap, Δ is the value of the energy gap in the nonequilibrium situation and $4N_0\Delta_0\, n$ is the excess number of quasiparticles per unit volume due to light illumination (N_0 is the density of states at the Fermi surface). A graph of Δ versus n in the (OS72) model is shown in Fig. III-6. In this model the superconducting state is energetically unfavorable at some critical value for n and the superconductor becomes normal (indicated by the dashed line in Fig. III-6).

Elesin (El73) pointed out that in the case of large excess quasiparticle number it is incorrect to assume that the distribution function of the nonequilibrium quasiparticles is described by a Fermi function. Based on the Gor'kov-Eliashberg formulation (GE68), (El73) showed that at zero temperature the dependence of Δ on n is given by

Fig. III-6: Normalized energy gap vs the excess quasiparticle number n as calculated from the Owen and Scalapino (OS72) theory, for a particular value of temperature. The dashed line indicates the region in which the superconducting state is energetically unfavorable.

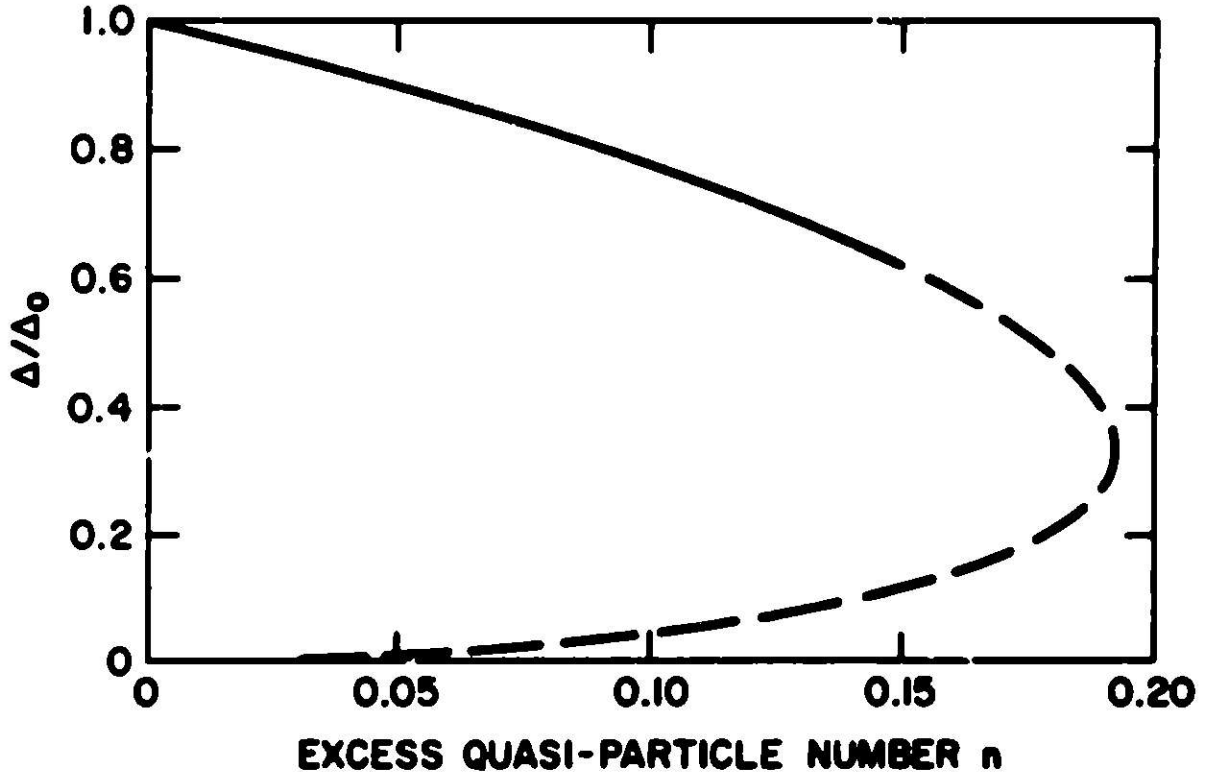
1.0
0.8
0.6
0.4
0.2
0
Δ/Δ₀
0
0.05
0.10
0.15
0.20
EXCESS QUASI-PARTICLE NUMBER n

$$\Delta = \Delta_o(1 - 2n)(1 + \ln \frac{4\Delta_o}{\Delta})^{-1} \qquad \text{(III-3)}$$

and that the distribution function does not show "population inversion" ($f(E) > 1/2$). A plot of Δ versus n is shown in Fig. III-7. It can be seen that for large values of n the energy gap is multivalued and consequently the system will probably be unstable. (This was not pointed out by Ek74).

An alternate theory was proposed by Parker (Pa75) in which the quasiparticles are in thermal and chemical equilibrium at an effective temperature T^* greater than the helium bath temperature.

The dependence of the gap Δ on n, for small n, is the same for all three models and is

$$\Delta/\Delta_o \cong 1 - 2n \qquad \text{(III-4)}$$

Various experiments relating to these theories will now be described. In two experiments (PW72, Pa74) the effective lifetime of quasiparticles were determined in lead and in tin with the use of the (OS72) theory. The dependence of μ^* on n was also determined from one of the experiments (PW72) although the role of the phonons was completely neglected, as will be described in Chapter IV. These experiments were performed by biasing a tunnel junction on the rapidly rising portion of the I-V characteristic. The change in the energy gap and hence the change in gap density due to illumination was measured as a function of temperature.

In a different experiment Hu et al. (HEW74) biased a tunnel junction at voltages less than the energy gap and hence measured the nonequilibrium quasiparticle density directly, during and after illumination by a fast risetime pulse of light. The quasiparticle lifetime measured in this

Fig. III-7: Normalized energy gap versus excess quasiparticle number n at high illuminations from the theory of Elesin (E73). Notice that the energy gap is multi-valued for large values of n indicating that the system will probably be unstable.

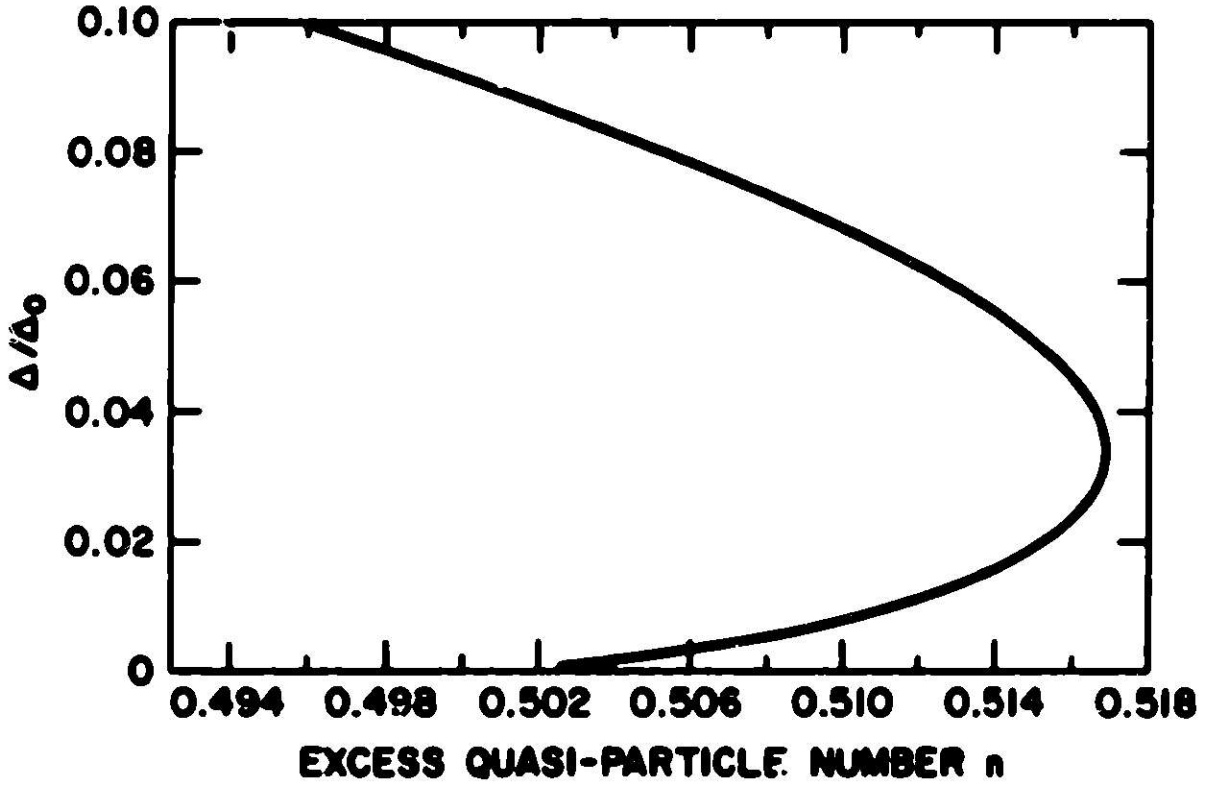
0.10
0.08
0.06
0.04
0.02
0
Δ / Δ0
0.494
0.498
0.502
0.506
0.510
0.514
0.518
EXCESS QUASI-PARTICLE NUMBER n

experiment is in agreement with the theoretical prediction, but for large values of n the first order phase transition predicted by (OS72) was not observed.

In studying the microwave reflectivity of thin films, Sai-Halasz et al. (Sa74) found agreement with the (OS72) theory at low temperatures and low values of n but failed to observe the phase transition predicted in the (OS72) model for "large" values of n.

In summary, at low light intensities the existing theories agree on the dependence of Δ on n, and this is consistent with the experimental results. At high light intensities the models of (OS72) and (El73) do not agree with the experimental results that fail to show a superconducting to normal phase transition.

IV. Acoustic Coupling of Thin Superconducting Films

IV.1. Introduction

In recent years there has been extensive work on nonequilibrium superconducting films to measure quasiparticle lifetimes (MD67, LH68, GLA69, LH71, PW72, HDM74) and to check theoretical calculations (OS72) about the nonequilibrium state. The nonequilibrium state was obtained by increasing the number of quasiparticles above the thermal equilibrium value and in most cases the role of the extra phonons was neglected. Although the importance of the phonons was recognized by Rothwarf and Taylor (RT67), only a few attempts (Gr71, Lo73) were made to account for these because of the difficulty of measuring and adequately estimating their effect.

In order to determine the role of the phonons in photoexcitation experiments, the data of (PW72) can be reanalyzed. As was described in Chapter III, using a tunnel junction, (PW72) measured the change in the energy gap of a superconductor due to laser illumination. From this they determined the variation of μ^*, the chemical potential introduced by (OS72) to characterize a nonequilibrium superconductor, with n, the excess quasiparticle number -- thermalized at the lattice temperature. (Gr73) reinterpreted the photoexcitation results of (PW72) by assuming that both films in their tin-tin tunnel junction are equally affected by the perturbation introduced by the light. If both films are equally affected, the true change in the energy gap is one half of their measurement and consequently n, the excess quasiparticle number, is one half of their quoted value, since

$$\frac{\Delta(n)}{\Delta(0)} = 1 - 2n \quad . \tag{IV-1}$$

In addition, the tunneling current due to the light perturbation is given by

$$\frac{I(n)}{I(0)} = 1 + \exp(\beta(\mu^*(n) + \Delta(0) - \Delta(n))) \tag{IV-2}$$

where I(n) is the tunneling current of the illuminated junction, I(0) is the current of the unilluminated junction, $\Delta(0)$ is the thermal equilibrium energy gap, $\Delta(n)$ is the energy gap of the illuminated superconductor and μ^* is the chemical potential.

The values of I(n)/I(0) from the experiment of (PW72) can be calculated from their data for $\mu^*(n)/kT_c$ versus n. $\mu^*(n)$ can then be recalculated from these experimental values for I(n)/I(0), assuming that both films are equally affected by the perturbation. These results are shown in Fig. IV-1 along with the original data of (PW72) and the comparison to the (OS72) theory. It can be seen that these recalculated results fit the (OS72) theory as well as the original data. Therefore (Gr73) concluded that photoexcitation experiments on tunnel junctions of similar metals are not very sensitive to the behavior of the phonons. Phonons are expected to readily pass the thin tunnel barrier (~ 10 Å thick), but this experiment leaves open the question of the perturbation in the second film.

On the other hand, if a tunnel junction is made of dissimilar metals it is possible to separate the contribution of the two films by their different temperature dependences. In this chapter we will describe an experiment similar to that of (PW72) but using tunnel junction of dis-

Fig. IV-1: Chemical potential versus excess quasiparticle number from the theory of Owen and Scalapino, the experiments of Parker and Williams, and the experiments of Parker and Williams reinterpreted as described in the text.

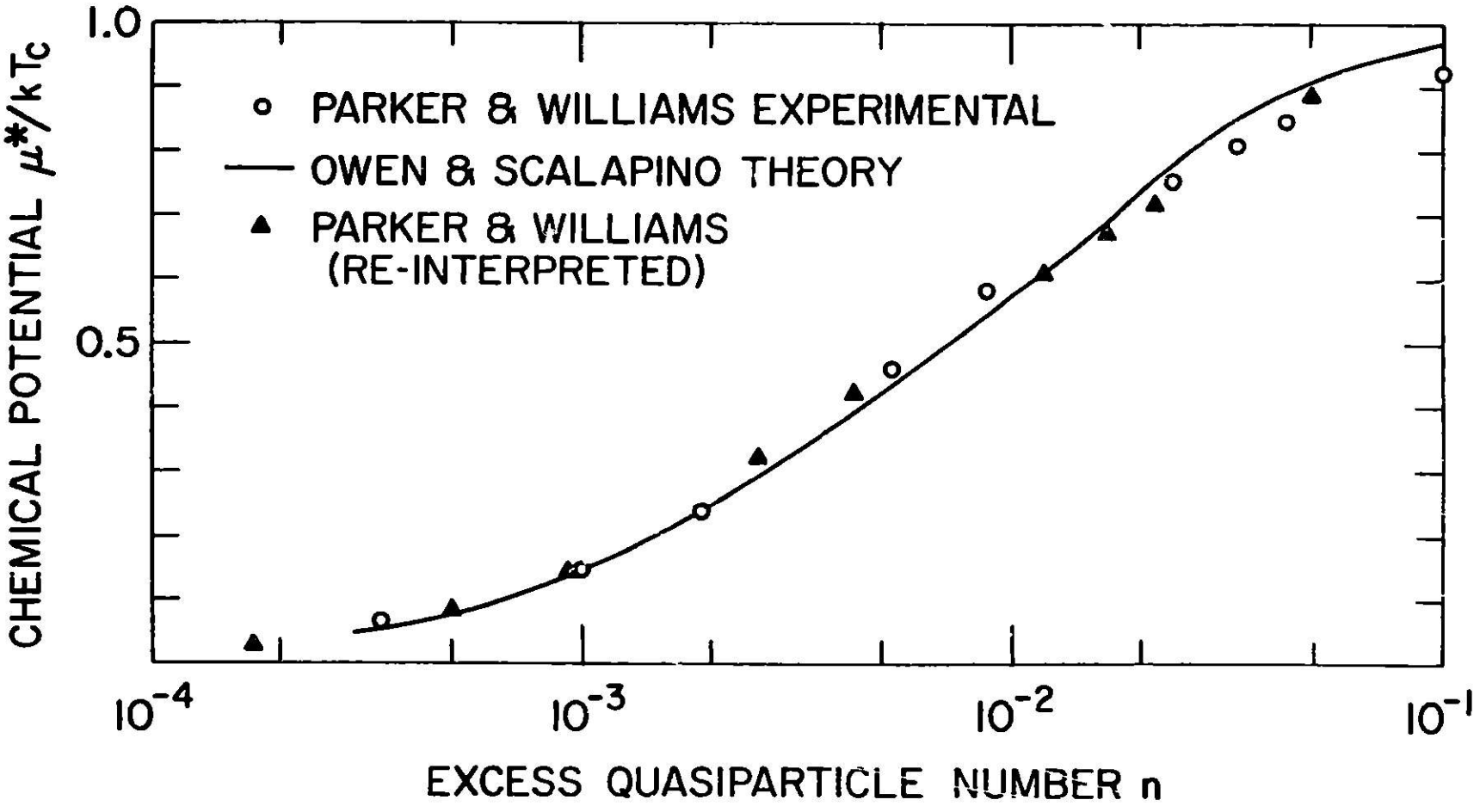
1.0
0.5
CHEMICAL POTENTIAL μ^*/kT_c
PARKER & WILLIAMS EXPERIMENTAL
OWEN & SCALAPINO THEORY
PARKER & WILLIAMS
(RE-INTERPRETED)
10^{-4}
10^{-3}
10^{-2}
10^{-1}
EXCESS QUASIPARTICLE NUMBER n

similar metals. We are able to separate the effects of the phonons from those of the directly-injected quasiparticles; the technique for separating these two contributions from the experimental data will be described later. From this experiment we can obtain the coupling of the films by phonons.

In Section 2 of this chapter we will discuss the theory for the acoustic coupling of solids. In Section 3 the theory for the excess number of quasiparticles will be described together with its relationship to ϵ, a coupling parameter between the films that will be defined. The interpretation of this coupling parameter in terms of phonon escape parameters will also be described in this section. Section 4 is devoted to a description of the experimental setup, and in Section 5 we describe the experimental procedure. In Section 6 we evaluate the temperature dependence for each film for various values of the coupling parameter ϵ and determine ϵ by choosing the best fit to the theory.

The results show that the phonon escape parameter from lead into tin agrees with calculated values. In addition to this the results are consistent with the assumption that the acoustic coupling of lead to helium is much higher than the coupling of lead to tin.

IV.2. Theory for Acoustic Coupling of Solids

The most successful theory for the transport of heat between solids at low temperature was advanced by Little (Li59). Corrections to this theory to account for the phonon attenuation in solids were made by Paterson and Anderson (PA72).

Following Little we consider two semi-infinite isotropic solids in contact in the plane zy at x = 0. In order to simplify the problem we consider only longitudinal phonons; transverse phonons can be accounted for by a simple generalization of the equations.

The heat flow across the interface from medium 1 to medium 2 is given by:

$$\frac{dQ}{dt} = \int N_1(\nu,\theta_1)\alpha_1(\theta_1)d\theta_1 d\nu dA - \int N_2(\nu,\theta_2)\alpha_2(\theta_2)d\theta_2 d\nu dA \qquad \text{(IV-3)}$$

where $N_i(\nu,\theta_i)$ is the number of phonons of frequency ν incident on the interface at an angle θ_i per unit area and unit time and $\alpha_i(\theta_i)$ is the transmission coefficient of the interface for phonons incident at an angle θ_i in the medium i (i = 1,2). It was shown by Rayleigh (Ra45) that for acoustical waves this coefficient is

$$\alpha_1(\theta_1) = \alpha_2(\theta_2) = \frac{\frac{4\rho_2 c_2}{\rho_1 c_1}\frac{\cos\theta_2}{\cos\theta_1}}{(\frac{\rho_2 c_2}{\rho_1 c_1} + \frac{\cos\theta_2}{\cos\theta_1})^2} \qquad \text{(IV-4)}$$

and it should be the same for longitudinal phonons. On the other hand

$$N_1(\nu,\theta_1) = \frac{1}{2} c_1 N_1(\nu)\cos\theta_1 \sin\theta_1 \qquad \text{(IV-5)}$$

where c_i is the group velocity of the longitudinal phonons and $N_i(\nu)d\nu$ is the number of phonons of energy between $h\nu$ and $h(\nu + d\nu)$ per unit volume. Since phonons obey the Bose-Einstein statistic, we have

$$N_i(\nu)d\nu = \frac{4\pi}{c_i^3}\frac{\nu^2 d\nu}{e^{h\nu/kT} - 1} \qquad \text{(IV-5)}$$

Inserting all this into the equation for dQ/dt and integrating over the area, we obtain

$$\frac{dQ}{dt} = \frac{2\pi k^4 \Gamma A}{h^3 c_1^3} [T_1^4 f(T_1) - T_2^4 f(T_2)] \frac{ergs}{sec} \qquad (IV-7)$$

where

$$f(T) = \int_0^{h\nu_m/kT} \frac{z^3 dz}{e^z - 1}$$

$$z = h\nu/kT \qquad (IV-8)$$

and

$$\Gamma = \int_0^{\pi/2} \alpha_1(\theta_1) \sin\theta_1 \cos\theta_1 d\theta_1 \qquad (IV-9)$$

At low temperatures ($T << \theta_{Debye}$), one can make the usual approximation $h\nu_m/kT = \infty$, and by performing the integral IV.8, one obtains

$$\frac{dQ}{dt} = \frac{2\pi k^4 \Gamma A}{h^3 c_1^2} \frac{\pi^4}{15} (T_1^4 - T_2^4)$$

$$= 5.01 \times 10^{16} \frac{\Gamma A}{c_1^2} (T_1^4 - T_2^4) \text{ ergs/sec} \qquad (IV-10)$$

with c_1 in cm/sec and T in °K.

This may be generalized to the contribution from the transverse phonons to obtain (Li59)

$$\frac{dQ}{dt} = 5.01 \times 10^{16} A[\frac{\Gamma_l}{c_l^2} + \frac{2\Gamma_t}{c_t^2}](T_1^4 - T_2^4) \text{ ergs/sec cm}^2 \qquad (IV-11)$$

with

Γ_ℓ = transmission coefficient of longitudinal phonons and Γ_t = transmission coefficient of transverse phonons.

When both types of waves (longitudinal and transverse) are present, the evaluation of the Γ's is not straightforward since each incident wave breaks into four waves, reflected transverse and longitudinal and refracted transverse and longitudinal. Since the velocities of the waves differ from each other there are two critical angles present. A phase shift occurs for these two angles between the reflected and refracted waves which depends on the angle of incidence. Little's numerical calculation for the contours of Γ are shown in Fig. IV-2.

In Little's theory it is required that as many phonons scatter into a solid angle $d\Omega$ and energy interval dE as scatter out. This has to be modified in order to take into account the fact that we have a uniform isotropic source of phonons throughout the film. (GLA69) introduced a quantity f, which is the fraction of phonons escaping the film. If the phonon mean free path Λ is much smaller than the thickness of the film d, the only phonons that will reach the interface will be those that are at a distance Λ from the interface. With this

$$f = \frac{\alpha\Lambda}{4d} \quad \text{for } \Lambda \ll d \qquad \text{(IV-12)}$$

where $\alpha = 2\Gamma$ is the average phonon-transmission coefficient at the boundary and can be obtained directly from Little's theory. A detailed calculation of f for arbitrary ratio d/Λ was done by Gray (Gr71) by assuming specular reflection at both surfaces of the film and by taking into account that phonons are damped due to pair breaking.

His results indicate that

Fig. IV-2. Transmission coefficients contours for longitudinal and transverse phonons, as a function of the ratio of sound velocities and of the ratio of densities of two media for Poisson's ratio of 0.33, as calculated by Little.

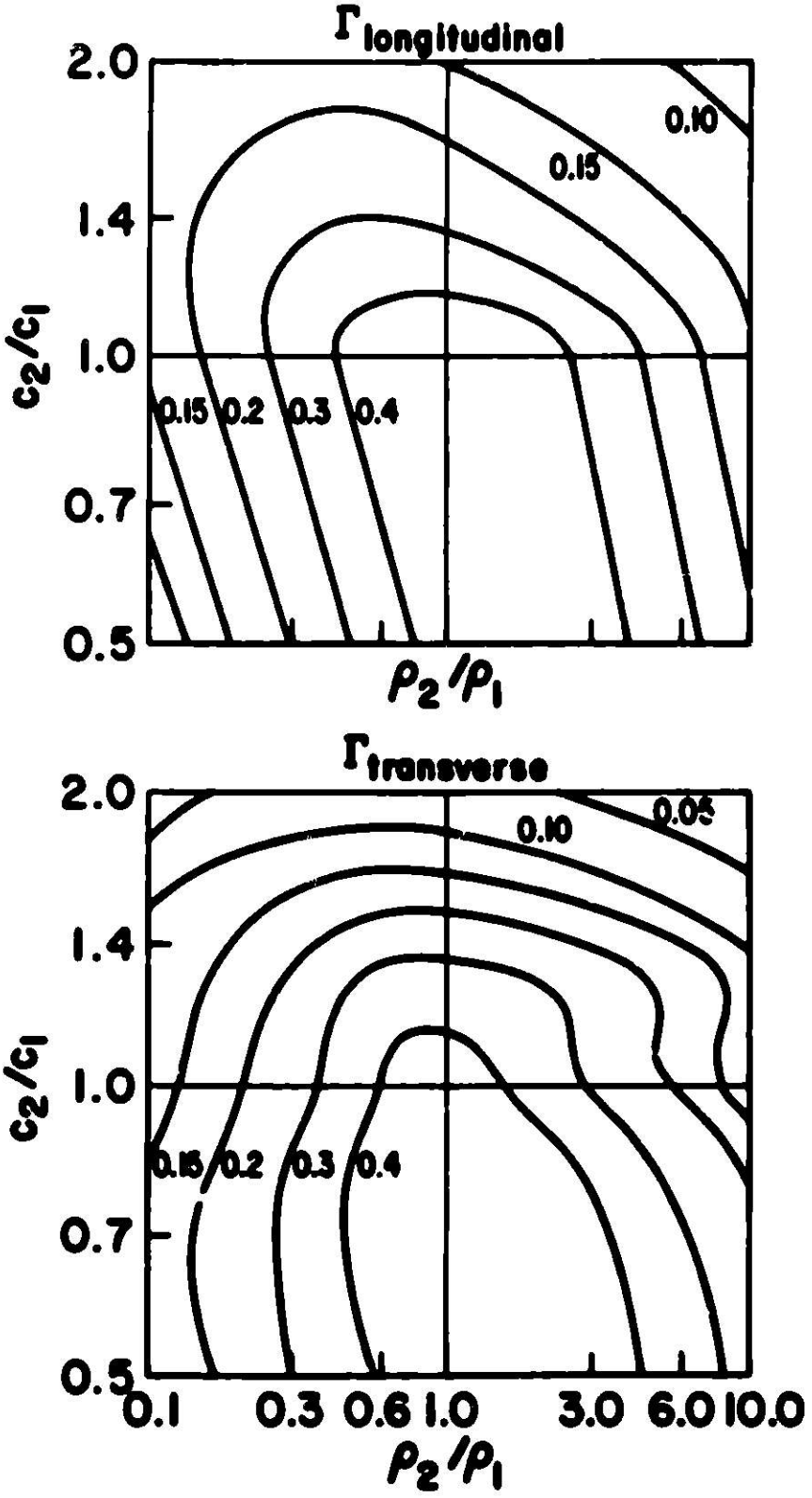
Γ longitudinal
2.0
1.4
1.0
0.7
0.5
c2/c1
0.10
0.15
0.15 0.2 0.3 0.4
ρ2/ρ1
Γ transverse
2.0
1.4
1.0
0.7
0.5
c2/c1
0.10
0.05
0.15 0.2 0.3 0.4
0.1 0.3 0.6 1.0 3.0 6.0 10.0
ρ2/ρ1

$$f = \frac{\alpha\Delta}{4d}\left(1 - \alpha \sum_{n=0}^{\infty} (1-\alpha)^n \Xi\left((n+1)\frac{2d}{\Lambda}\right)\right) \qquad \text{(IV-13)}$$

where

$$\Xi(\xi) = (1-\xi)e^{-\xi} - \xi^2 E_1(-\xi)$$

with

$$E_1(-\xi) = \int_{-\infty}^{\xi} \frac{e^{-v}}{v}\, dv \quad .$$

IV.3. Theory for the Excess Number of Quasiparticles

The equations that describe the nonequilibrium quasiparticle and phonon densities in a superconducting film (RT67) are

$$\frac{\partial N}{\partial t} = I_0 + \beta N_\omega - RN^2 \qquad \text{(IV-14)}$$

$$\frac{\partial N_\omega}{\partial t} = K_0 + \frac{RN^2}{2} - \frac{\beta}{2} N_\omega - \gamma(N_\omega - N_\omega(T)) \qquad \text{(IV-15)}$$

where N is the total number of quasiparticles, R is the recombination coefficient, N_ω is the total number of phonons with energy $\hbar\omega \geq 2\Delta$, $N_\omega(T)$ is the value in thermal equilibrium, β is the probability for pair breaking by such phonons, γ is the probability for phonons to be lost out of the energy range $\hbar\omega \geq 2\Delta$ by processes other than pair breaking, I_0 is the number of quasiparticles injected per cm^3 per sec and K_0, a term introduced by us, is the number of phonons injected per cm^3 per sec.

In thermal equilibrium there is a dynamic equilibrium between pairs and quasiparticles, i.e., $\beta N_\omega(T) = RN(T)^2$ where $N(T)$ is the thermal equilibrium quasiparticle density. Using this relation the steady state

solution of Eqs. (IV-14) and (IV-15) is given by

$$S \quad \Delta N^2 + 2N(T)\Delta N = \frac{I_0}{R}\left(1 + \frac{\beta}{2\gamma}\right) + K_0 \frac{P}{\gamma R} \qquad \text{(IV-16)}$$

where $\Delta N = N - N(T)$. Equation (IV-16) is valid in both superconductors of a tunnel junction. However, if we illuminate only one film of the junction the nonilluminated film will have no direct injection of quasiparticles since the films are opaque so that Eq. (IV-16) becomes

$$S' \equiv \Delta N'^2 + 2N'(T)\Delta N' = K_0' \frac{\beta'}{\gamma' R'} \quad . \qquad \text{(IV-17)}$$

where primed quantities refer to the nonilluminated film. In each equation the term on the right is the "source" perturbing the quasiparticle population. When it is zero, ΔN is zero.

The relative effect of the illumination on the nonilluminated film is determined by the ratio c of the perturbing sources; i.e.,

$$c = \frac{S'}{S} = \frac{K_0'\beta'}{\gamma' R'} \Big/ \left[\frac{I_0}{R}\left(1 + \frac{\beta}{2\gamma}\right) + K_0 \frac{\beta}{\gamma R}\right] \qquad \text{(IV-18)}$$

and this c is the phonon coupling parameter that we determine experimentally.

Equations (IV-16) and (IV-17) are additionally coupled through the experimentally measured change in the energy gap ($\delta\Delta_{exp}$) due to illumination. In the theory of (OS72) and the theory of (Pa75) for small values of $\delta\Delta/\Delta_0$, we have in each film $\delta\Delta = -\Delta N/2N_0$, where N_0 is the single spin, phonon enhanced, density of states at the Fermi energy in the normal metal and Δ_0 is the energy gap at zero temperature. We measure $\delta\Delta_{exp} = \delta\Delta + \delta\Delta'$.

We use the very convenient simplification

$$n(T) = \frac{N(T)}{N_0}, \quad n'(T) = \frac{N'(T)}{N_0'}, \quad c' = c\left(\frac{N_0}{N_0'}\right)^2 \tag{IV-19}$$

Using Eqs. (IV-16)-(IV-19) we obtain

$$\Delta N_{exp} = \frac{N_0}{1 - c'}\left[2\delta\Delta_{exp} + n'(T) + c'n(T)\right]$$

$$- \sqrt{\left[\frac{2\delta\Delta_{exp} + n'(T) + c'n(T)}{1 - c'}\right]^2 - \frac{4\delta\Delta_{exp}(\delta\Delta_{exp} + n'(T))}{1 - c'}} \tag{IV-20}$$

$$\Delta N'_{exp} = \frac{-N_0'c'}{1 - c'}\left[2\delta\Delta_{exp} + n(T) + \frac{1}{c'}n'(T)\right]$$

$$+ \sqrt{\left[\frac{c'(2\delta\Delta_{exp} + n(T) + \frac{1}{c'}n'(T))}{1 - c'}\right]^2 + \frac{4c'\delta\Delta_{exp}(\delta\Delta_{exp} + n(T))}{1 - c'}}$$

(IV-21)

where the signs were chosen to give positive values for ΔN_{exp} and $\Delta N'_{exp}$.

To determine N(T) we note that the BCS density of quasiparticle states is given by

$$\mathcal{D}(E)dE = 2N_0 \frac{EdE}{(E^2 - \Delta^2)^{1/2}}$$

where N_0 is the single spin, phonon enhanced density of states at the Fermi surface and E is measured with respect to the Fermi energy. Since the quasiparticles (quasielectrons and quasiholes) obey the Fermi-Dirac statistic, we have

$$N(T) = 4N_0 \int_{\Delta}^{\infty} \frac{E}{(E^2 - \Delta^2)^{1/2}} (1 + e^{E/kT})^{-1} \, dE$$

so that at low temperatures

$$N(T) \simeq 4N_0\Delta_V \sqrt{\frac{\pi}{2}} \left(\frac{kT}{\Delta}\right)^{1/2} e^{-\Delta/kT}\left(1 + \frac{3}{8}\frac{kT}{\Delta} + \ldots\right) \qquad \text{(IV-22)}$$

Using this expression for N(T) and the experimentally determined $\delta\Delta_{exp}$, we can evaluate ΔN_{exp} and $\Delta N'_{exp}$ for a given value of the parameter ϵ.

ϵ can then be related to phonon processes in the films in the following way. Assuming that the phonons can escape the lead by various mechanism, we write

$$\gamma = \gamma_{PbSn} + \gamma_{PbHe} + \gamma_{Pb^*} \qquad \text{(IV-23)}$$

where γ_{PbSn} relates to phonons lost into the tin, γ_{PbHe} into helium and γ_{Pb^*} to any inelastic processes in the lead film other than pair breaking. (Note that if the phonon energy is degraded below 2Δ it is effectively lost (ED67, MD71), since it cannot break pairs.) The rate of phonons going from the lead film to the tin is $\gamma_{PbSn}\Delta N_{\omega}$ (from Eq. (IV-15)), and this is the only perturbation in the tin film, giving the term K'_0 in Eq. (IV-17). The steady state solution of Eqs. (IV-14) and (IV-15) in the lead (if we neglect K_0) is

$$\gamma\Delta N_{\omega} = \frac{I_0}{2} \qquad \text{(IV-24)}$$

so we write $K'_0 = 2\left(\frac{\gamma_{PbSn}}{\gamma}\right)\frac{I_0}{2}$. The extra factor of two accounts, roughly, for the fact that $2\Delta_{Pb} \sim 2(2\Delta_{Sn})$ and two tin pairs may be broken by each $2\Delta_{Pb}$ phonon. Substituting this in Eq. (IV-18) and neglecting K_0,

$$c = \frac{\beta' R}{\beta R'} \frac{\gamma_{PbSn}}{\gamma'} \frac{\beta}{\gamma} \frac{1}{(1 + \frac{\beta}{2\gamma})} \qquad \text{(IV-25)}$$

In order to simplify this expression it is necessary to examine the lifetime experiments in lead (PW72, JPK76) and tin (HDN74). These experiments measure an effective lifetime which is related to the quasiparticle lifetime by $\tau_{eff} = \tau(1 + \beta/2\gamma)$ so that we can write for the experimental recombination coefficient R_{exp}

$$\frac{\beta}{1 + \frac{\beta}{2\gamma}} = (\frac{\beta}{R})R_{exp} \qquad \text{(IV-26)}$$

On the other hand, in thermal equilibrium $\beta N_{\omega}(T) = RN(T)^2$. $N_{\omega\lambda}(T)$ can be calculated by using the Debye spectrum and the fact that phonons obey the Bose-Einstein statistic

$$\mathcal{D}_{\lambda}(\omega)d\omega = 4\pi \frac{V}{N} \frac{1}{(2\pi S_{\lambda})^3} \omega^2 d\omega$$

and

$$N_{\omega\lambda}(T) = \frac{N}{V} \int_{\omega_0}^{\omega_D} \mathcal{D}_{\lambda}(\omega)(e^{\hbar\omega/kT} - 1)^{-1} d\omega$$

with $\hbar\omega_0 = 2\Delta$. Solving the integral we obtain

$$N_{\omega\lambda}(T) = 4\pi(\frac{kT}{hS_{\lambda}})^3 \sum_{n=1}^{\infty} \frac{1}{n}[(\frac{2\Delta}{kT})^2 + \frac{2}{n^2}(\frac{2\Delta}{kT} + 1)]e^{-2n\Delta/kT} \quad .$$

At low temperatures only the term n = 1 is important. Using the expressions for N(T) and $N_{\omega\lambda}(T)$, β/R can be determined independently from the detailed recombination processes involved. Using this and Eq. (IV-26), we see that the lifetime experiments are a measurement of $\beta/(1 + \beta/2\gamma)$. The measurements

done in aluminum indicates that (Gr71) $0.2 \leq \beta/2\gamma \leq 1.0$ or (SM75, Sm75) $7.6 \leq \beta/2\gamma \leq 8.7$. We can expect this to be the case in tin and lead since they are stronger coupling superconductors and the phonon mean free path is much shorter. We solve the simpler case $\beta/2\gamma \gg 1$ and $\beta'/2\gamma' \gg 1$, since if $\beta/2\gamma \sim 1$ or $\beta'/2\gamma' \sim 1$ our results will still be in error only by a factor of ~ 2 but the conclusions will still be valid. With this, Eq. (IV-25) becomes

$$c = 2\,\frac{\beta' R}{\beta R'}\,\frac{\gamma_{PbSn}}{\gamma'} \tag{IV-27}$$

To determine c we note that for each film we can write, using Eqs. (IV-14) and (IV-15),

$$\Delta N = -N(T) + \sqrt{N^2(T) + \frac{I_0}{R}\left(1 + \frac{\beta}{2\gamma}\right)}$$

$$\Delta N' = -N'(T) + \sqrt{N'^2(T) + \frac{K_0' R'}{\gamma' R'}}$$

where the nonprimed equation refers to the illuminated film and the primed refers to the nonilluminated one. The signs were chosen to give positive values for ΔN and $\Delta N'$. From these equations for low light intensities, and using the BCS expressions (IV-22) for $N(T)$ and $N'(T)$ at low temperature,

$$\Delta N = \frac{I_0}{2R}\left(1 + \frac{\beta}{2\gamma}\right)\frac{1}{N(T)} = \frac{I_0}{2R}\left(1 + \frac{\beta}{2\gamma}\right)\sqrt{\frac{2}{\pi}}\,\frac{1}{4N_0\Delta}\left(\frac{\Delta}{kT}\right)^{1/2} e^{\Delta/kT} \tag{IV-28}$$

$$\Delta N' = \frac{K_0'\beta'}{2\gamma' R'}\,\frac{1}{N'(T)} = \frac{K_0'\beta'}{2\gamma' R'}\sqrt{\frac{2}{\pi}}\,\frac{1}{4N_0'\Delta'}\left(\frac{\Delta'}{kT}\right)^{1/2} e^{\Delta'/kT} \tag{IV-29}$$

As can be seen ΔN varies nearly exponentially with Δ/kT and the slope of log (ΔN) versus Δ/kT at low light intensities is independent of film.

coupling or relaxation parameters. From a plot of log (ΔN) versus Δ/kT, it was determined that this theoretical slope varies between 1.087 and 1.165 due to the additional temperature dependent factor $(T\Delta(T))^{-1/2}$.

In order to determine ϵ we recall that ΔN_{exp} is a function of T as well as of ϵ'. ΔN_{exp} is then plotted versus Δ/kT for various values of ϵ' and ϵ' is chosen to be that value for which the slope of log (ΔN_{exp}) versus Δ/kT lies between 1.087 and 1.165. ϵ is determined from ϵ' by using Eq. (IV-19). Recalling Eq. (IV-27) for ϵ, since ϵ can be determined as described and β/R and β'/R' can be calculated from statistics, our experiment is a direct determination of γ_{PbSn}/γ'. The relevant physical properties of lead and tin are summarized in Table II.

Finally we would like to point out that in a naive way of looking at the problem (if all phonons are of energy 2Δ) since $\Delta_{Pb} > \Delta_{Sn}$ it is expected that when tin is illuminated ϵ will be zero since $2\Delta_{Sn}$ phonons cannot break pairs in the leak, as illustrated in Fig. IV-3.

IV.4. Experimental Setup

To study the acoustic coupling of superconducting films, we illuminate one film of a tunnel junction with a laser and we study the resulting change in the I-V characteristic.

In this section we will describe the preparation of the tunnel junctions, and the electronics and optics used.

For convenience we used glass substrates instead of sapphire substrates since (PW72) found no difference in similar optical excitation experiments below the λ point of helium, where our experiments were performed. We found the cleaning of the substrates to be crucial in obtaining junctions that

Fig. IV-3. When lead is illuminated $2\Delta_{Pb}$ phonons can break pairs in the tin; when tin is illuminated $2\Delta_{Sn}$ phonons cannot break pairs in the lead.

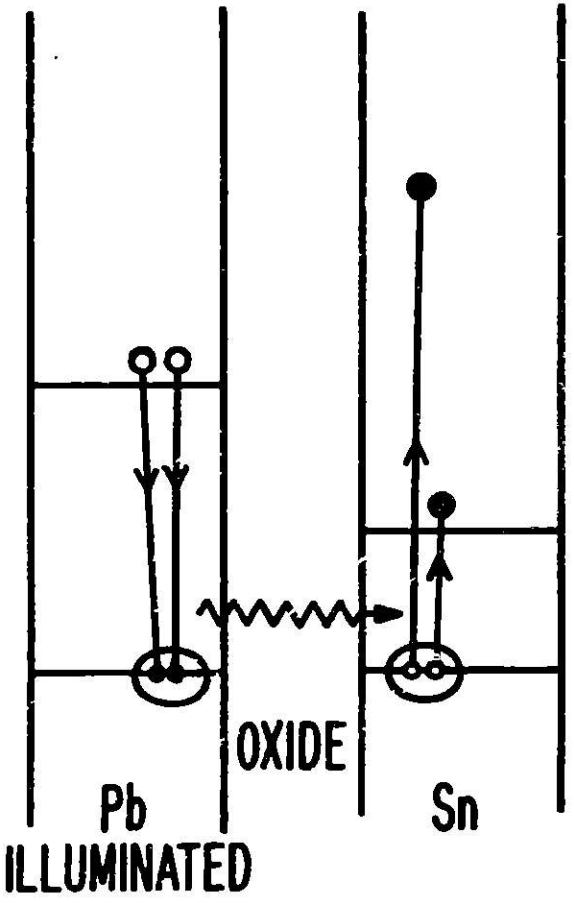
OXIDE
Pb
Sn
ILLUMINATED

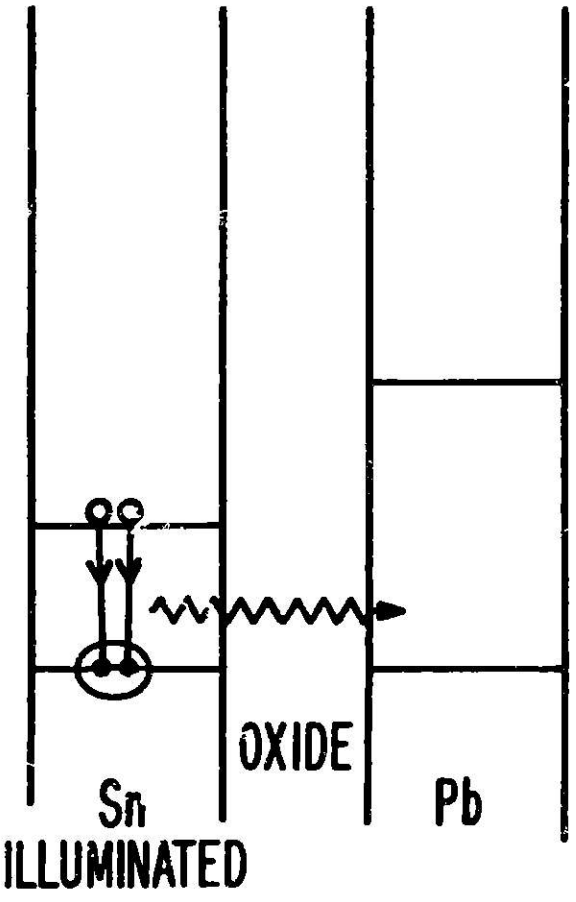
OXIDE
Sn
Pb
ILLUMINATED

were not shorted. We will describe now several cleaning procedures that gave good results:

Procedure #1: The substrate was held in a gem holder and was blown for 3-5 minutes with dry nitrogen in order to remove dust particles. It was then held over boiling trichloroethylene until the vapors condensed on the substrate, at which time it was removed and again blown with dry nitrogen. This step was repeated 4-5 times.

Procedure #2: The substrate was blown with Freon* to remove dust particles and washed in an Alconox** solution in the ultrasonic cleaner. After this the substrate was rinsed successively in distilled water and acetone and dried with Freon. The substrate was then boiled in methyl-ethyl-ketone and washed again in a solution of Alconox in the ultrasonic cleaner. It was then immersed in several baths of boiling water and dried in an oven at a temperature of about 150°C for 15 minutes.

We feel that the important steps in cleaning are the removal of dust particles by blowing with a dry nonreactive gas and the subsequent removal of grease with a strong solvent.

The tunnel junctions were prepared under a pressure of 2×10^{-7} Torr with standard evaporation techniques. First a 2500 Å tin film was condensed and a tunnel barrier formed by glow discharge oxidation (MS61) for one hour under a pressure of 50 mTorr of oxygen. This was followed by

---

*"Aero-Duster" MS-220 from Miller Stephanson Chemical Co., 7615 N. Paulina, Chicago.

**A cleaning compound from Sargent-Welch Scientific Co., 7300 Linden Ave., Skokie, Ill. 60076.

depositing a 2500 Å lead film to form a tunnel junction of area ~ 0.04 mm^2 having typical normal resistance of $\sim 1\ \Omega$ at 4.2 K. Immediately after evaporation the junction was mounted inside the cryostat and the cryostat was evacuated so as to expose the junction to air for as short a time as possible.

Light from a Spectra-Physics 15 mW He-Ne laser was mechanically chopped at 100 Hz and introduced into the cryostat through a 1/8" fiber optic bundle, illuminating one side of the tunnel junction. At the bottom of the cryostat the fiber optic bundle was held in a double threaded brass holder which permitted the displacement of the bundle with respect to the junction without any twisting. With this holder the junction could be positioned as close as 5×10^{-2} mm from the end of the fiber optic bundle. The room temperature end of the optic bundle was epoxied into a brass fitting and held by an X-Y micropositioner fixed to an optical bench. This permitted us to displace the optical fiber with respect to the light beam until the signal was maximized. Before reaching the fiber optic bundle, the chopped light traveled through a partially silvered mirror. The small reflected light from this mirror was fed into a photomultiplier and used as a reference signal for the lock-in amplifier. The intensity of the light was varied with a set of Oriel laser interference filters for the 6328 Å He-Ne line.

The junction was biased with a battery powered current source and the I-V characteristic of the junction was recorded with a Honeywell 560A X-Y recorder. The signal due to the chopped light illumination was measured with a HR-8 PAR lock-in amplifier. The output of the lock-in was also applied to an X-Y recorder.

A block diagram of the optics and electronics is shown in Fig. IV-4.

Fig. IV-4. Block diagram of electronics and optics. The temperature stabilizer was built into the system although it was not used for this experiment.

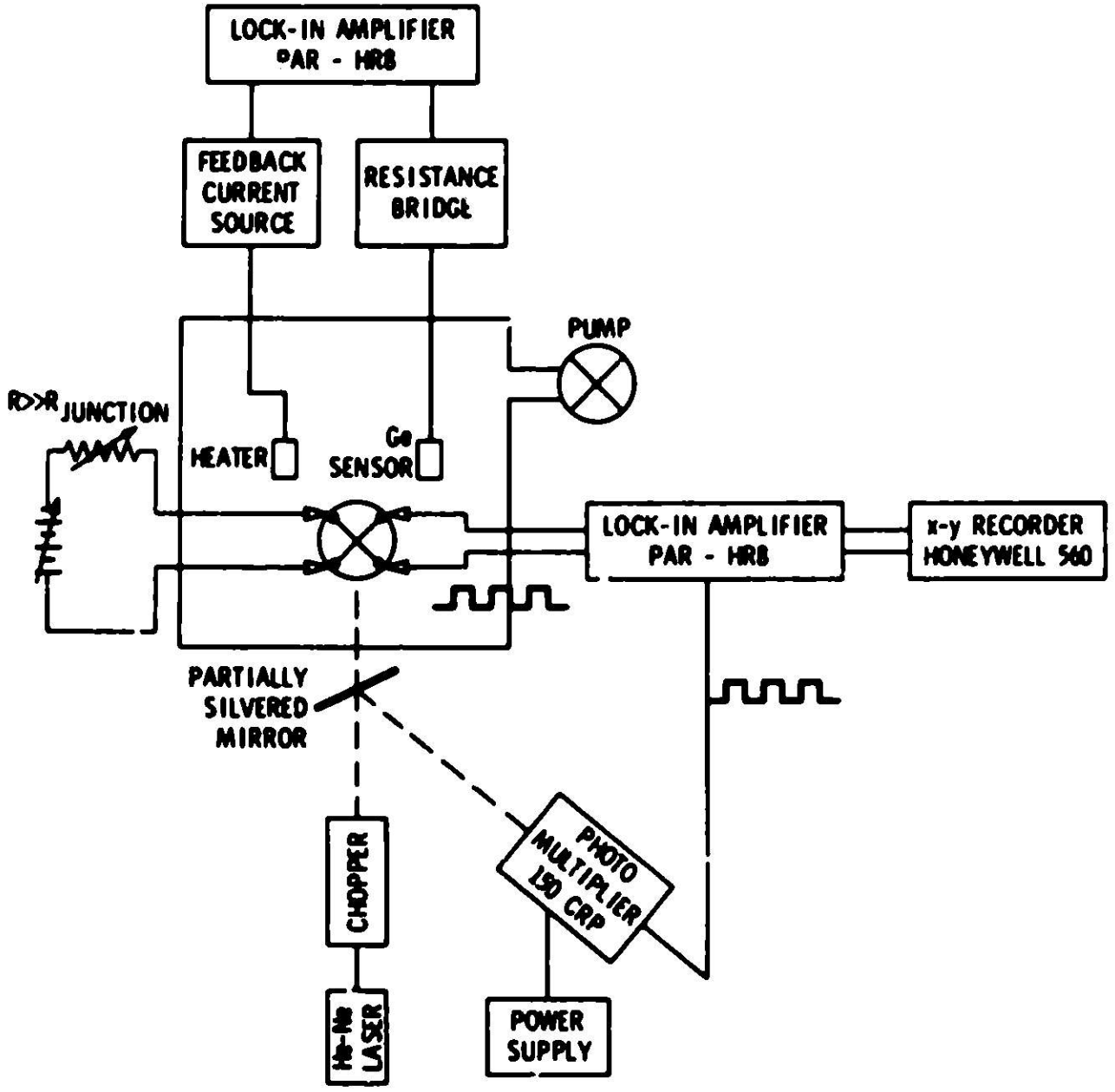
LOCK-IN AMPLIFIER
PAR - HRB
FEEDBACK CURRENT SOURCE
RESISTANCE BRIDGE
PUMP
R>>R JUNCTION
HEATER
Ge SENSOR
LOCK-IN AMPLIFIER
PAR - HRB
x-y RECORDER
HONEYWELL 560
PARTIALLY SILVERED MIRROR
CHOPPER
PHOTO MULTIPLIER 150 CRP
He-Ne LASER
POWER SUPPLY

IV.5. Experimental Procedure

The junction was biased at the sum of the energy gaps at approximately the middle of the rising portion of the tunneling characteristic, as shown in Fig. IV-5. Since a light pulse decreases the energy gap of the illuminated film, the voltage across the junction is modulated by the chopped light. The modulated voltage across the junction is $\delta\Delta_{exp}$, described in Section 3 of this chapter. The variation of the signal was recorded while the bath temperature was allowed to rise slowly to the λ point after being first lowered to about 1.28 K by pumping on the helium bath. This process took about 1/2 hour, insuring a good approximation to thermal equilibrium. The smallest signals detected were of the order of 100 nV whereas the average noise and pickup without illumination was less than 10 nV. Several checks at a chopping frequency of 500 Hz did not differ appreciably, and some runs were made several times to check consistency in the results. The experiment was repeated for several samples, with slightly different normal resistances, and the results obtained were essentially the same. This experiment was done also with a pulsed Ga-As injection laser, immersed in the liquid helium and the results are in good quantitative agreement with the chopped laser light experiments.

A typical signal as recorded on the X-Y recorder is shown in Fig. IV-6. The signal versus the current through the junction is shown in Fig. IV-7. The details of this signal have not been explained and will be the subject of further experiments.

Fig. IV-5. I-V characteristic of one of the Sn-SnO-Pb junctions at 1.28°K. The junction was biased at point A to measure the modulation of the energy gap by the illumination.

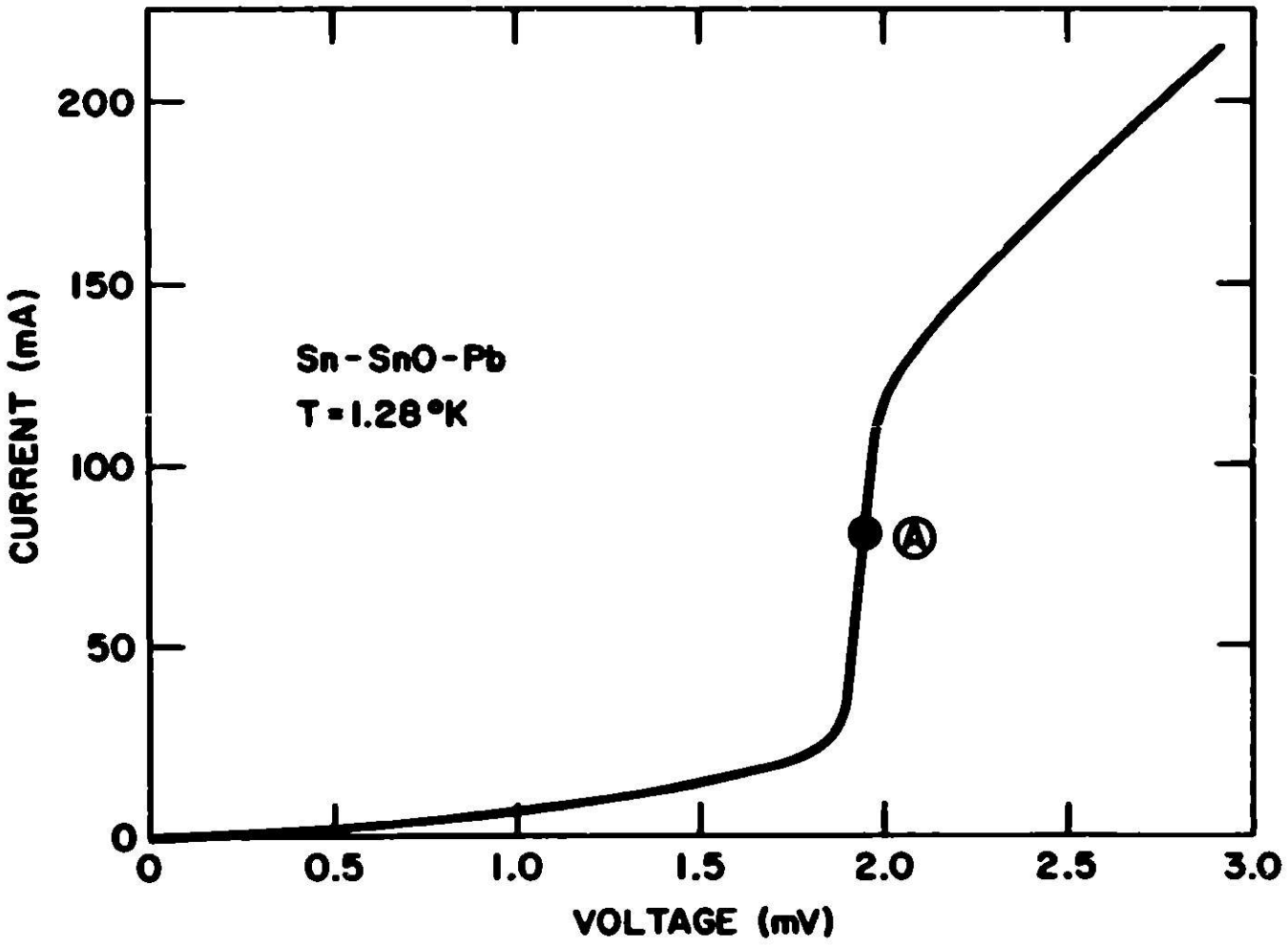
200
150
100
50
0
CURRENT (mA)
Sn-SnO-Pb
T=1.28°K
A
0
0.5
1.0
1.5
2.0
2.5
3.0
VOLTAGE (mV)

Fig. IV-6. Modulation signal versus time, with the appropriate temperatures indicated. These were determined from the helium bath vapor pressure measured at corresponding times.

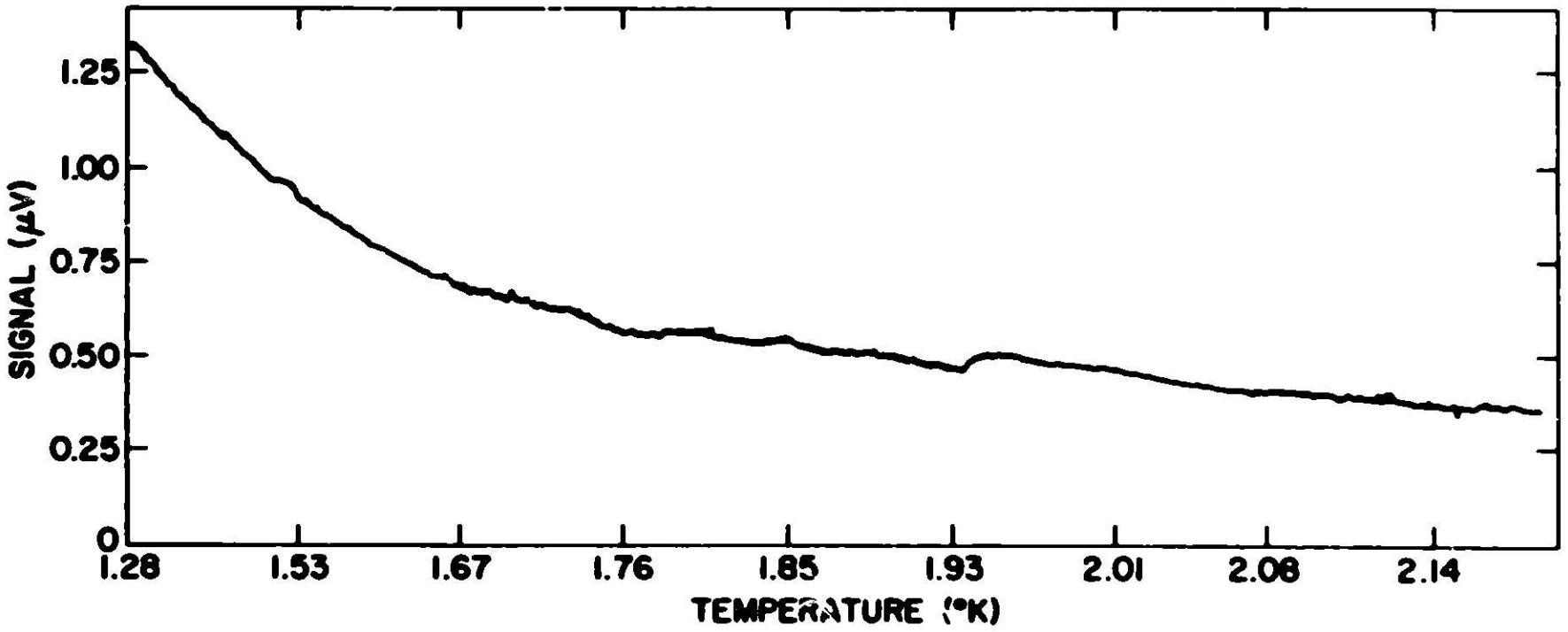
SIGNAL (μV)
1.25
1.00
0.75
0.50
0.25
0
1.28
1.53
1.67
1.76
1.85
1.93
2.01
2.08
2.14
TEMPERATURE (°K)

Fig. IV-7. Modulation signal versus current through the junction. Structure is observed at $\Delta_{Sn} \pm \Delta_{Pb}$ and some very reproducible oscillations at 1.0 mA.

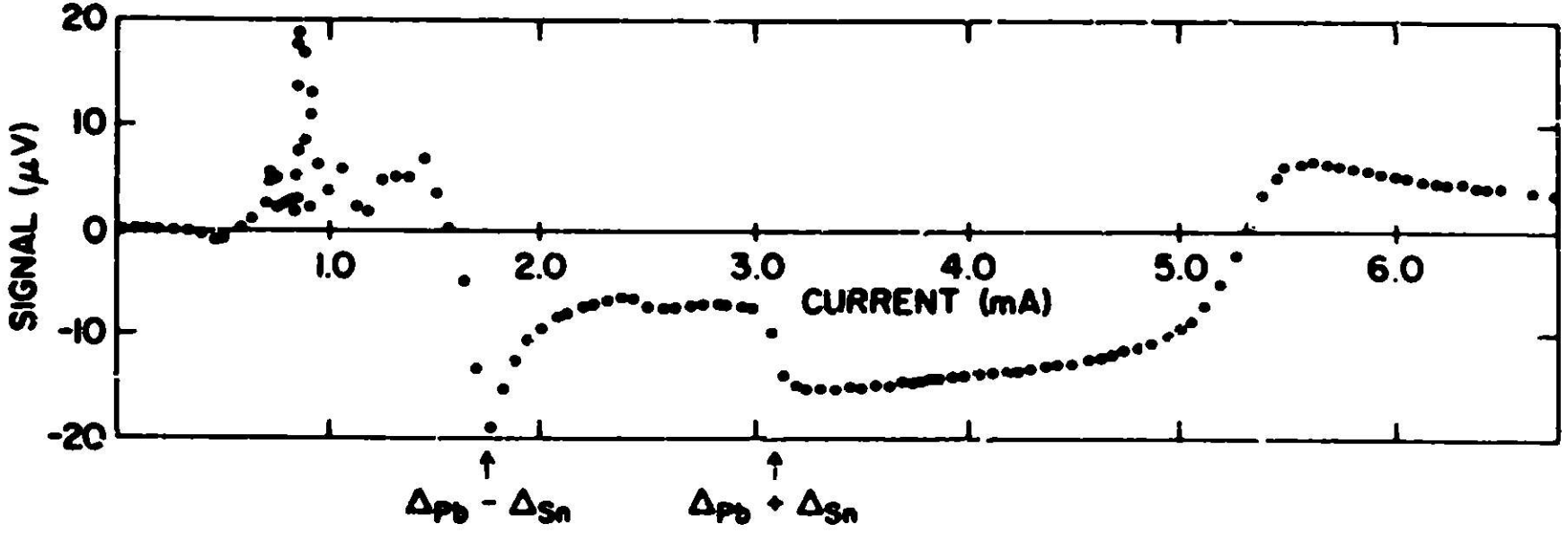
20
10
0
-10
-20
SIGNAL (μV)
1.0
2.0
3.0
4.0
5.0
6.0
CURRENT (mA)
Δ_Pb - Δ_Sn
Δ_Pb + Δ_Sn

IV.6. Results and Discussion

The data was analyzed by using Eqs. (IV-20) and (IV-21) to evaluate ΔN and $\Delta N'$ for several values of T and light intensity, which resulted in different values of $\delta\Delta_{exp}$. Briefly, it was found in Section IV-3 that $\Delta N_{exp} = f(N(T), N'(T), \delta\Delta_{exp}, \varepsilon)$, where f is an algebraic function of its variables. N(T) and N'(T) can be calculated from the BCS theory and $\delta\Delta_{exp}$ is experimentally determined. Therefore ΔN_{exp}, as a function of temperature, can be calculated for different values of the parameter ε. The calculation was done using the IBM 360/195 computer of Argonne National Laboratory as described in Appendix 1. On the other hand, the temperature dependence of ΔN can be calculated theoretically as in Eqs. (IV-28) and (IV-29) above. The comparison of temperature dependence of the theoretical ΔN with the experimentally determined ΔN_{exp} allows us to obtain ε. This can be related to phonon escape parameters using Eq. (IV-27).

The slopes of $\ln(\Delta N_{exp})$ or $\ln(\Delta N'_{exp})$ versus Δ/kT or Δ'/kT were determined by fitting a straight line to these curves at low values of Δ/kT or Δ'/kT. At high values of Δ/kT, the curve $\ln(\Delta N_{exp})$ versus Δ/kT saturates because it is no longer valid to approximate Eq. (IV-22) only by the first term of its series expansion. The saturation shows up as a "flattening" of the curve at high Δ/kT values. Because the lead film showed saturation for most of the light intensities used, in the determination of ε' the best fit for the tin film was used. An example of the curve ΔN^{Sn}_{exp} versus Δ_{Sn}/kT for a particular value of ε' is shown in Fig. IV-8 together with the theoretical curve N(T) when tin is illuminated. For this fit only a vertical adjustable parameter was used which does not modify the slope of this curve. Figure IV-9 shows an example of the

Fig. IV-8. Values of $\ln(\Delta N_{Sn})$ derived from the experiment with the tin illuminated at low intensity using unenhanced densities of state. The value of ϵ' is 0.04 and the solid line is a fit to the theoretical N(T) for tin.

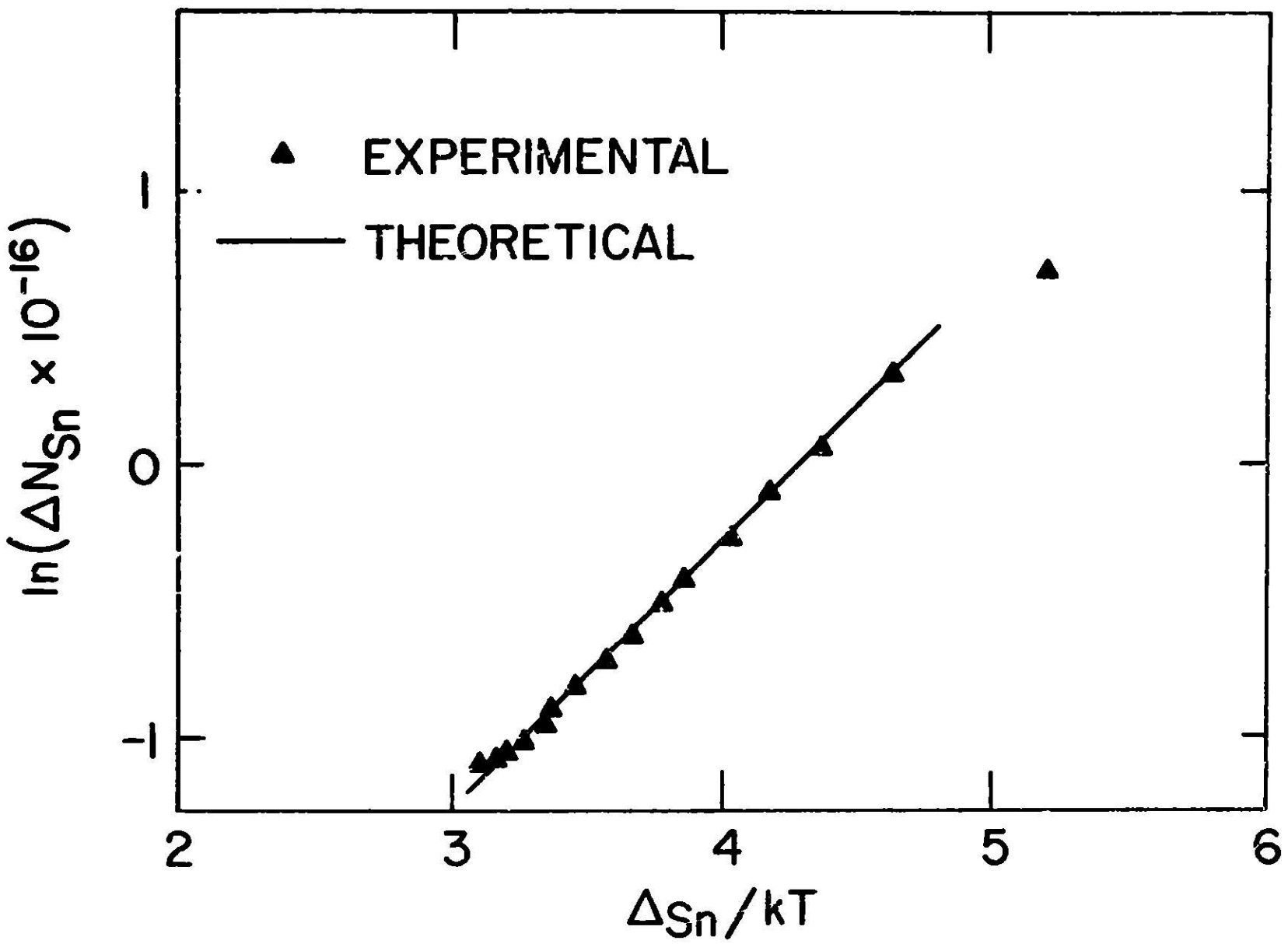
EXPERIMENTAL
THEORETICAL
$\ln(\Delta N_{Sn} \times 10^{-16})$
1
0
-1
2
3
4
5
6
Δ_{Sn}/kT

Fig. IV-9. Values of $\ln(\Delta N_{Pb})$ derived from the experiment with the tin illuminated at relatively low intensity using unenhanced densities of state. The value of $\epsilon' = 0.04$ as in Fig. IV-9.

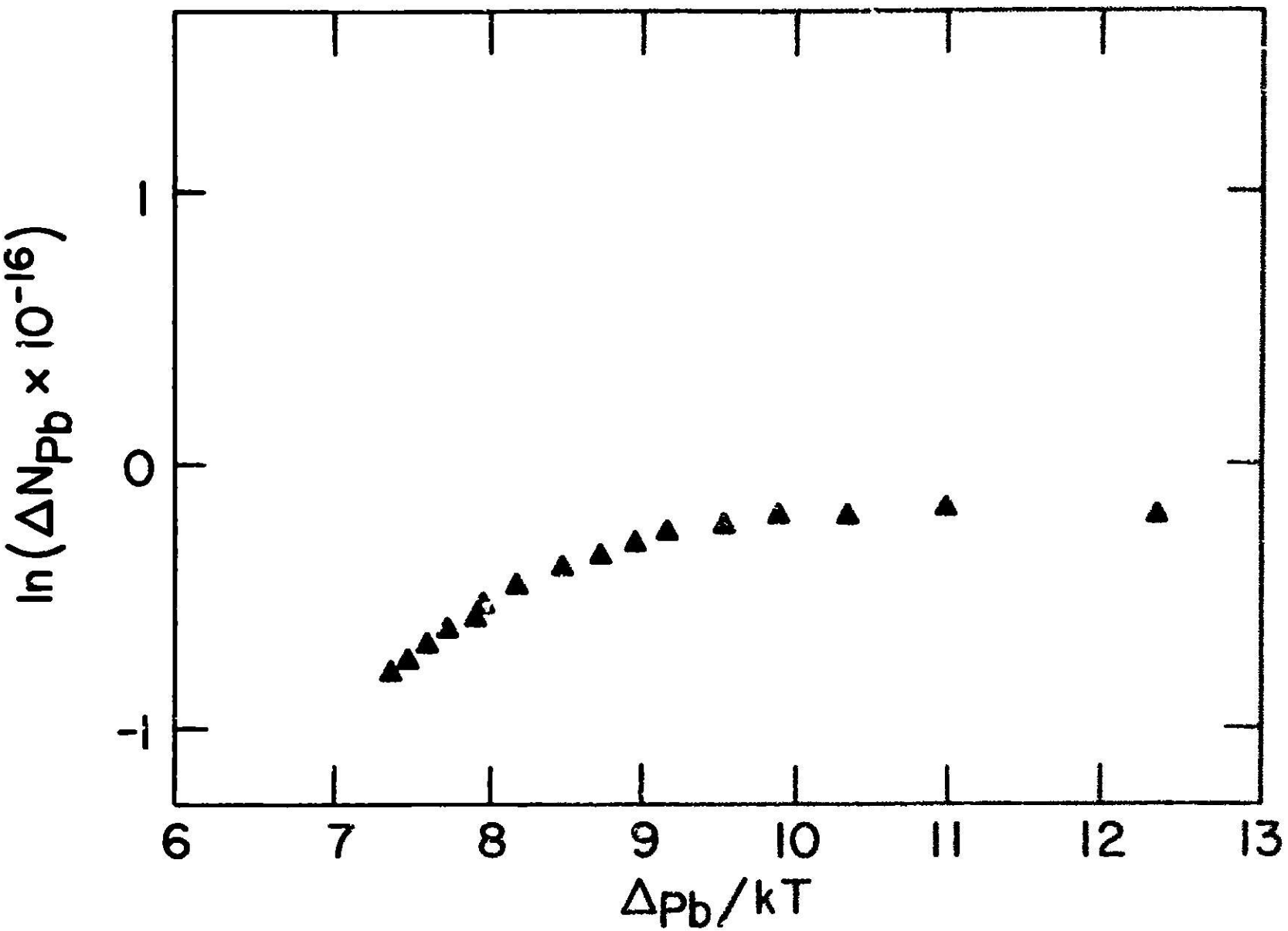
ln(ΔNPb x 10-16)
1
0
-1
6
7
8
9
10
11
12
13
ΔPb/kT

curve ΔN^{Pb}_{exp} versus Δ_{Pb}/kT for the same value of ϵ'. It can be seen that the lead curve shows saturation.

To determine ϵ' we plot the slop of $\ln(\Delta^{Sn}_{exp})$ versus Δ_{Sn}/kT versus the coupling parameter ϵ'(when lead is illuminated) for different relative illuminations, as shown in Fig. IV-10. As explained earlier these low temperature slopes have to lie, theoretically, between 1.087 and 1.165, which is indicated by the shaded area in the graph. (The correct value of ϵ was determined from a graph similar to IV-10.) The mean value plus or minus one standard deviation from the mean for ϵ is 0.75 ± 0.3. Figure IV-11 shows the values of the slopes for different ϵ''s, for various light intensities when tin is illuminated. The nonzero value of ϵ, in the latter case, indicates generation of phonons with energy larger than $2\Delta_{Pb}$ in the tin, so that pairs are broken in lead. However, most of the phonons have energy $2\Delta_{Sn}$ and will not be able to break pairs in the lead, so we will concentrate on the results with lead illuminated where the analysis of the acoustic coupling is simplified,since most phonons have energy $\geq 2\Delta_{Pb}$ and can be detected by the tin film.

Since most determinations of the lifetimes are not direct, in order to compare our results with other experiments, it was necessary to correct the reported lifetimes so as to conform to the same values for densities of states, film thicknesses, etc.

We will compare our experimental values of γ_{PbSn} with available calculations. If ΔS_ω is the rate of production of phonons per unit volume, then its source is the quasiparticles recombining, given by $\Delta N/\tau = (I_0/2)(1 + \beta/2\gamma)$, where τ is the true quasiparticle recombination time. The rate of phonons escaping is the fraction (f) escaping times the ratio of production; so

Fig. IV-10. Slope of $\ln(\Delta N_{Sn})$ versus Δ_{Sn}/kT plotted as a function of the coupling parameter ε' for the case when lead is illuminated for different relative illuminations. The dashed area indicates the theoretical values of the slope for low reduced temperature. (For this graph ΔN_{Sn} was determined by using unenhanced densities of states.)

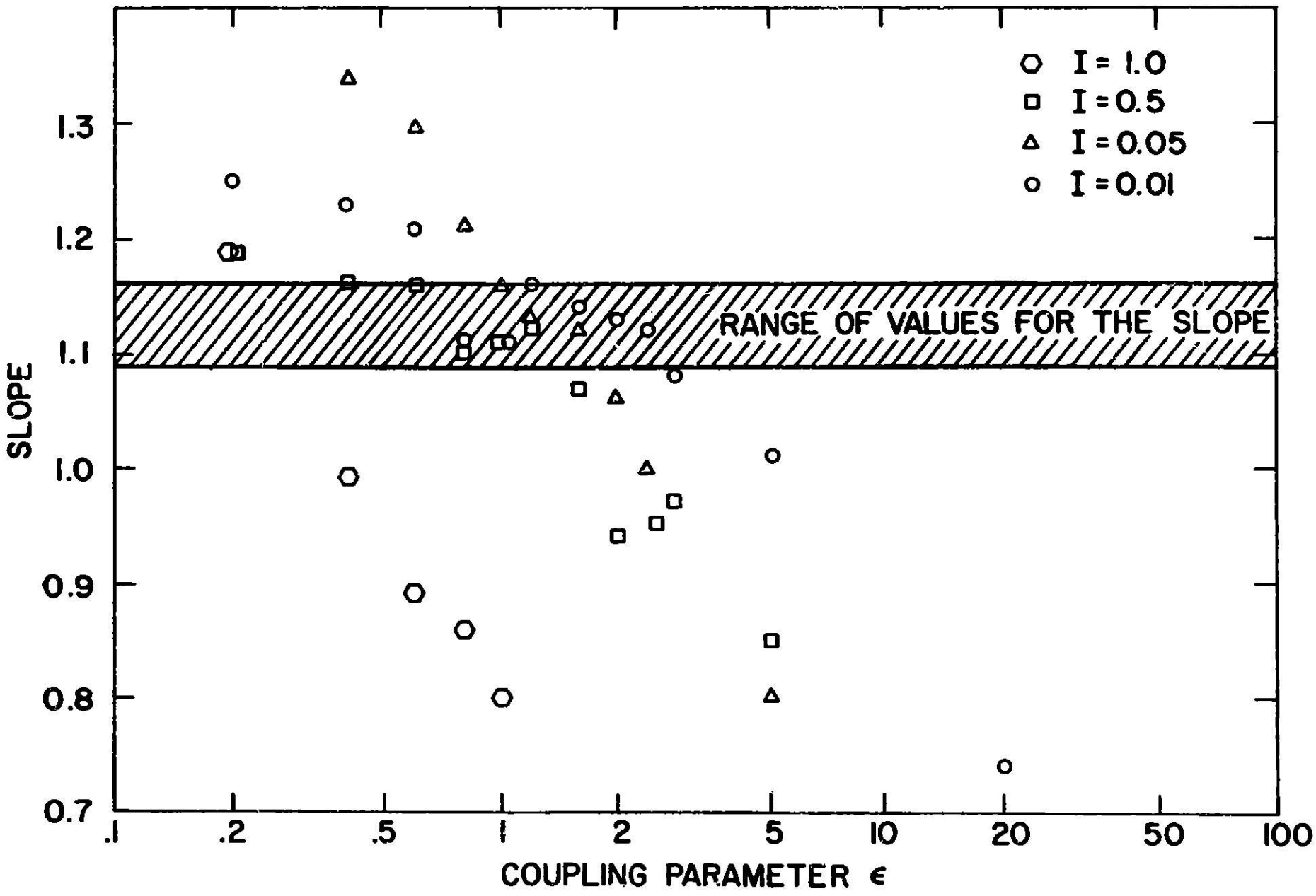
I = 1.0
I = 0.5
I = 0.05
I = 0.01
RANGE OF VALUES FOR THE SLOPE
SLOPE
1.3
1.2
1.1
1.0
0.9
0.8
0.7
.1
.2
.5
1
2
5
10
20
50
100
COUPLING PARAMETER ϵ

Fig. IV-11. Slopes of $\ln(\Delta N_{Sn})$ versus Δ_{Sn}/kT plotted as a function of the coupling parameter ϵ' for the case when Sn is illuminated for different relative illuminations. The dashed area indicates the theoretical values of the slopes for low reduced temperatures. (For this graph ΔN_{Sn} was determined using unenhanced densities of state.)

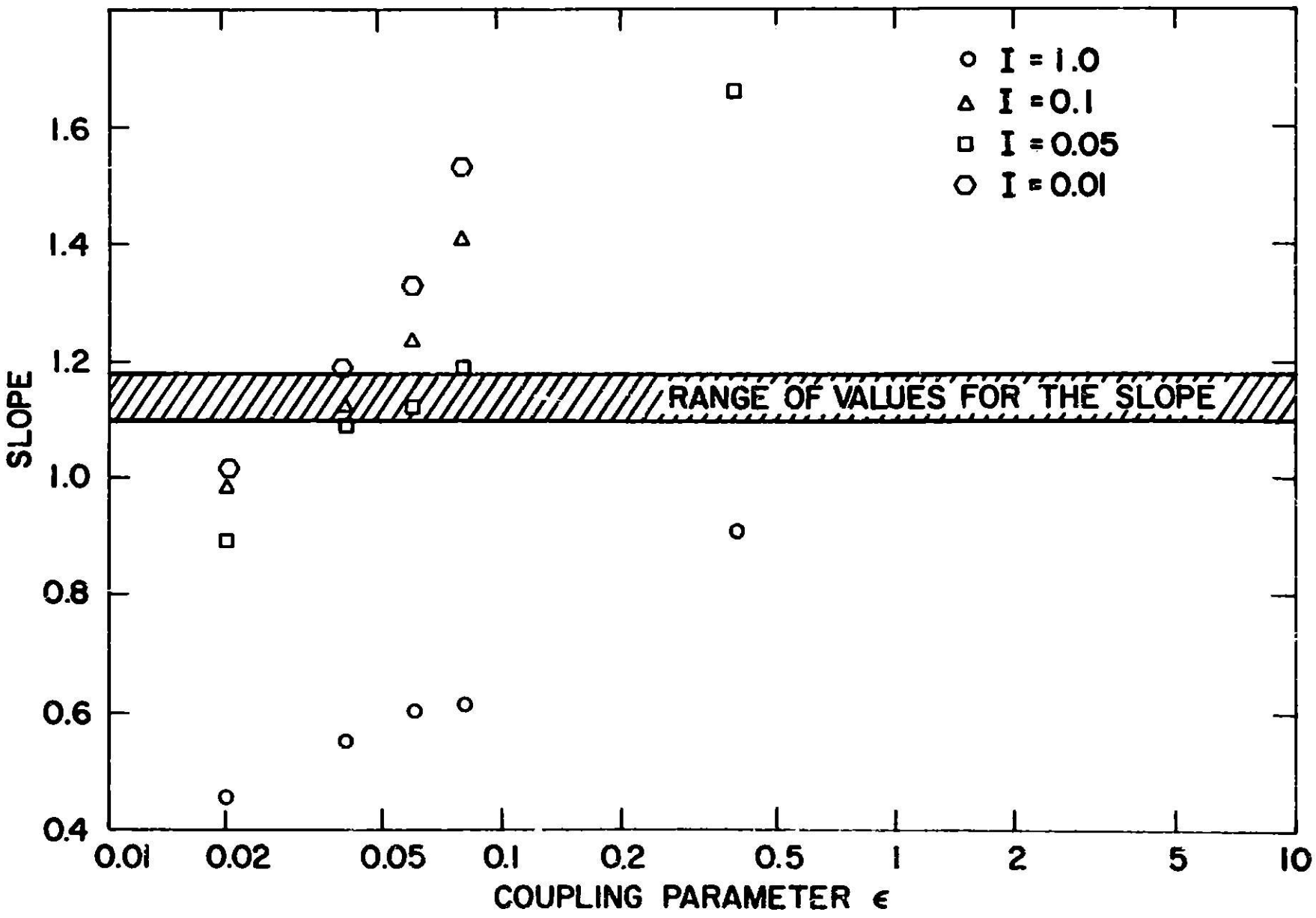
I = 1.0
I = 0.1
I = 0.05
I = 0.01
RANGE OF VALUES FOR THE SLOPE
SLOPE
1.6
1.4
1.2
1.0
0.8
0.6
0.4
0.01
0.02
0.05
0.1
0.2
0.5
1
2
5
10
COUPLING PARAMETER ϵ

$$\gamma_{PbSn} \quad \Delta N_{\omega} = f \, \Delta S_{\omega} \tag{IV-30}$$

Using Eq. (IV-24) together with the condition that $\beta/2\gamma >> 1$, we get

$$\gamma_{PbSn} = \frac{1}{2} f \, \beta. \tag{IV-31}$$

Using Eq. (IV-12) $f = \frac{\alpha\Lambda}{4d}$ and substituting the expression for the phonon mean free path $\Lambda = [\bar{S}/(\gamma + \beta/2)]$ into Eq. (IV-31)

$$\gamma_{PbSn} = \frac{S_T}{4d} \frac{\alpha}{1 + 2\gamma/\beta} \tag{IV-32}$$

Since $\beta/2\gamma >> 1$, the calculated value for our lead films is $\gamma_{PbSn} = 1.27 \times 10^{9} \, \alpha \, sec^{-1}$. The value of α at the lead-tin interface can be calculated by comparing the theoretically found value for γ_{PbSn} and the experimentally determined valur of γ_{PbSn} with the use of Eq. (IV-27).

Using Little's theory described in Section 2 of this Chapter, α is calculated to be about 0.15, which is within factors of 2-3 of the experimental value. The values obtained are considered to be in good agreement with Little's calculation in view of the uncertainties about the microscopic nature of the interface and small numerical uncertainties when using the results of different experiments.

A comparison of our determined values for γ_{PbSn} with experimental determination of γ of other workers (PW72, JPK76) indicates that most of the phonon escape is into the helium and not into the underlying film. If we assume that all the phonons escape into the helium bath, the results of (PW75) give a value of $\alpha > 1$, indicating the presence of inelastic processes mentioned earlier in our discussion related to Eq. (IV-23). On the other hand if we use the most recent results for the lifetimes in lead, the ratio of α_{PbHe} obtained is 0.5. The relevant properties of lead and tin are shown in Table II.

Table II. Relevant physical properties of tin and lead.

Corrections applied to the quoted lifetime, indicated in parenthesis in the table:

1. Only thickness of one film was used in the calculation of τ.
2. τ was determined using the band structure value for N_T. Include enhancement $(1 + \lambda)$.
3. Experiment measures $\tau/2$ not τ.
4. The value of N_0 used does not agree with (LH68).
5. Lifetime was corrected to confora to a thickness of 2500 Å.

The formulas used were:

N_T from Eq. (IV-22)

$$R_{exp} = 1/\tau_{exp}\, N_T$$

$$\frac{\beta}{R} = \frac{N_T^2}{2N_{\omega_T}} = \frac{(1+\lambda)^2 N_0^2 h^3}{4\Delta}\, \bar{S}^3$$

The fact of 2 in the denominator comes from the two transverse modes.

γ from Eq. (IV-26).

γ_{PbSn} from Eq. (IV-27)

α as explained in the text.

Table II

Parameter		Tin		Lead	Units
$\Delta(0)$		0.60×10^{-3}		1.35×10^{-3}	eV
N_0 (LH68)		0.89×10^{22}		0.92×10^{22}	$eV^{-1}\ cm^{-3}$
S_T (AIP72, TEC69)		1.67×10^{5}		1.13×10^{5} (100) 0.80×10^{5} (110) 0.57×10^{5} (111)	cm/sec
S_L (AIP72, TEC69)		3.32×10^{5}		2.03×10^{5} (100) 2.25×10^{5} (110) 2.32×10^{5} (111)	
$\bar{S}_T$		1.67×10^{5}		0.9×10^{5}	
λ (EMD)		0.72		1.55	
N(T)		4.09×10^{19}		15.84×10^{19}	$(\frac{\Delta}{kT})^{-1/2} e^{\Delta/kT}\ cm^{-3}$
τ_o		3.5×10^{-10} (HDN74)		1×10^{-12} (PW72)	sec
(quoted)		8.7×10^{-10} (P74)		48×10^{-12} (JPK76)	
τ_o	(3,5)	5.5×10^{-10} (HDN74)	(1,2,3)	10×10^{-12} (PW72)	
(corrected)	(2,4,5)	8.4×10^{-10} (P74)	(5)	34×10^{-12} (JPK76)	
R_{exp}		4.0×10^{-11} (HDN74) 2.6×10^{-11} (P74)		6.3×10^{-10} (PW72) 1.8×10^{-10} (JPK76)	$eV\ cm^3\ sec^{-1}$

Table II (contd.)

Parameter	Tin	Lead	Units
$\frac{\beta}{R}$	3.2×10^{19}	5.3×10^{18}	cm^{-3}
γ	6.4×10^{8} (HDN74)	1.7×10^{9} (PW72)	sec^{-1}
	4.2×10^{8} (P74)	4.7×10^{8} (PK76)	
γ_{PbSn}	3.1×10^{7} (HDN74)		
	1.8×10^{7} (P74)		
α_{PbSn}	2.5×10^{-2} (HDN74)		
	1.4×10^{-2} (P74)		
α_{PbHe}	1.13 (PW72 - 3000 Å)		
	0.53 (JPK76 - 3500 Å)		

In conclusion, this experiment determined the excess number of quasiparticles $\Delta N = f(N(T), N'(T)), \delta\Delta_{exp}, \varepsilon)$, with the coupling coefficient ε being an adjustable parameter. ε was determined by fitting ΔN_{Sn} to the theoretical temperature dependence. It was then related to γ_{PbSn}, the phonon escape parameter from lead into tin. If we use an enhanced density of states in the calculation, the value obtained for γ_{PbSn} agrees reasonably well with the acoustic mismatch theory of Little modified to take into account that we have a uniform isotropic source of phonons throughout the film. The recent experimentally determined value for the lifetime in tin, together with our results, indicate that most of the phonons escape into the helium with an average phonon transmission coefficient of the boundary $\alpha_{PbHe} \approx 0.5$.

V. Relaxation of the Superconducting Order Parameter

V.1. Introduction

One of the most fundamental quantities in nonequilibrium superconductivity is the time response of the order parameter or energy gap to external perturbations which break Cooper pairs, thereby decreasing the order parameter.

Landau and Khalatnikov (LK54) developed a theory for the temperature dependence of the relaxation time of the order parameter "near a second order phase transition point". This was studied experimentally in liquid helium by Chase (Ch58). Later, Schmid (Sch66) modified the Landau-Khalatnikov theory by essentially postulating a gauge invariant form of the Landau-Khalatnikov equation. Several theories (LS67, WA68, Sch69, SS75) were developed, using different assumptions or starting points, which disagree on the temperature dependence of the relaxation time of the superconducting order parameter. There has been only one attempt to measure this relaxation time experimentally (PM73), the results being inconclusive.

In this Chapter we describe a direct measurement of the relaxation time τ for the superconducting energy gap. We find a transition from single particle behavior at low temperatures to collective behavior very near the superconducting transition temperature T_c where the relaxation time diverges. We have also measured the equilibrium energy gap Δ, and find $\tau \propto \Delta^{-1}$ very near T_c in agreement with the theoretical predictions of Schmid and Schön (SS75).

In Section 2 of this Chapter we will describe a macroscopic phenomenological theory for the relaxation of the order parameter in systems that

show a second order phase transition. In Section 3 we will briefly delineate the several microscopic theories. A detailed description of these theories is beyond the scope of this work, and because of this we will only outline the main ideas. In Section 4 a description of the experimental setup will be given and in Section 5 we will describe the experimental procedure. In Section 6 the experimental results and their relationship to the various theories will be described and in Section 7 we will briefly summarize the results and conclusions of this work.

V.2. The Phenomenological Gauge Invariant Landau-Khalatnikov Theory

Since the Ginzburg-Landau equation has proven to be very successful when applied to equilibrium superconductivity, it is reasonable to try to formulate a time-dependent theory based on this equation. The following gauge invariant modification of the (LK54) theory was advanced by Schmid (Sch66).

Let us assume that in a nonequilibrium situation the free energy of a superconductor can be written as

$$F(P,T,\psi,t) = F_0(P,T) + A(P,T)\psi^2(t) + C(P,T)\psi^4(t) \qquad (V\text{-}1)$$

where the time dependence enters through the time dependence of the order parameter ψ and the assumptions are the same as in the Ginzburg-Landau theory. For completeness we will rewrite the assumptions. Below T_c, $C > 0$ and $A < 0$, and above T_c, $A > 0$; the transition point is determined by the condition $A(P,T) = 0$. In the vicinity of the transition temperature T_c we expand $A(P,T)$ in series in the difference $T - T_c$, and neglecting higher order terms we have

$$A(P,T) = a(P)(T - T_c) \quad . \tag{V-2}$$

The temperature dependence of the order parameter ψ is determined from the condition that the free energy has to be a minimum in equilibrium. This gives

$$\psi_{eq}^2 = - \frac{A}{2C} = \frac{a}{2C} (T_c - T) \tag{V-3}$$

which is the BCS temperature dependence of the energy gap, close to T_c.

The approach of the order parameter ψ to its equilibrium value is determined from the transport equation

$$\frac{d\psi}{dt} = \gamma \frac{\delta F}{\delta \psi} \tag{V-4}$$

where the transport coefficient γ was assumed by Landau and Khalatnikov, not to have any singularity at T_c. Schmid (Sch66), using the Gorkov (Go58) formulation, showed that $\gamma = - \frac{4k}{a\hbar\pi}$ for a superconductor. Let us assume that we have a small deviation from equilibrium, that is to say $\psi(t) = \psi_{eq} + \delta\psi(t)$ with $|\delta\psi/\psi_{eq}| << 1$. Then using Eqs. (V-4) and (V-1)

$$\frac{d\delta\psi}{dt} = 2\gamma A(\psi_{eq} + \delta\psi) + 4\gamma C(\psi_{eq} + \delta\psi)^3$$

and, since the perturbation is small,

$$\frac{d\delta\psi}{dt} \simeq 2\gamma A(\psi_{eq} + \delta\psi) + 4\gamma C\, \psi_{eq}^3 (1 + 3 \frac{\delta\psi}{\psi_{eq}})$$

But, from Eq. (V-3), $C = -(A/2\psi_{eq}^2)$ and $d\delta\psi/dt = -4A\,\gamma\delta\psi$, implying that the order parameter relaxes exponentially with a relaxation time,

$$\tau = \frac{1}{4A\gamma} = \frac{1}{4a\gamma} \frac{1}{T - T_c} \qquad \text{(V-5)}$$

It should be pointed out that the temperature dependence of τ is independent of the temperature dependence of ψ_{eq}. If, in addition to the time dependence, the order parameter has a spatial dependence and, allowing for a complex order parameter, the Ginzburg-Landau equation is (Th75, Eq. (4-1)

$$F = F_0 + A\psi^2 + C\psi^4 + \frac{1}{2m} \left| \left(\frac{\hbar}{i} \nabla - \frac{2e}{c} A\right)\psi \right|^2 + \frac{H^2}{8\pi}$$

where $H = \nabla \times A$ is the magnetic field, A is the vector potential and ψ is now a complex order parameter or the "superconducting wavefunction". If this form of the free energy is introduced in the Landau-Khalatnikov Eq. (V-4), we obtain

$$\frac{\partial \psi}{\partial t} = 2\gamma \left\{ \frac{1}{2m} \left(\frac{\hbar \nabla}{i} - \frac{2e}{c} A\right)^2 \psi + A\psi + 2C|\psi|^2 \psi \right\} \qquad \text{(V-6)}$$

We notice that a quantum mechanical gauge transformation consists of replacing simultaneously (Schiff68, p. 399)

$$A \to A + \nabla \Xi$$

$$\tilde{\phi} \to \tilde{\phi} - \frac{1}{c} \frac{\partial \Xi}{\partial t}$$

$$\psi \to \psi \, e^{ie\Xi/\hbar c}$$

where $\tilde{\phi}$ is the effective potential and Ξ is an arbitrary function of $\vec{r}$ and t. In order to make Eq. (V-6) gauge invariant, a term has to be added so as to obtain

$$\left(\frac{\partial}{\partial t} - 2ie\tilde{\phi}\right)\psi = 2\gamma \left\{ \frac{1}{2m} \left(\frac{\hbar \nabla}{i} - \frac{2eA}{c}\right)^2 \psi + A\psi + 2C|\psi|^2 \psi \right\} . \qquad \text{(V-7)}$$

It was proposed by Schmid (Sch66) that the effective potential $\tilde{\phi}$ should be written as $\tilde{\phi} = \phi - \mu/e$ where ϕ is the electric potential and μ is the chemical potential. Physically μ is the energy necessary to add an electron in thermal equilibrium when the fields are kept constant. With this assumption, in the case where there are no electro-magnetic fields present and ψ does not vary spatially, Eq. (V-7) reduces to

$$(\frac{\partial}{\partial t} + 2i\mu)\psi = 2\gamma(A\psi + 2C|\psi|^2\psi) \qquad \text{(V-8)}$$

In writing the "wavefunction" as $\psi = |\psi|e^{i\theta}$ and separating the real and imaginary parts of Eq. (V-8), two modes are obtained:

$$\frac{\partial|\psi|}{\partial t} = 2\gamma[A|\psi| + 2C|\psi|^3] \qquad \text{Real part} \qquad \text{(V-9)}$$

$$\frac{\partial\theta}{\partial t} + 2\mu = 0 \qquad \text{Imaginary part} \qquad \text{(V-10)}$$

Equation (V-9) is the same as Eq. (V-4) except that now ψ is a complex order parameter. The earlier calculation for the relaxation time is still valid, and so the relaxation time for the magnitude of ψ is

$$\tau_{|\psi|} = \frac{1}{4A\gamma} = \frac{1}{4\alpha\gamma}\frac{1}{T - T_c} \qquad \text{(V-11)}$$

The relationship between the superconducting order parameter (wavefunction) and the energy gap was determined by Gorkov (Go60, see Chapter II)

$$\psi(\vec{r},t) = \left[\frac{7\zeta(3)n_o\chi(\rho)}{16\pi^2k^2T_c^2}\right]^{1/2}\Delta(\vec{r},t) \qquad \text{(V-12)}$$

where $\zeta(3) = 1.202$, n_o is the density of electrons, $\rho = \frac{1}{2}\pi T_c \tau_{tr}$ with τ_{tr} the mean time between collisions for an electron, and

$$\chi(\rho) = \frac{8}{7\zeta(3)} \frac{1}{\rho} \left[\frac{\pi^2}{8} + \frac{1}{2\rho} \left(G(\tfrac{1}{2}) - G(\tfrac{1}{2} + \rho)\right)\right]$$

with G the logarithmic derivative of the Γ function.

Since the superconducting order parameter and the energy gap differ only by a constant, the relaxation time of the energy gap will be given by Eq. (V-11).

The imaginary part of Eq. (V-8) describes the evolution of the phase of the order parameter. Equation (V-10) implies that the phase of the order parameter will change in time at a constant rate. It will be shown later that the relaxation time associated with Eq. (V-10) is related to the branch imbalance relaxation described in Chapter III. We will just point out that Eq. (V-10) is expected to be related to the branch imbalance relaxation (determined by the difference between the chemical potential of quasiparticle and pairs) since the evolution of the phase θ is determined by the chemical potential μ of the "superelectrons".

V.3. The Microscopic Theories for the Relaxation of the Order Parameter in a Superconductor

The first attempt to determine the time variation of the Ginzburg-Landau order parameter from a microscopic theory was done by Abrahams and Tsuneto (AT66). They extended the Gorkov (Go60) formulation to the non-equilibrium situation and found that if the time variations are sufficiently small, a time-dependent Landau-Ginzburg equation exists near the transition temperature and near absolute zero temperature. Close to the transition

temperature they found a differential equation which is diffusive-like in character, and at zero temperature they found an equation which is wave-like. One of the main limitations of the (AT66) theory is that they assumed that the thermal excitations in the superconductor are at rest and in equilibrium with the local values of the energy-gap and the external fields. This occurs only if the characteristic interaction time between phonons and thermal excitations is faster than the characteristic time for the "normal to superfluid" conversion.

Later, Lucas and Stephen (LS67) studied the relaxation of the order parameter in a superconductor and also found that the main mechanism for this relaxation is through the interaction of the quasiparticles with the phonon field. To calculate the relaxation time τ they started from the Hamiltonian for the electron-phonon interaction written in the conventional form (dG66, p. 32) and used a Boltzmann equation (BRT59) for the quasi-particle distribution. The relaxation time for the order parameter derived as described has the form

$$\tau \propto \lambda^2 n \left[\frac{(T_c - T)}{T_c}\right]^2 \quad \text{for } \frac{T}{T_c} \sim 1 \quad . \qquad \text{(V-13)}$$

Woo and Abrahams (WA68) pointed out that the calculation of (LS67) is not correct since they used the Boltzman equation (BRT59), which assumes local equilibrium between the quasiparticles and the energy gap. In the case where the energy gap is time dependent, there is no local equilibrium between the quasiparticles and the energy gap at a time scale shorter than the electron-phonon inelastic collision time. (WA68) derive a transport equation for the superconductor in the presence of electron-phonon interaction. This transport equation is obtained by a technique of thermodynamic

Green's functions developed by Kadanoff and Baym (KB62). Their conclusion is that for weak coupling materials, for $0.9 \leq T/T_c \leq 0.99$ the relaxation time of the energy gap (10^{-9} - 10^{-8} sec) is about an order of magnitude faster than the quasiparticle recombination rate, but very close to T_c it diverges as

$$\tau \propto \frac{1}{T - T_c} \tag{V-14}$$

This temperature dependence agrees with the prediction of the phenomenological Landau-Khalatnikov theory.

Schmid (Sch68) calculated the relaxation of the order parameter starting from a dynamical version of the BCS theory (E160). He included both the electron-electro and the electron-phonon collision times since, at the temperatures considered, they are comparable in weak coupling materials, especially in aluminum (La72). For small deviations from equilibrium (Sch68) finds that the relaxation time for the superconducting order parameter is

$$\tau = \begin{cases} \dfrac{\pi}{16(T_c - T)} & \text{if } \Delta_{eq} < \dfrac{1}{\tau_e} \\ \dfrac{\pi^3}{7\zeta(3)} \dfrac{T}{\Delta_{eq}} \tau_e & \text{if } \Delta_{eq} > \dfrac{1}{\tau_e} \end{cases} \tag{V-15}$$

where τ_e is the inelastic electron collision time, Δ_{eq} is the equilibrium energy gap and $\zeta(3) = 1.2$. The condition $\Delta_{eq} < 1/\tau_e$ is the condition of gapless superconductivity where the energy gap is smaller than the collision broadening of the energy levels. For the relaxation of the phase of the order parameter (Sch68) obtains

$$\tau = \begin{cases} \dfrac{6}{v_0^2 k^2}\,\tau_e\,\Delta_{eq}^2 & \text{if } v_0 k \ll \dfrac{1}{\tau_e} \text{ and } \Delta_{eq} \gg \dfrac{1}{\tau_e} \\ \dfrac{12\pi^3 T_c}{\zeta(3) v_0^3 k^3}\,\Delta_{eq} & \text{if } v_0 k \gg \dfrac{1}{\tau_e} \end{cases} \qquad \text{(V-16)}$$

where v_0 is the Fermi velocity and k is the wavevector of the particular mode under consideration.

The most recent theory was developed by Schmid and Schön (SS75) based on a temperature-dependent Green's function technique introduced by Eliashberg (El61) and Eilenberger (Ei68). The calculation is based on a model of a superconductor where the electrons interact via phonons. The phonons are assumed to be in thermal equilibrium and the deviations from equilibrium of the electronic system are small so that a linearized theory applies. The linearization of the theory also permits the classification of various modes, especially useful when the theory is applied close to the transition temperature T_c. (SS75) obtain an equation for energy gap that is very similar to the Landau-Khalatnikov Eq. (V-8).

$$\left(\frac{\partial}{\partial t} + 2iM\right)\Delta = -\frac{8T}{\pi N_0}\ \text{linearized}\ \left(\frac{\delta F_{GL}}{\delta \Delta}\right) \qquad \text{(V-17)}$$

where N_0 is the density of states at the Fermi energy and M is a complex valued function, unlike in Eq. (V-8), where it was μ the chemical potential, a real quantity.

$$M = \frac{4T}{\pi|\Delta|} \int dE' \beta(E') \delta f_{E'} \qquad \text{(V-18)}$$

where $\delta f_{E'}$ is the quasiparticle distribution and $\beta(E')$ is related to the details of the theory.

In addition to Eq. (V-17), the energy gap and the quasiparticle distribution are coupled together through a Boltzman-type equation for the quasiparticle distribution,

$$\frac{d\delta f_E}{dt} - K(\delta f) - P_E - Q_E = \dot{h}_E \qquad \text{(V-19)}$$

where the term $\delta f_E/dt$ is the time derivative of the quasiparticle distribution, $K(\delta f)$ is the collision integral as in a Boltzmann equation for a gas, P_E is the perturbation term since we are considering nonequilibrium situations, $\dot{h}_E$ is the term that couples the energy gap and the quasiparticle distribution and Q_E is an additional correction term that arises from a detailed theory. It should be pointed out that Q_E and $\dot{h}_E$ are different for the different modes that arise.

There are two modes, that can be distinguished by studying Eq. (V-17), associated with the imaginary and real parts of M. This is similar to the two modes obtained in Section 2 of this Chapter, when studying the real and imaginary parts of Eq. (V-8).

The real part of Eq. (V-17) gives rise to the relaxation of the magnitude of Δ, the so-called "longitudinal mode". Accordingly to Schmid and Schön the longitudinal mode can be excited by a superposition of a DC and an AC current (PM73), or by irradiation of the superconductor by an electromagnetic wave. The relaxation time for this mode was found to be

$$\tau^{(L)} = \frac{\pi^3}{7\zeta(3)} \frac{T}{\Delta_{eq}} \tau_e \qquad \zeta(3) = 1.2 \qquad \text{(V-20)}$$

The imaginary part of Eq. (V-17) gives rise to the relaxation of the phase of Δ, the so-called "transverse mode". This equation is the same as Eq. (V-10), obtained from a simple phenomenological theory (μ has to be replaced in Eq. (V-10) by Re(M)). This mode can be excited by electron tunneling injection at high voltage (C72, Pa73, CP74), or by driving a current in the direction of a spatial change of the order parameter, as at a normal-superconductor interface (Yu74). The relaxation time associated with this mode was found to be

$$\tau^{(T)} = \frac{4}{\pi} \frac{T}{\Delta_{eq}} \tau_e \qquad \text{(V-21)}$$

It should be pointed out that in both modes the relaxation time diverges as $1/\Delta_{eq}$ for $T \to T_c$, and that although the processes involved are quite different, the relaxation times of the two modes are quite close. It is pointed out by (SS75) that a divergence should occur in any mode that involves the order parameter essentially.

Since the details of the calculations are quite involved and beyond the scope of this work, we are going to recapitulate the main ideas and conclusions of this theory. The equations that govern the relaxation of the superconducting order parameter are a pair of coupled differential equations for the energy gap and the quasiparticle distribution. One of the equations has the form of the Landau-Khalatnikov equation for the energy gap, the other equation is a Boltzmann-like equation for the quasiparticle distribution function. In solving these equations one obtains two different modes, one associated with the relaxation of the magnitude of the order parameter, the other associated with the phase of the order parameter. Both these modes have similar relaxation times that diverge as

$1/\Delta_{eq}$ for $T \to T_c$. The difference between superconductors and other systems that exhibit second order phase transitions (He, ferromagnets, etc.) can be understoody physically (Co75). Superconductors exhibit a forbidden energy gap unlike other systems. When a Cooper pair is broken into quasiparticles, by perturbing the energy gap (with electromagnetic radiation for instance), the energy gap will decrease. Since the energy gap decreases more final states are made available for the quasiparticles and consequently more quasiparticles are thermally excited into these newly available states. Because of this we would expect the behavior of the energy gap to be coupled to that of the quasiparticles, and we expect the relaxation time of the order parameter to be a different dependence in superconductors than in systems that exhibit a second order phase transition but do not have an energy gap.

To check this hypothesis in other systems besides superconductors it would be very interesting to study the relaxation of the order parameter in liquid He^3 in B phase, which also has a real energy gap that presumably is BCS-like. This could be done by studying the low frequency sound attenuation in the B phase of He^3 in a similar way to that done by Chase (Ch58) for the relaxation time of the order parameter in He^4.

V.4. Experimental Setup

In order to study the relaxation time of the order parameter we illuminate a tunnel junction with a fast risetime light pulse. The light will break Cooper pairs in the illuminated film and thereby will decrease the energy gap. The relaxation of the energy gap back to equilibrium is measured by studying the real time response of the I-V characteristic of the junction.

In this section we will describe the selection of suitable materials for the experiment, the electronics and optics used and the behavior of the GaAs solid state laser (used in the experiment) at low temperatures.

Since the relaxation times to be measured are expected to be short ($\sim$ nsec), it is convenient to perform the experiment on a material that is expected to have the longest relaxation time. Also, it would be convenient to have a metal that can be oxidized easily and that has the transition temperature under the λ point of helium so that any thermal problems are minimized.

A calculation of the electron collisions times τ_e can be made from the thermal conductivities. The thermal conductivity K of a metal is given by (Kittel 71, p. 262)

$$K = \frac{\pi^2}{3} \frac{n}{m} k^2 T \tau_e \qquad \text{(V-22)}$$

where n is the electronic concentration per unit volume, m is the mass of the electron, k is the Boltzmann constant and T is the temperature. n is not expected to vary much with temperature since the linear coefficient of thermal expansion for metals is a few times 10^{-6}. Because of this we use the room temperature values of n. The relevant quantities for some metals, as well as the calculated values of τ_e, are listed in Table III. It can be seen from this table that aluminum and tin have almost the same collision time if one considers the fact that thermal conductivities are reliable at best to within 20%.

Although the calculations made from thermal conductivities indicate that the collision times in aluminum and tin are similar, calculations made using the low frequency behavior of $\alpha^2(\Omega)F(\Omega)$ (phonon density of states $F(\Omega)$ weighted by the electron-phonon interaction $\alpha^2(\Omega)$), (Ka75),

Table III. Relevant physical properties, and calculated values for electron collision times for selected metals.

	T_c[°K]	K (T_c)[W/cm deg] (Ro55)	n[10^{22}/cm^3] (Kittel 71, p. 248)	τ_e[sec]
Al	1.2	8.0	18.0	0.54×10^{-11}
Pb	7.2	4.0	13.2	0.061×10^{-11}
Sn	3.7	22.5	14.5	0.61×10^{-11}

indicate that the collision times in aluminum are much longer ($\sim$ 500 times) than the collision times in tin. In addition to this we expect a measurement of the relaxation of the energy gap at low temperatures to yield the recombination lifetime of the individual quasiparticles. From Table III-1 we can see that the recombination lifetimes are longer in aluminum than in tin, and consequently it is expected that at temperatures close to T_c this will also be the case. Quasiparticle recombination rates (Gr69) also indicate that the relaxation time will be longer in aluminum. In addition to all this, aluminum has its transition temperature below the λ point and can be oxidized easily. Consequently these facts support our choice of studying the relaxation time of the order parameter in aluminum.

In order to compare our measurements of the relaxation times with the theoretical dependence on equilibrium energy gaps, we measure the equilibrium energy gaps also. Since the measurements are of interest close to T_c, where the relaxation time diverges, it is more convenient to use a tunnel junction made of dissimilar metals for the measurement of the energy gaps. In a junction made of the same materials the energy gap structure close

to T_c is smeared out due to thermal effects. On the other hand, for a junction made of dissimilar metals, sharp structure is seen in the I-V characteristic (at $\Delta_1 \pm \Delta_2$) even as close as $\frac{1}{2}$ mK from T_c of the weaker superconductor.

Aluminum (1000 Å) - tin (2500 Å) tunnel junctions were prepared on glass substrates with standard evaporation techniques. The junction has an approximate area of 0.04 mm^2. The procedure for the cleaning of the substrates was described in Chapter IV.3. In order to more easily obtain non-shorted, low resistance junctions, it was found helpful to put a shield around the electron beam gun so that electrons that escaped the bending magnetic field were not able to hit the junction, thereby presumably breaking the oxide layer. The preparation of the samples on a substrate cooled to liquid nitrogen temperatures did not increase the yield of "good" junctions. Cooling the substrate had an effect on the appearance of the tin film, which looked "shinier" when the substrate was cooled, compared to the evaporation on room temperature substrates.

The normal resistances of the junctions were $\leq$ 25 Ω at liquid helium temperature. Since we are interested in measuring short times (nsec), it is important to take into consideration the electronic (RC) junction time constant. The relevant resistance for this calculation is the differential resistance at which the junction is biased for the relaxation time measurement. Using the highest observed differential resistance ($\sim$ 5 Ω), conservative values for the thickness of the oxide layer of 10 Å, and a dielectric constant of 10 (AIP 72, p. 9-109), the RC time constant of the junction is $\sim$ 18 nsec.

After the junctions were evaporated they were immediately mounted in the cryostat and cooled to liquid nitrogen temperature. In junctions stored at room temperature for an extended period of time (2-3 days), increases of up to 3 orders of magnitude in the room temperature resistance were observed. The characteristics of the tunnel junctions stored at liquid nitrogen temperature did not change significantly over periods of up to 3 weeks.

The aluminum film of the tunnel junction was illuminated by a pulsed GaAs injection laser (RCA, SG2012) of about 10 nsec risetime, which was also immersed in the liquid helium. The tunnel junction and the laser were encased in separate niobium shields to avoid direct electromagnetic pickup (seen as a ringing at the beginning and end of the pulse). In addition to this, 50 Ω solid coaxial lines (UT-141SS) were used for the electrical pulses for the laser, and for the biasing and detecting channels. Also all the 115V supplies for the different amplifiers, scopes, etc., were floated so as to eliminate all possible ground loops. In this way, the only possible source of pickup was direct electromagnetic radiation from the laser through the niobium shield to the junction and to a metallic coil protecting part of the fiber optic bundle. The total pickup at the junction was less than 15 μV peak to peak. A block diagram of the experimental setup is shown in Fig. V-1.

The junction was optically connected to the laser via a fiber optic bundle that had a loss of less than $\frac{1}{2}$ dB. The biasing of the junction was done with a battery-operated power supply, and the high frequency pulses were blocked out from this power supply with a low pass RC filter. The pulsed modulation signal from the junction was fed into a series of low noise, fast risetime (∿ 4 nsec) amplifiers, which then were fed into a sampling

Fig. V-1 Experimental setup for the measurement of the relaxation time of the superconducting order parameter.

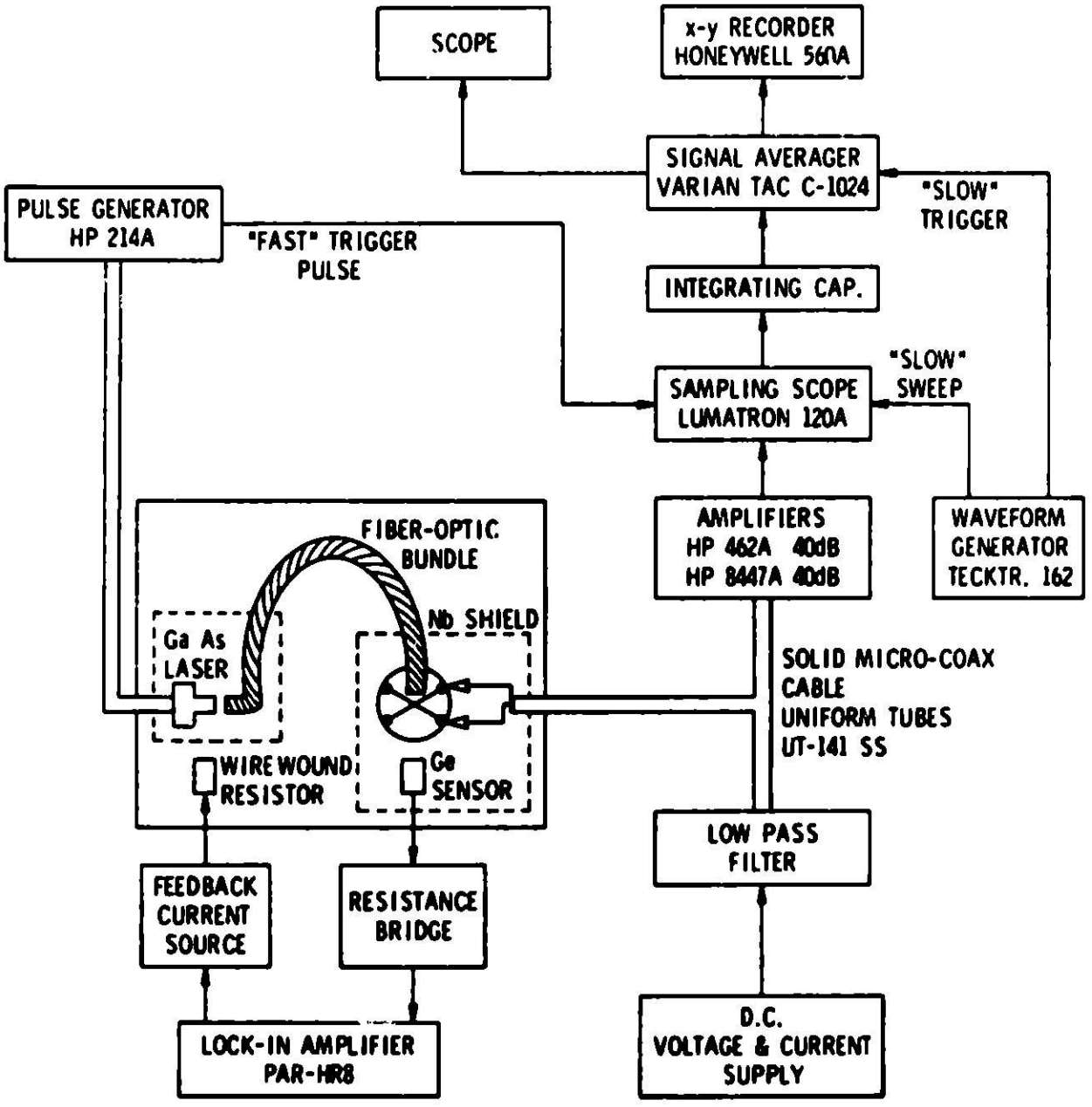
SCOPE
x-y RECORDER
HONEYWELL 560A
SIGNAL AVERAGER
VARIAN TAC C-1024
"SLOW"
TRIGGER
PULSE GENERATOR
HP 214A
"FAST" TRIGGER
PULSE
INTEGRATING CAP.
"SLOW"
SWEEP
SAMPLING SCOPE
LUMATRON 120A
AMPLIFIERS
HP 462A 40dB
HP 8447A 40dB
WAVEFORM
GENERATOR
TECKTR. 162
FIBER-OPTIC
BUNDLE
Nb SHIELD
Ga As
LASER
SOLID MICRO-COAX
CABLE
UNIFORM TUBES
UT-141 SS
WIRE WOUND
RESISTOR
Ge
SENSOR
LOW PASS
FILTER
FEEDBACK
CURRENT
SOURCE
RESISTANCE
BRIDGE
LOCK-IN AMPLIFIER
PAR-HR8
D.C.
VOLTAGE & CURRENT
SUPPLY

scope (Lumatron 120A), integrated with a capacitor and fed into a digital memory and signal averager (Varian TAC C-1024). The output from the signal averager could be displayed on a scope or X-Y recorder. The triggering of the sampling scope was done with a signal obtained from the pulse generator (HP 214A) for the laser (labeled "fast" trigger pulse). In order not to have the signal distorted by the integrating capacitor, a sawtooth ramp (waveform generator, Tektronix 162) was used to sweep slowly ($\sim$ 10 sec) through the signal in the sampling scope (labeled "slow" sweep). Simultaneously with the beginning of the "slow" sweep, a trigger signal (labeled "slow" trigger) was used to trigger the signal averager. The system equivalent noise referred to the input was about 20 μV peak to peak before averaging, and $< \frac{1}{4}$ μV after averaging.

The temperature was electronically controlled using a feedback system with a germanium sensor. The helium was pumped somewhat below the temperature that was to be obtained. Then the germanium sensor, which was part of a resistance bridge, produced an error signal in the bridge which was detected with a lock-in amplifier, amplified and fed into a wire-wound resistor which heated the helium bath. In this way the temperature was stabilized to better than $\frac{1}{2}$ mK.

A GaAs laser (RCA SG 2012) was used, we believe, for the first time in the temperature range 1.3-4.2°K. The light output versus the current through the laser has the form shown in Fig. V-2. (This particular curve was taken at 4.2°K after approximately 4 months of use.) There is first a linear region up to a current labeled "lasing threshold", then there is a sharp break in the curve where the laser starts emitting coherent radiation. Deterioration has been observed in the performance of the laser (the change

Fig. V-2 Light output versus current for a solid state GaAs laser (SG 2012, RCA). The breaking point in the curve is the point at which the laser starts to emit coherent radiation.

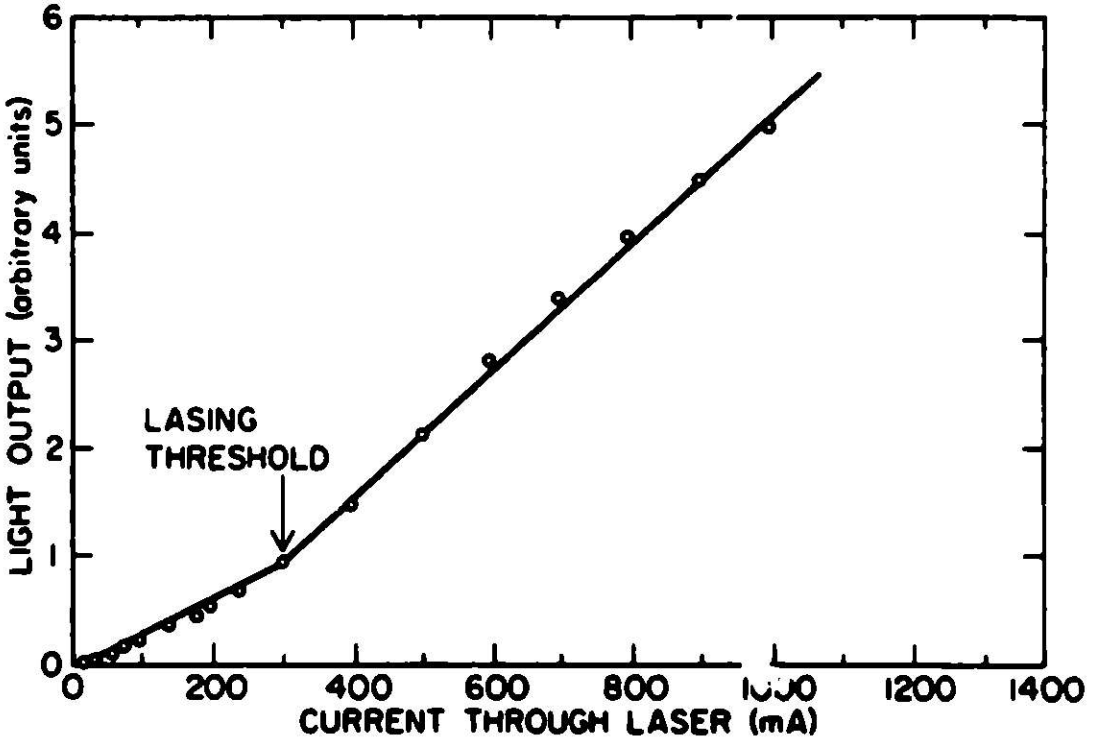
LIGHT OUTPUT (arbitrary units)
0
1
2
3
4
5
6
LASING
THRESHOLD
0
200
400
600
800
1000
1200
1400
CURRENT THROUGH LASER (mA)

in the derivative of the light output versus current at the lasing threshold decreases) after several months of use. This is possibly due to thermal recycling and self-induced damage due to heating.

In general the performance of the laser improves at lower temperatures, particularly under the λ point of helium. This is probably due to the fact that at helium temperature the heat is conducted away from the laser more efficiently than at higher temperatures. A comparison of the performance of the laser at different temperatures is given in Table IV. A systematic study of the operation of this laser, at helium temperatures, can shed more light (CD65, Ke70, CP71, EL73, LMM74) on problems relating to the operation and degradation due to thermal processes in semiconductor lasers.

V.5. Experimental Procedure

For the measurement of the relaxation time the tunnel junction was current biased with a battery supply, and the change in its voltage due to the laser pulse was amplified and fed into the sampling scope. Since the aluminum film is opaque, the pulse of light decreases directly only Δ_{Al}. The change in Δ_{Sn} is due only to the phonons that cross the tunneling barrier and since $\Delta_{Al} < \Delta_{Sn}$, this will be small (SG75, Chapter IV of this thesis). Therefore when the junction is biased at point B (Fig. V-3), a positive decay signal is seen and when the junction is biased at point A, the signal is negative. Note that these signals are shown inverted in Fig. V-3.

The noise was adequately averaged by the sampling scope, but the pickup, which was much larger than the signal ($\sim$ 1 μV) near T_c, had to be

Fig. V.3. The change in the junction voltage versus time at bias points A and B (shown in the inset). The laser illumination occurs during the risetime of the pulse. Note that the signal is shown inverted.

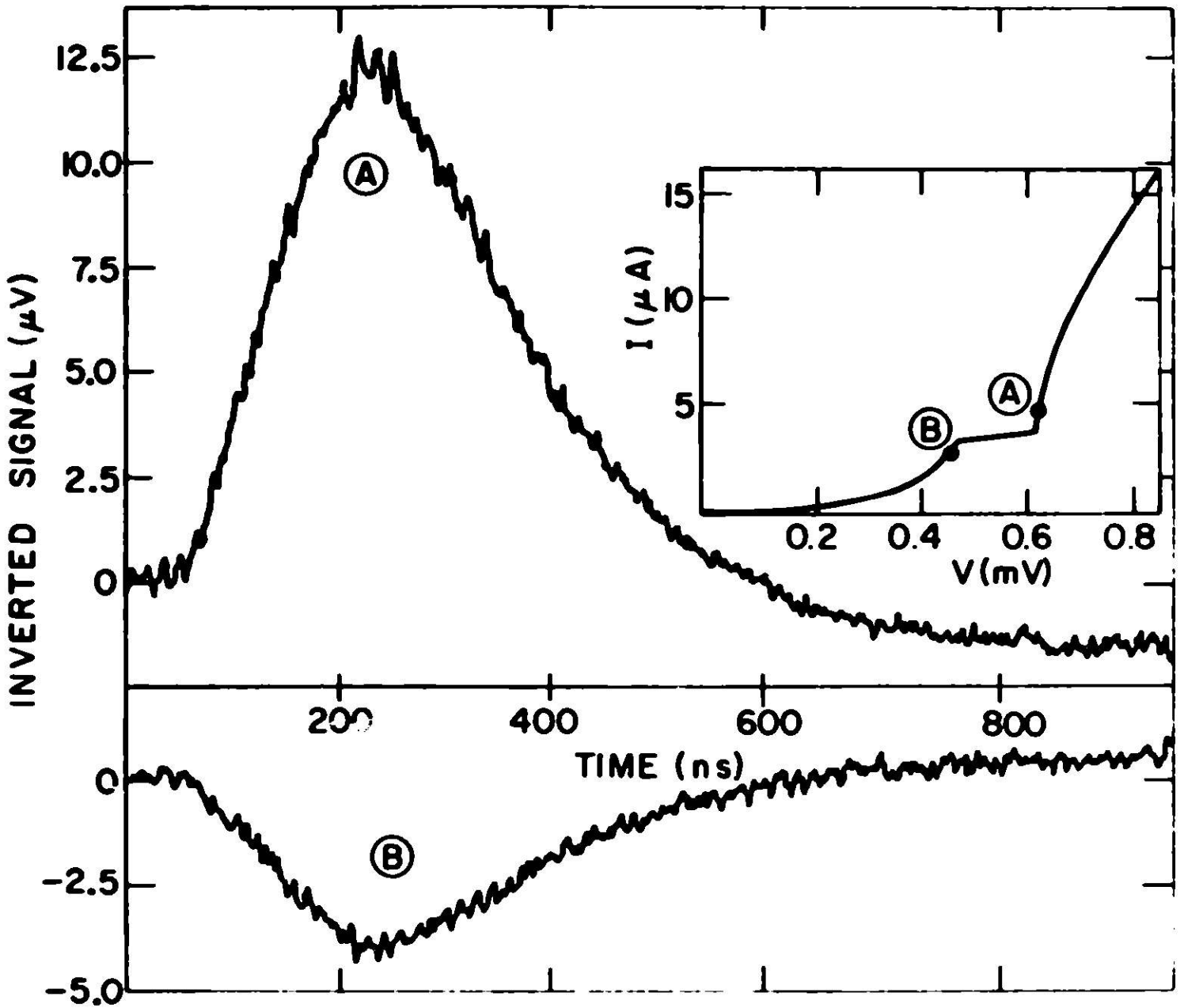
12.5
10.0
7.5
5.0
2.5
0
-2.5
-5.0
INVERTED SIGNAL (μV)
200
400
600
800
TIME (ns)
A
B
15
10
5
I (μA)
0.2
0.4
0.6
0.8
V(mV)

Table IV. Comparison of laser parameters at different temperatures.

	77°K	4.2°K	1.3°K
Maximum pulse width (μsec)	0.7	30	150
Lasing threshold (mA)	600	300	200
Forward voltage (V)	2.0	1.5	0.7
Maximum duty factor	5%	12%	25%

subtracted in the following manner. Data (including pickup) at bias point A was stored in the digital memory. Then the battery connections of the current supply to the junction were reversed, reaching a point on the characteristic symmetrical to A but with opposite voltage. In this way all the impedances, including the junction differential resistance, were the same so that the pickup should be identical. However, the signal is reversed. When the second set of data is subtracted, the pickup subtracts and the signal adds. A signal before and after subtraction and signal averaging is shown in Fig. V-4.

The pulses of Fig. V-3 were obtained in this way. The signal to noise ratio was 5 in the worst case, with neglibile evidence of direct pickup. The decay signal shows a slight undershoot caused by the low frequency threshold of one amplifier (0.1 mHz). An amplifier with lower threshold did not show the undershoot but had a much poorer signal to noise ratio.

The equilibrium energy gaps Δ_{eq} were measured in the same run the relaxation times were measured. Δ_{eq} was determined from the DC tunneling characteristic using a method suggested by Douglas and Meservey (DM64). The characteristic was plotted when the current was increased and when the

Fig. V.4. Signal versus time before end and after subtraction and averaging as explained in the text.

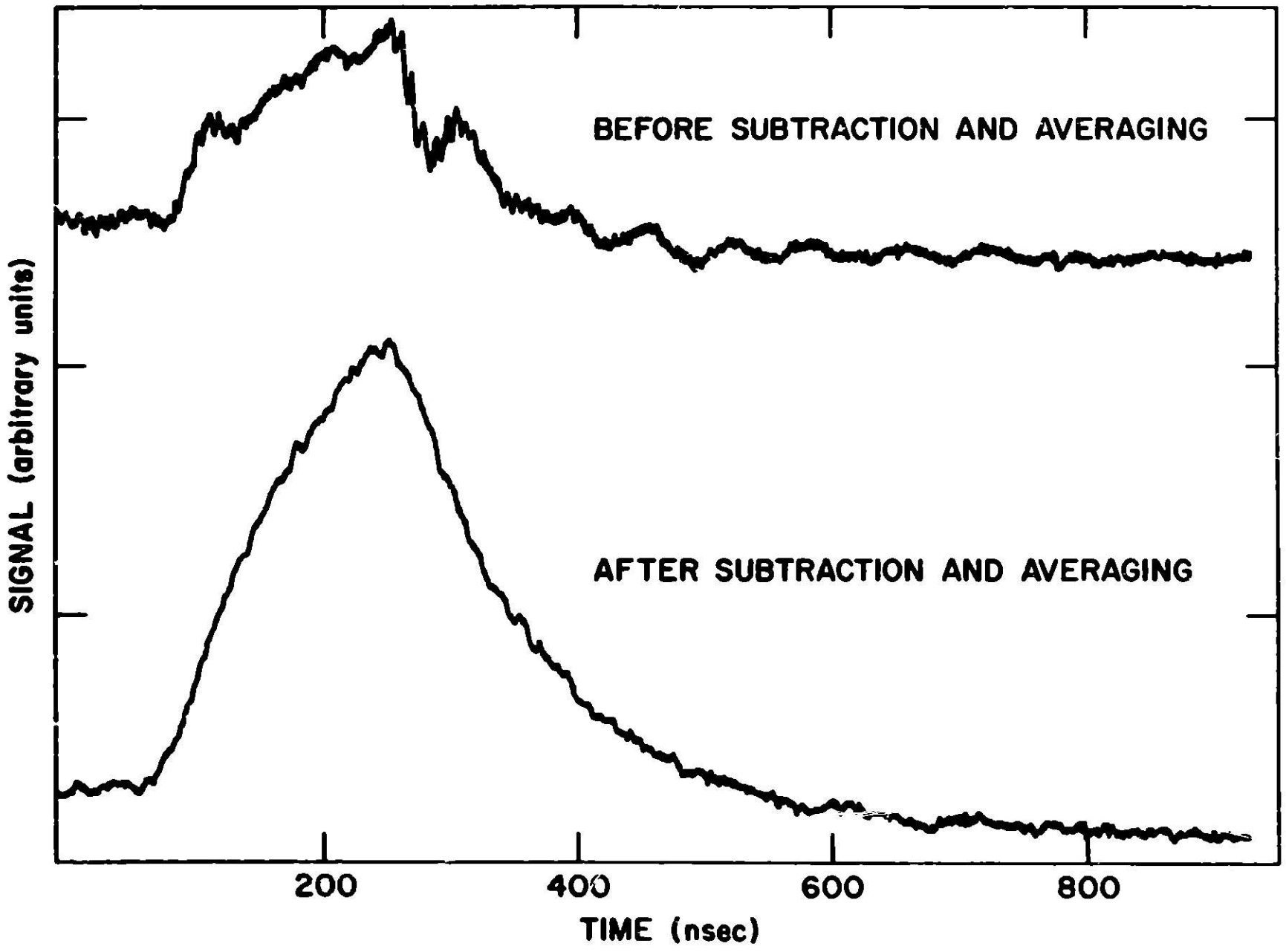
BEFORE SUBTRACTION AND AVERAGING
AFTER SUBTRACTION AND AVERAGING
SIGNAL (arbitrary units)
200
400
600
800
TIME (nsec)

current was decreased. The energy gap of aluminum was determined by the hysteresis loop as described in Fig. V-5. At about 10 mK from T_c, the hysteresis became very small but the structure due to Δ_{Al} was clearly discernable and we were still able to use the method of (DM64). The square of the energy gap determined this way is plotted against the temperature in Fig. V-6. The plot is done in this fashion so that later a direct comparison can be made with the BCS theory, which predicts a straight line.

V.6. Results and Discussion

In order to extract the relaxation times the experimental data (signal vs time, Fig. V-3) was plotted on semi-log paper. The baseline was chosen to give the best exponential decay and was slightly below the undershoot seen in Fig. V-3. Provided that the change in Δ was small compared to Δ_{eq}, we found a good fit to an exponential decay over about 3 time constants with an average deviation of less than 5%. The relaxation time is just the slope of such a plot. At high levels of light intensity, saturation could be observed in the signal, as is expected. In this case the light drives normal the illuminated film and the maximum signal that can be seen is approximately the size of the equilibrium energy gap at that temperature.

A plot of the relaxation time τ against the reduced temperature T/T_c is shown in Fig. V-7 for two different samples. It is clear from this graph the dramatic increase of the relaxation time close to T_c and the agreement between the two different samples is very good. In order to plot both samples in a universal curve, T_c was determined from an extrapolation of the data for Δ_{eq} vs T.

Fig. V.5. Procedure for the measurement of the equilibrium energy gaps from the I-V characteristic. Line (a) is tangent to the curve at the first point of inflection and line (b) is parallel to (a) and tangent to the curve. The energy gap is half the horizontal distance between (a) and (b).

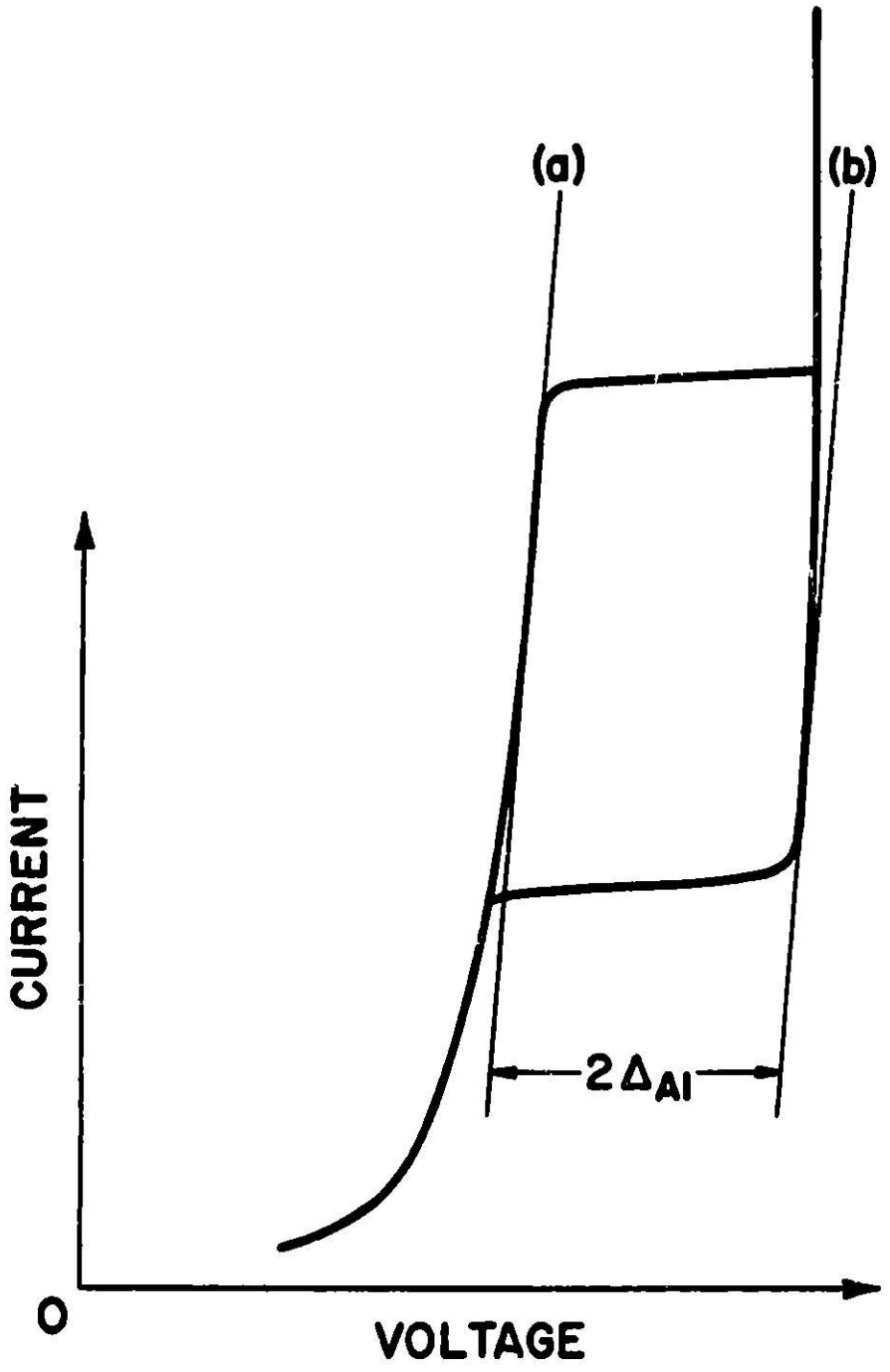
(a)
(b)
CURRENT
0
VOLTAGE
$2\Delta_{Al}$

Fig. V.6. Temperature dependence of the equilibrium energy gap. The solid line is the BCS prediction.

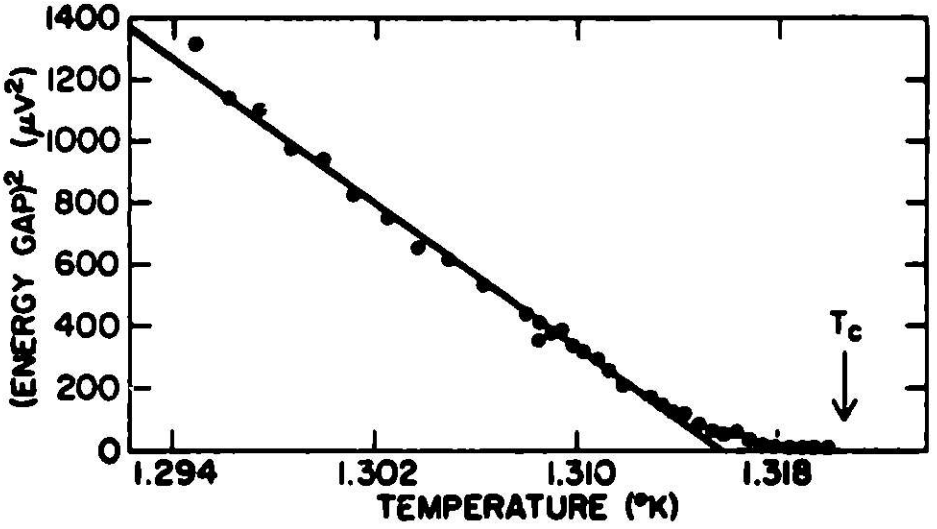
1400
1200
1000
800
600
400
200
0
(ENERGY GAP)² (μV²)
1.294
1.302
1.310
1.318
TEMPERATURE (°K)
Tc

Fig. V.7. Relaxation time τ versus reduced temperature T/T_c. The triangles and the hexagons are data measured in two different samples.

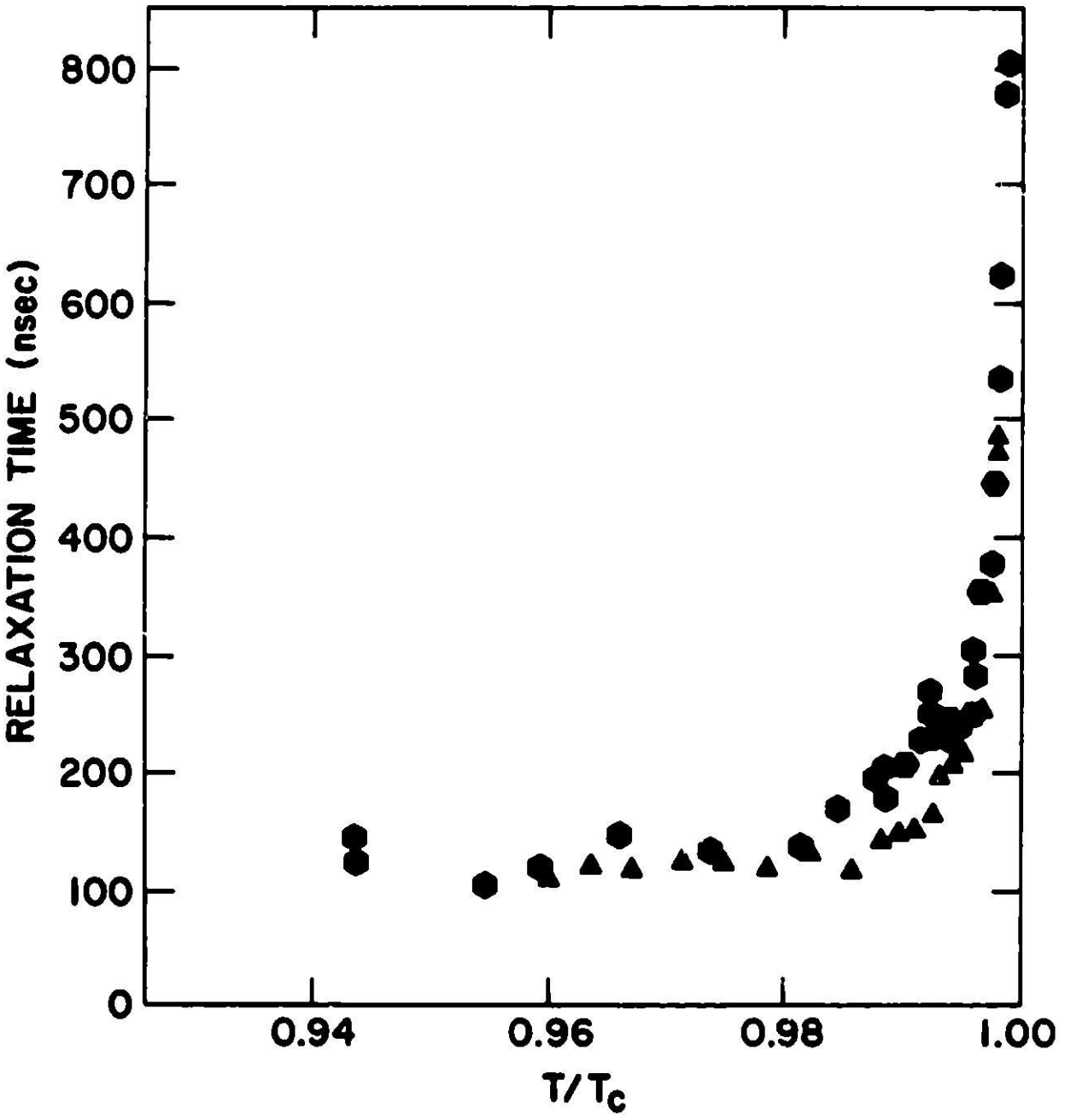
RELAXATION TIME (nsec)
800
700
600
500
400
300
200
100
0
0.94
0.96
0.98
1.00
T/Tc

In both samples a deviation from the BCS temperature dependence of Δ_{eq} was observed close to T_c, as seen in Fig. V-6. The BCS prediction close to T_c is

$$\Delta_{eq} \sim 3.2\, k_B\, T_c [1 - T/T_c]^{1/2} \qquad \text{(V-23)}$$

In Fig. V-6 the solid line represents a temperature dependence of the type (V-23) as in the BCS prediction. However within about 7 mK of the transition temperature, the energy gap depends linearly on the temperature. Deviations from the BCS behavior for the energy gap have been seen before (DM64) and they were attributed to grains with slightly different T_c (DM64) or to enhanced superconductivity at the edges of the junction (Gre75) due to strains in the film. Calculations show that fluctuations cannot produce such a large effect in reasonably clean, 1000 Å, thick aluminum films (Tinkham 75, p. 238); consequently we believe that the deviation is due to spatial inhomogeneities in the films.

Returning to the data of Fig. V-7, we note that it is traditional (PM73) to fit the relaxation times to $(T_c - T)^n$ to compare with the various theoretical predictions (see Chapter III) of the constant n. However, this may not be appropriate in our case since our measured equilibrium energy gaps do not follow the BCS temperature dependence close to T_c where the divergence in τ occurs. Hence we chose to plot τ vs Δ_{eq} as shown in Fig. V-8.

Schmid and Schön (SS75) predicted $\tau \propto \Delta_{eq}^{-1}$ whereas for a gapless superconductor (LS67, GE68) (fluctuations above T_c or with magnetic impurities) the dependence is $\tau \propto \Delta_{eq}^{-2}$. In Fig. V-8 we find $\tau \propto \Delta_{eq}^{-1}$ close to T_c in

Fig. V.8. Measured relaxation times for one sample vs the equilibrium energy gap, showing good agreement with the solid line whose slope is -1. The other sample showed essentially the same behavior.

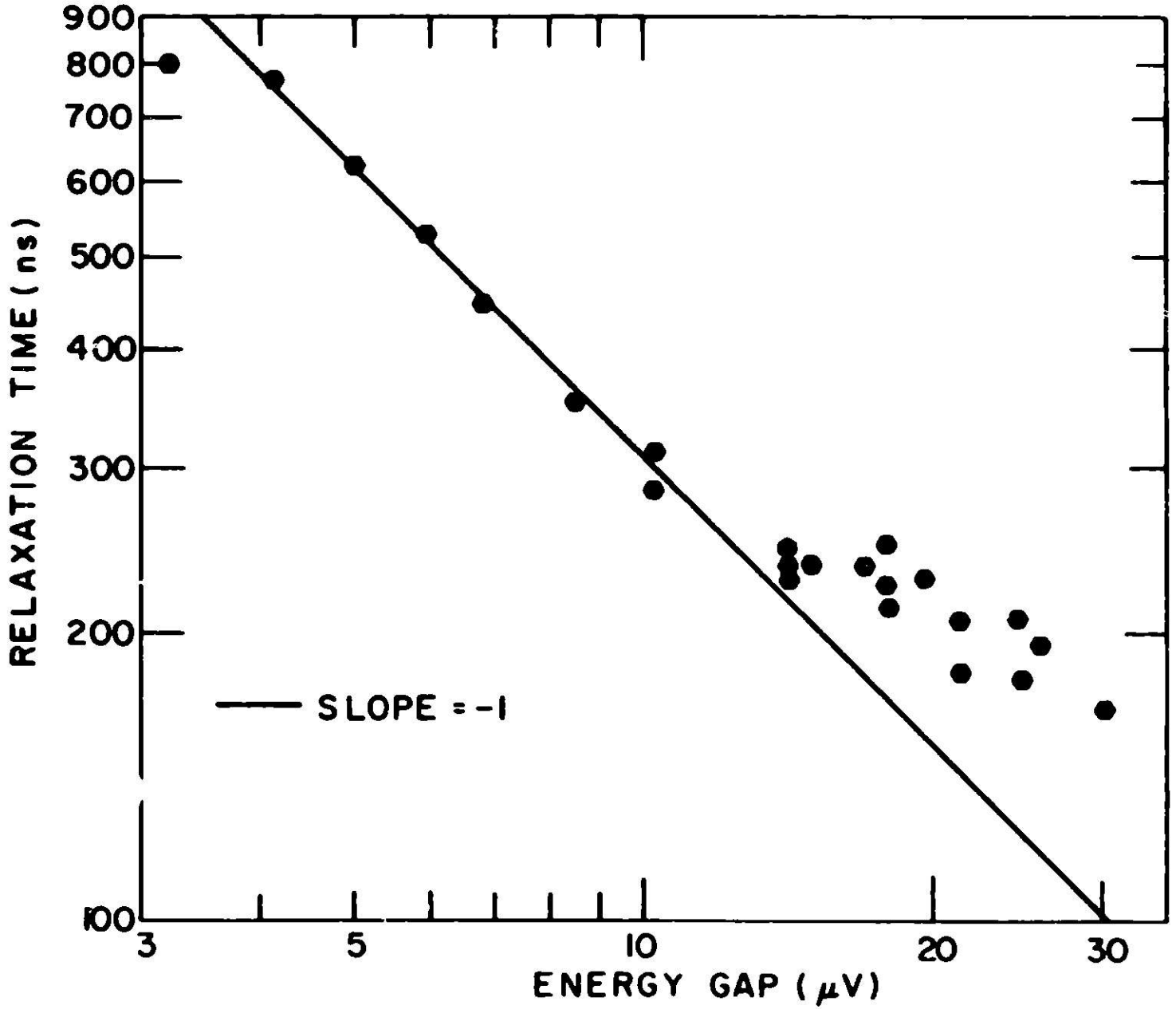
900
800
700
600
500
400
300
200
100
RELAXATION TIME (ns)
SLOPE = -1
3
5
10
20
30
ENERGY GAP (μV)

agreement with the theories of (SS75). It should be pointed out that over the same temperature range the best fit of τ against temperature indicates that $\tau \propto (T_c - T)^{-1}$ in agreement with gapless superconductors and the theory of (LK54), but we feel this is only an artifact of the linear temperature dependence of Δ_{eq} near T_c, which is non-BCS, and the important dependence is on the energy gap.

The possibility of thermal time constant associated with the junction can be ruled out. From the theory of Little (Li59) the thermal time constant of the junction can be calculated using Eq. (IV-11), and the values of the transmission coefficient for longitudinal and transverse phonons obtained from Fig. IV-2. The thermal time constant is simply the heat capacity divided by the thermal conductivity and is found to be $\leq$ 30 nsec, which is smaller than our measured times. The junction RC time constant was shown to be less than 18 nsec (this Chapter, Section 4) and is expected to be weakly temperature-dependent. There is, however, a possibility that heating is affecting the results, but in the following we give some strong arguments to show that this is not so.

There are two possible contributions to the signal we observe at the time the laser is turned off. One (S_T) is due to a change in the film temperature, which then affects Δ_{eq} and relaxes with the thermal time constant τ_T. Another contribution (S_R) is due to direct pair breaking and decays with the order parameter relaxation time τ which we wish to measure. We make the reasonable assumption that for the highest temperature (i.e., the longest measured relaxation time), $\tau_T \ll \tau$. We also point out the fact that in none of our decays is it possible to fit the data to two

exponentials. These facts imply that at high temperatures S_T, the faster decaying component of the signal, must be negligible compared to S_R. We also point out that experimentally the total signal $S_T + S_R$ decreases as T increases. However S_T is expected to increase with T since $\frac{d\Delta}{dT}$ increases with T and $\frac{dT}{dt}$ is approximately independent of T. Hence the ratio S_T/S_R is expected to decrease with decreasing T, and we conclude that S_T is negligible for all T. Any other assumption about the relative magnitude of τ_T and τ leads to the same conclusion, so we feel confident that we are measuring τ and not τ_T at <u>all</u> temperatures.

The first reported experiments that showed an increase of the relaxation time near T_c were the steady state quasiparticle lifetime measurements (GLA69, Gr71). However these measurements were not sufficiently detailed to establish this behavior (see Fig. III-1). In these experiments the relaxation time was measured by injecting quasiparticles through a tunnel junction and measuring the perturbed quasiparticle population. The complete relaxation time curve for aluminum is shown in Fig. V-9. The data of (Gr71) was scaled vertically so as to overlap our data in the common temperature range. At $T/T_c \sim 0.99$ a transition is observed between the single particle behavior and the collective behavior described in Sections 2 and 3 of this Chapter. This is the first time that the complete relaxation curve has been established for a superconductor.

Using Eq. (V-20) and the experimental results of Fig. V-7, we find that the inelastic electron collision time τ_e is 7 nsec. The inelastic electron-phonon collision time can be obtained from a surface-Landau-level-resonance experiment (PN68), and is approximately 200 nsec along most of the Fermi surface, although it is quite anisotropic (DW75). An average

Fig. V.9. Relaxation time vs reduced temperature in aluminum. The full circles are the results of the present experiment and the empty squares are the steady state measurements.

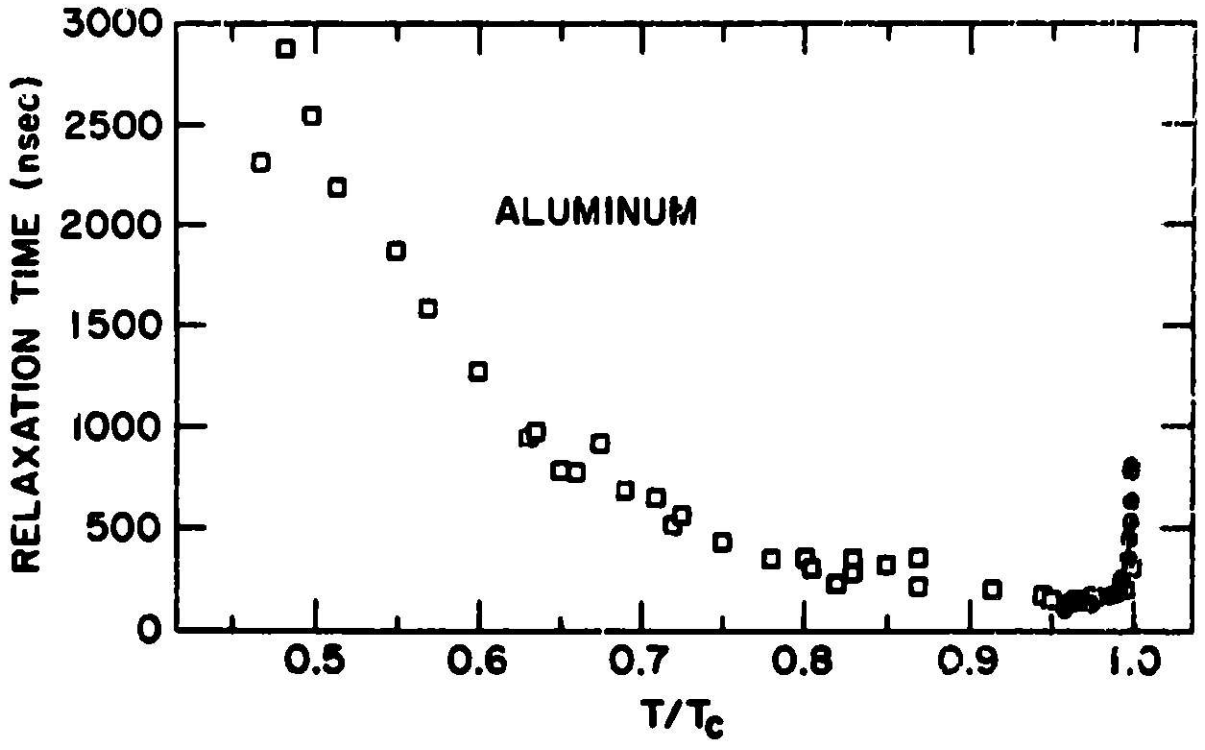
3000
2500
2000
1500
1000
500
0
RELAXATION TIME (nsec)
ALUMINUM
0.5
0.6
0.7
0.8
0.9
1.0
T/T_c

over the whole Fermi surface might alter somewhat these results. It should be pointed out that our measurement is sensitive to all inelastic collisions (including electron-electron and electron-phonon collisions) so that our measurements are not inconsistent with (DW75). A theoretical calculation of the quasiparticle recombination time (KA75) indicates that close to T_c the recombination time is 104 nsec, in good agreement with our low temperature results.

Our measurements determine the relaxation of the magnitude of the order parameter. The relaxation of the phase of the order parameter was done in the experiments of (Cℓ72) and (CP74) for the branch imbalance relaxation. They also obtain a time that diverges as $1/\Delta_{eq}$ in good agreement with the theory of (SS75).

V.7. Conclusions

We have measured directly for the first time, the relaxation time of the superconducting order parameter and the equilibrium energy gap close to T_c. The results indicate that the relaxation time of the magnitude of the order parameter diverges as $1/\Delta_{eq}$ for $T/T_c \geq 0.99$, in agreement with the theory of (SS75). The inelastic collision time for electrons τ_e determined from this experiment is consistent with surface-Landau-level-resonance experiments (DW75) and theory (Ka75).

Additional experiments are under way to measure the relaxation time of the order parameter in a sample in which the equilibrium energy gap obeys BCS more closely.

Appendix I: Computer program for the calculation of the excess quasi-particle number vs the coupling parameters and vs the experimentally-determined change in the energy gap.

The computer program for the deconvolution of ΔN_{exp} vs ε and $\delta\Delta_{exp}$ was done using the SPEAKEASY computer language developed at Argonne National Laboratory. Essentially the computer program calculates Eqs. (IV-20) and (IV-21) in a matrix form where the rows give the value of ΔN_{exp} vs T for fixed ε, and the columns give ΔN_{exp} vs ε for fixed T.

The parameter called EPS in the program is the coupling parameter ε.

```
1   PROGRAM
2   ETA=4.4*NO*DEXP
3   EPS=GRID (.2,.8,.2),1.5,2,3,4,5
4   K=.8617E-4
5   N=.0464*NO*SQRT(DELTA*T)*EXP(-DELTA/(K*T))
6   NPR=.0464*NOPR*SORT(DELTAPR*T)*EXP(-DELTAPR/(K*T))
7   DN=VECTOR(1/(1-EPS))**VECTOR(ETA+NPR)
8   DN=DN+VECTOR(EPS/(1-EPS))**VECTOR(N)
9   A=VECTOR(1/((1-EPS)**2))**VECTOR((ETA+NPR)**2)
10  B=VECTOR(EPS/((1-EPS)**2))**VECTOR((ETA+NPR)*N)*2
11  C=VECTOR((EPS/(1-EPS))**2)**VECTOR(N**2)
12  D=VECTOR(1/(1-EPS))**VECTOR(ETA*(ETA+2*NPR))
13  I=GRID(1,4,1)
14  J=GRID(5,9,1)
15  DN(I,)=DN(I,)-SORT(A(I,)+B(I,)+C(I,)-D(I,))
16  DN(J+1,)=DN(J,)+SORT(A(J,)+B(J,)+C(J,)-D(J,))
17  FREE(A,B,C,D)
18  DNPR=VECTOR(EPS/(EPS-1))**VECTOR(ETA+N)
19  DNPR=DNPR+VECTOR(1/(EPS-1))**VECTOR(NPR)
20  A=VECTOR((EPS/(EPS-1))**2)**VECTOR((ETA+N)**2)
21  B=VECTOR(EPS/((EPS-1)**2))**VECTOR((ETA+N)*NPR)*2
22  C=VECTOR(1/(EPS-1)**2)**VECTOR(NPR**2)
23  D=VECTOR(EPS/(EPS-1))**VECTOR(ETA*(ETA+2*N))
24  DNPR(I,)=DNPR(I,)+SQRT(A(I,)+B(I,)+C(I,)-D(I,))
25  DNPR(J+1,)=DNPR(J,)-SQRT(A(J,)+B(J,)+C(J,)-D(J,))
26  DN(5,)=(ETA*(ETA+2*NPR))/(2*(N+NPR+ETA))
27  DNPR(5,)=(ETA*(ETA+2*N))/(2*(N+NPR+ETA))
28  FREE(A,B,C,D)
```

References

ACG72 J. T. Anderson, et al., J. Low Temp. Phys. 8, 29 (1972).

AIP72 American Institute of Physics Handbook, Dwight E. Gray, Ed. (McGraw-Hill Co., N.Y., Third Edition, 1972).

AR63 P. W. Anderson and J. M. Rowell, Phys. Rev. Letters 10, 230 (1963).

AT66 Elihu Abrahams and Toshihiko Tsuneto, Phys. Rev. 152, 416 (1966).

BCS57 J. Bardeen, L. N. Cooper, and J. P. Schrieffer, Phys. Rev. 106, 162 (1957); and Phys. Rev. 108, 1175 (1957).

BRT59 J. Bardeen, et al., Phys. Rev. 113, 982 (1959).

Ca75 R. V. Carlson, Thesis, University of Minnesota, 1975 unpublished.

CD65 M. Ciftan and P. D. Debye, Appl. Phys. Letters 6, 120 (1965).

Ch58 C. E. Chase, Phys. Fluids 1, 193 (1958).

Cl72 J. Clarke, Phys. Rev. Letters 28, 1363 (1972).

Co57 L. N. Cooper, Phys. Rev. 104, 1189 (1956).

Co75 Morrel Cohen, private communication.

CP71 A. N. Chakravarti and D. P. Parui, Intern. J. Electronics 30, 589 (1971).

CP74 John Clarke and James L. Paterson, J. Low Temp. Phys. 15, 491 (1974).

Da72 A. H. Dayme, J. Phys. 33 (Suppl. C-4), 15 (1972).

dG66 P. G. deGennes, "Superconductivity of Metals and Alloys" (W. A. Benjamin Inc., Publishers, N.Y., 1966).

DM64 D. H. Douglas and R. Meservey, Phys. Rev. 135, A19 (1964).

DW75 R. E. Doezema and T. Wegehaupt, Solid State Commun. 17, 631 (1975).

ED67 W. Eisenmenger and A. H. Dayem, Phys. Rev. Letters 18, 125 (1967).

E168 G. Eilenberger, Z. Phys. 214, 195 (1968).

El60 G. M. Eliashberg, Soviet Physics-JETP 11, 696 (1960).

El61 G. M. Eliashberg, Soviet Physics-JETP 12, 1000 (1961).

El73 V. I Eliseev, J. Luminescence 7, 338 (1973).

Fa75 C. M. Falco, Private communication.

Fr50 H. Fröhlich, Phys. Rev. 79, 845 (1950).

CE68 L. P. Gorkov and G. M. Eliashberg, Soviet Physics-JETP 27, 328 (1968).

Gi60 Ivar Giaver, Phys. Rev. Letters 5, 464 (1960).

GL50 V. L. Ginsburg and L. D. Landau, Soviet Physics-JETP 20, 1064 (1950).

GLA69 K. E. Gray, A. R. Long, and C. J.Adkins, Phil. Mag. 20, 273 (1969).

Go58 L. P. Gorkov, Soviet Physics-JETP 8, 505 (1958).

Go59 L. P. Gorkov, Soviet Physics-JETP 9, 1364 (1959).

Go60 L. P. Gorkov, Soviet Physics-JETP 37, 998 (1960).

Gr69 K. E. Gray, Phil. Mag. 20, 267 (1967).

Gr71 K. E. Gray, J. Phys. F: Metal Phys. 1, 290 (1971).

Gr75 K. E. Gray, private communication.

Gre75 W. D. Gregory, private communication.

HDN74 P. Hu, R. C. Dynes, and V. Narayanamurti, Phys. Rev. B10, 2786 (1974).

Jo62 B. D. Josephson, Phys. Letters 1, 251 (1962).

JPK76 F. Jaworski, W. H. Parker, and S. Kaplan, to be published.

Ka76 S. B. Kaplan, private communication.

KB62 L. P. Kadanoff and G. Baym, "Quantum Statistical Mechanics" (W. A. Benjamin Inc., Publishers, N.Y., 1962).

Ke70 R. W. Keyes, IBM Journal Res. Develop. 14, 158 (1970).

Kittel71 C. Kittel, "Introduction to Solid State Physics" (John Wiley & Sons Inc., N.Y., 4th Edition, 1971).

La72 D. C. Lancanshire, J. Phys. F: Metal Phys. 2, 107 (1972).

La74 D. N. Langenberg, in Festerkörpeprobleme-Advance in Solid State Physics, Vol. XIV, p. 67, H. J.Queisser Editor (F. Vieweg & Son Inc., Braunschweig, 1974).

La75 D. N. Langenberg, in Low Temperature Physics LT-14, Vol. 5, p. 223 M. Krusius and M. Vuorio, Editors (North-Holland Publishing Co., Amsterdam, 1975).

LH68 J. L. Levine and S. Y. Hsieh, Phys. Rev. Letters 20, 994 (1968).

LH71 J. L. Levine and S. Y. Hsieh, Physica 55, 471 (1971).

Li59 W. A. Little, Can. J. Phys. 37, 334 (1959).

LK54 L. D. Landau and I. M. Khalatnikov, Dokladii Academii Nauk CCCP 96, 469 (1954). English version in "Collected Papers of L. D. Landau" (Gordon and Breach Publishers, N.Y), edited by D. ter Haar.

Lo73 A. R. Long, J. Phys. F: Metal Phys. 3, 2040 (1973).

LMM74 V. F. Livinov, et al., Soviet Physics-JETP 19, 384 (1974).

LS67 G. Lucas and M. J. Stephen, Phys. Rev. 154, 349 (1967).

MB56 W. P. Mason and H. E. Brommel, J. Acoust. Soc. Am. 28, 930 (1965).

MD67 Barry I. Miller and Aly H. Dayem, Phys. Rev. Letters 18, 1000 (1967).

Me70 J. E. Mercereau, Rev. Phys. Appliquee 5, 13 (1970).

MS63 J. L. Miles and P. H. Smith, J. Electrochem. Soc. 110, 1240 (1963).

ND71 V. Narayanamurti and R. C. Dynes, Phys. Rev. Letters 27, 410 (1971).

OS72 C. S. Owen and D. J. Scalapino, Phys. Rev. Letters 28, 1559 (1972).

Parks69 "Superconductivity", R. D. Parks, editor (Marcell Dekker, Inc., N.Y., 1969).

A72 R. E. Peterson and A. C. Anderson, Solid State Commun. 10, 891 (1972).

Pa73 J. L. Paterson, Thesis, University of California, 1973, unpublished.

Pa74 W. H. Parker, Solid State Commun. 15, 1003 (1974).

Pa75 W. H. Parker, Phys. Rev. B12, 3667 (1975); Bull. Am. Phys. Soc. 20, 331 (1975).

PM73 R. Peters and H. Meissner, Phys. Rev. Letters 30, 965 (1973).

PN68 R. E. Prange and T. W. Nee, Phys. Rev. 168, 779 (1968).

PW72 W. H. Parker and W. D. Williams, Phys. Rev. Letters 29, 924 (1972).

Ra45 J. W. S. Rayleigh, "The Theory of Sound" (Dover Publications, N.Y., 1945).

RC63 A. Rothwarf and M. Cohen, Phys. Rev. 130, 1401 (1963).

RMD J. M. Rowell, W. C. McMillan, and R. C. Dynes, "A Tabulation of the Electron-Phonon Interaction in Superconducting Metals and Alloys. Part I", unpublished.

Ro55 H. M. Rosenberg, Phil. Trans. - Royal Soc. of London 247, 441 (1955).

RT67 A. Rothwarf and B. N.Taylor, Phys. Rev. Letters 19, 27 (1967).

RWNH75 F. J. Rachford, et al., Phys. Rev. Letters 35, 305 (1975).

Sa74 G. A. Sai-Halasz, et al., Phys. Rev. Letters 33, 215 (1974).

Sch66 Albert Schmid, Phys. Kondens, Materie 5, 302 (1966).

Sch68 Albert Schmid, Phys. Kondens Materie 8, 129 (1968).

Sch69 Albert Schmid, Phys. Rev. 186, 420 (1969).

Schiff68 L. I. Schiff, "Quantum Mechanics" (McGraw-Hill Co., N.Y., 1968).

SG62 J. R. Schrieffer and D. M. Ginsberg, Phys. Rev. Letters 8, 207 (1962).

SG75 I. Schuller and K. E. Gray, Phys. Rev. B12, 2629 (1975).

SG76 Ivan Schuller and K E. Gray, Phys. Rev. Letters 36, 429 (1976).

Sm75 L. N. Smith, Thesis, University of Illinois, 1975, unpublished.

SM75 L. N. Smith and J. M. Mochel, Phys. Rev. Letters 35, 1597 (1975).

SS75 Albert Schmid and Gerd Schön, J. Low Temp. Phys. 20, 207 (1975).

Ta63 B. N. Taylor, Thesis, University of Pennsylvania, 1963, unpublished.

TC72 M. Tinkham and John Clarke, Phys. Rev. Letters 28, 1366 (1972).

Te71 L. R. Testardi, Phys. Rev. B4, 2189 (1971).

TEC69 R. Truell, C. Elbaum, and B. B. Chick, "Ultrasonic Methods in Solid State Physics" (Academic Press, N.Y., 1969).

Ti72 M. Tinkham, Phys. Rev. B6, 1747 (1972).

Tinkham75 M. Tinkham, "Introduction to Superconductivity" (McGraw-Hill Co., N.Y., 1975).

VK74 A. F. Volkov and S. M. Kogan, Soviet Physics-JETP 38, 1018 (1974).

WA68 J. W. F. Woo and E. Abrahams, Phys. Rev. 169, 407 (1968).

YM72 M. L. Yu and J. E. Mercereau, Phys. Rev. Letters 28, 1117 (1972).

Yu74 M. L. Yu, Thesis, California Institute of Technology, 1974, unpublished.

VITA

Name: Ivan Schuller

Birthplace: Cluj, Rumania

Birthdate: June 8, 1946

Education: University of Chile: Bachiller en Matematicas (1965)

Licenciado en Ciencias (1970)

Northwestern University: Master of Science (1972)

Publications:

1. Development of a System for the Measurement of Half Lives of Isomeric States and Study of the Excited States of Sn^{115}
   Thesis, University of Chile, 1970

2. Isomeric States with Half Lives Longer than 10^{-5} sec
   T. W. Conlon, J. L. Romero, and I. Schuller
   Proc. of the 10th Meeting of the Chilean Physical Society
   Concepcion, Chile, A2 (1970)

3. Acoustic Coupling of Thin Superconducting Films
   I. Schuller and K. E. Gray
   Bull. Am. Phys. Soc. 20, 416 (1975).

4. Acoustic Coupling of Thin Superconducting Films
   I. Schuller and K. E. Gray
   Phys. Rev. B12, 2629 (1975)

5. Experimental Observation of the Relaxation Time of the Order Parameter in Superconductors
   Ivan Schuller and K. E. Gray
   Phys. Rev. Letters 36, 429 (1976)

6. Relaxation of the Superconducting Order Parameter
   Ivan Schuller and K. Gray
   Bull. Am. Phys. Soc. 21, 404 (1976)